Stony Brook University

Mathematical Modeling of G-protein-coupled Receptor Signaling Pathways

A Dissertation presented

by

Tao Jiang

to

The Graduate School

in Partial Fulfillment of the

Requirements

for the Degree of

Doctor of Philosophy

in

Applied Mathematics and Statistics

Stony Brook University

May 2014

Stony Brook University

The Graduate School

Tao Jiang

We, the dissertation committe for the above candidate for the

Doctor of Philosophy degree, hereby recommend

acceptance of this dissertation

David F. Green - Dissertation Advisor
Associate Professor, Department of Applied Mathematics and Statistics

Robert C. Rizzo - Chairperson of Defense
Associate Professor, Department of Applied Mathematics and Statistics

Thomas MacCarthy
Assistant Professor, Department of Applied Mathematics and Statistics

Suzanne Scarlata
Professor, Department of Physiology and Biophysics

This dissertation is accepted by the Graduate School

Charles Taber
Dean of the Graduate School

Abstract of the Dissertation

Mathematical Modeling of G-protein-coupled Receptor Signaling Pathways

by

Tao Jiang

Doctor of Philosophy

in

Applied Mathematics and Statistics

Stony Brook University

2014

G-protein-coupled receptor (GPCR) signaling plays an important role in converting extracellular stimuli into cellular responses. Many biological functions are regulated by GPCR signaling, and nearly 40% of current pharmaceuticals target GPCRs. In this work, mathematical modeling is used to investigate the initial steps of GPCR signaling with two major aims: 1) to understand the causes for non-canonical signaling behaviors; 2) to understand how signaling specificity is reacted to in the individual reactions of the pathway.

The classic ternary complex model describing the interaction between a single ligand, receptor and G-protein served as our basic model for the initial investigation. Dose response curves were generated using computer simulations and qualitative differences were observed due to variations in the model parameters. A systematic study on individual parameters demonstrates that the rate for the binding of ligand-receptor complex to G-protein is the key determinant.

In the next step, models containing two signaling pathways were built. The two signaling pathways can be considered to interact with each other when interactions between

the components of both pathways exist. When nonspecific interactions exist in both the binding of the ligand to the receptor and the binding of the receptor to the G-protein, a biphasic dose response is observed. Specificity for the steady state response and dynamics of the signal were defined and how the strength of interactions and concentration of molecules affect signaling specificity were investigated.

Other processes involved in GPCRs signaling were also considered. GPCRs undergo internalization upon ligand activation; they also form homo/hetero-dimers. A double-peaked dynamical response was observed due to the internalization of the receptors, while dimerization of the receptors may produce a double-peaked steady state response. Specificity as previous defined was also calculated and shown to be affected by both internalization and dimerization.

Contents

List of Figures

List of Tables

Acknowledgements

First, I would like to express my deep appreciation to my advisor Dr. David F. Green for introducing me to the systems biology field and for his trust, support and guidance along the way. He has given me freedom to pursue what Im interested in and taught me to critically think about research problems.

I am deeply grateful to Dr. Robert C. Rizzo, Dr. Thomas MacCarthy, Dr. Suzanne Scarlata for serving as my committee members and for their valuable suggestions on my research and on improving this thesis.

I would like to thank all lab members for their support and suggestions, especially Dr. Vadim Patsalo and Dr. Yukiji Fujimoto, who gave me great help when I first joined the group. I would also like to thank Loretta Au for proofreading my presentation slides and posters and all the fun activities she organized for the lab.

I would like to thank all my friends, especially Guangtao Li and Yikang Chai. We came here in the same year, became friends and still are after so many years. I really appreciate their support and help on figuring out my life.

Finally, I also want to thank my family, especially my parents and my grandparents, for their love and support. It was hard to be alone away from home and I would not be able to get this far without their encouragement.

Chapter 1
General Introduction

1.1 Introduction to the G-protein-coupled receptor signaling pathways

When cells communicate with each other, signaling molecules such as hormones and neurotransmitters secreted by one cell usually do not directly enter its neighboring cells. Instead, they can be detected by a group of proteins located on the membrane of other cells called "receptors". The origination of the concept of receptor can be traced back to 100 years ago and the receptor theory has been a key element in the pharmacological sciences [1, 2].

G-protein-coupled receptors constitute one of the largest families of cell surface receptors and represent approximately 1% of the human genome [3, 4, 5]. Various ligands can be detected by GPCRs, including hormones, neurotransmitters, odor molecules as well as light. Malfunctioning of GPCRs can lead to retinal, endocrine, metabolic and developmental disorders [6, 7]. In consequence, GPCRs account for one of the most important drug targets and about 40% of pharmaceuticals target GPCRs [8, 9, 10]. In 2012, Brian Kobilka and Robert Lefkowitz were awarded the Nobel Prize in Chemistry for their contributions in understanding GPCRs.

G-protein-coupled receptors are also called 7-transmembrane receptors and heptahelical receptors because they possess 7 α-helices spanning across the cell membrane (Figure 1.1). Their N-terminus is extracellular and C-terminus is in the cytoplasm. Several classification systems exist for GPCRs based either on sequence similarity, function or phylogenetic trees [4, 10, 12, 13, 14]. Three major families are grouped similarly using different classification methods. The rhodopsin receptor family contains the largest num-

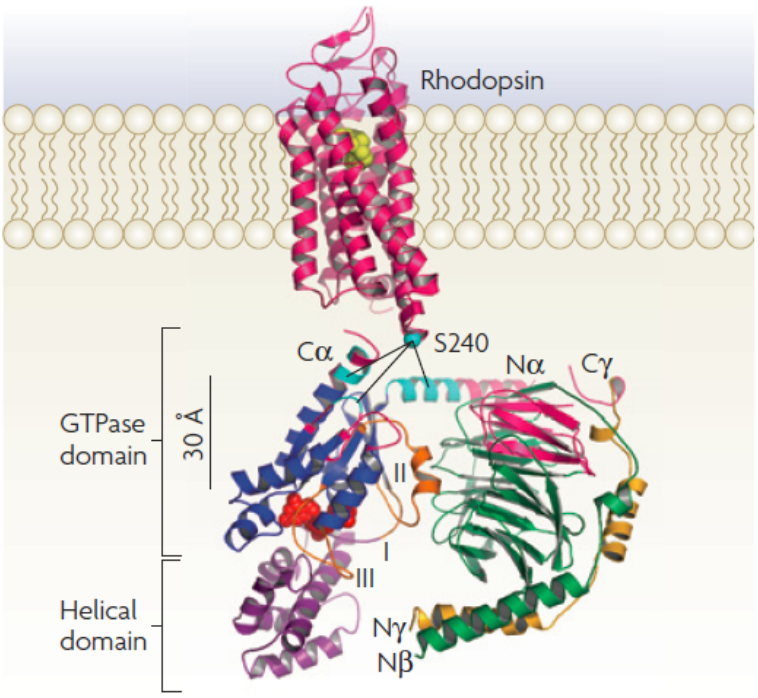

Figure 1.1: **The structures of the G-protein-coupled receptor and heterotrimeric G-protein.** G-protein-coupled receptors are also called 7-transmembrane receptors since they have 7 α-helices spanning across the cell membrane. GPCRs transmit signals by activating the heterotrimeric G-proteins. G-proteins consist of 3 subunits (α, β and γ). When G-protein is activated, the α subunit is separated from the $\beta\gamma$ dimer and both of them can regulate downstream signaling processes. This figure is taken from [11].

ber of GPCRs and includes most of the sensory receptors. The secretin receptor family contains the majority of the peptide hormone G-protein-coupled receptors. The glutamate receptor family includes the metabotropic glutamate receptors and others that can detect neurotransmitters.

G-protein coupled receptors transmit signals primarily through activating heterotrimeric G-proteins. The heterotrimeric G-proteins consist of 3 subunits, α, β and γ. The α subunit has a GTPase activity and is the primary component for transmitting signals to the downstream signaling pathways. Various biological functions can be regulated by GPCR signaling pathways (Figure 1.2). Based on the sequence similarity of the α subunit, G-proteins can be divided into 4 groups: G_s, G_i, G_q and G_{12}. Both G_s and G_i regulate

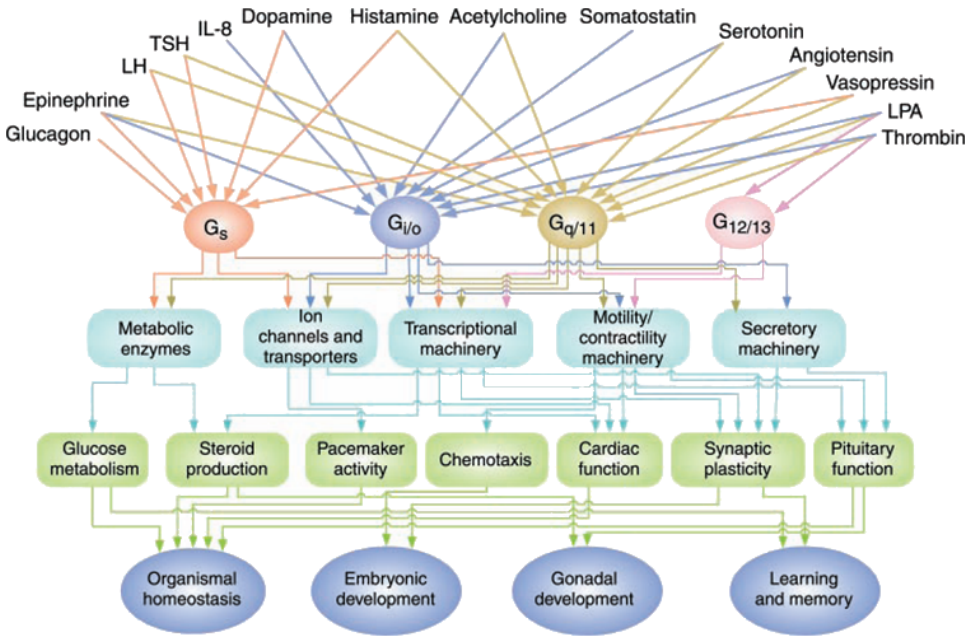

Figure 1.2: **G-protein-coupled receptor signaling pathways.** Various ligands can signal through the four families of G-protein by interacting with G-protein-coupled receptors to regulate systemic functions. This figure is taken from [15]. Reprinted with permission from AAAS.

the down-stream cAMP-dependent pathways by modulating the enzymatic activities of adenylate cyclase. Adenylate cyclase converts adenosine triphosphate (ATP) to cyclic adenosine monophosphate (cAMP). The rate is accelerated by the G_s proteins and impeded by the G_i proteins. cAMP is an important second messenger and can regulate a number of biological functions by activating protein kinase A (PKA). The activated G_q proteins can activate the membrane-bound phospholipase C beta (PLCβ), which in turn cleaves phosphatidylinositol-4,5-bisphosphate (PIP_2) into second messengers inositol trisphosphate (IP_3) and diacylglycerol (DAG). IP_3 interacts with the IP_3 receptors on the endoplasmic reticulum to control the release of Ca^{2+} to the cytoplasm. DAG and Ca^{2+} together can activate protein kinase C (PKC). G_αs in the G_{12} family can regulate the activity of the Rho family small G-proteins.

Due to the complexity of cellular signaling, mathematical models are often helpful for understanding system behaviors [16, 17, 18, 19, 20]. GPCR signaling pathways have

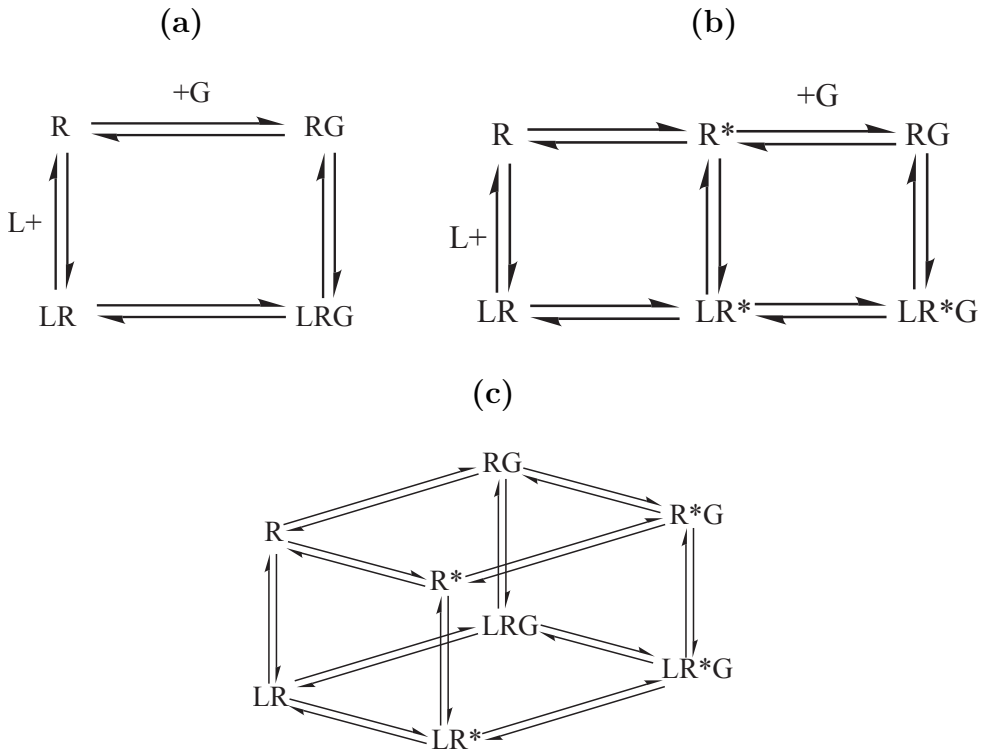

Figure 1.3: **G-protein-coupled receptor models.** (a) The ternary complex model (TCM). (b) The extended ternary complex model (eTCM). (c) The cubic ternary complex mode (CTC). L, R and G represent ligand, receptor and G-protein, respectively. R^* represents the active form of the receptor.

been investigated using different modeling techniques [21, 22]. The first model describing the interactions between ligand, receptor and G-protein was proposed in 1980 by De Lean et. al. [23]. Ligand and G-protein are considered to be able to interact with the receptor simultaneously to from a ternary complex, and thus the model is named the ternary complex model (TCM) (Figure 1.3(a)). In 1993, the ternary complex model was extended by Samama et. al. by considering both an active and an inactive state of the receptor in the model and G-protein is only activated by the active state of the receptor (Figure 1.3(b)) [24]. A more thermodynamically complete model was proposed by Weiss et. al. by considering the interactions between the inactive receptor and the G-protein (Figure 1.3(c)) [25, 26, 27]. All these models are equilibrium models and the

main focus was on the steady state distribution of the receptor states. The activation of G-protein and the dynamics of the signal was later considered in the TCM as well the CTC [28, 29, 30, 31]. These models and their variations represent a large body of theoretical works on the GPCR signaling pathways. Models describing other related processes besides the interactions between a single ligand, receptor and G-protein also exist and are reviewed in each relevant chapters.

1.2 Overview of the present work

The G-protein-coupled receptor signaling pathways exhibit both diversity and specificity [32]. The diversity can be originated from the numerous variants of the components in GPCR signaling pathways as well as the regulations on the GPCRs such as dimerization and internalization. However, such diversity may potentially undermine signaling specificity. For example, the components in GPCR signaling pathways may have the ability to interact with multiple partners due to structural similarities, and result in crosstalk between signaling pathways. How signaling specificity is affected by the interactions between components in different pathways and regulations on the receptors is an interesting question. Ordinary differential equation models are used in this thesis to give an insight into this question. In addition, the underlying mechanisms for diverse signaling patterns are also explained using models.

In Chapter 2, a minimal model describing the initial steps of GPCR signaling is first used to give an insight into the transferability of knowledge gained from one system to another system. Sensitivity analysis on the model parameters sheds light on the key determent on the qualitative behaviors of the dose-response curves. In Chapter 3, a model containing two GPCR signaling pathways is introduced. Interactions between the two pathways are considered and how they affect signaling behavior and signaling specificity are investigated. In Chapter 4, heterodimerization of GPCRs is further considered in the

two-pathways model. The effects of allosteric regulations associated with receptor heterodimerization on signaling are examined. In Chapter 5, trafficking of the receptors are considered in both the one-pathway model and two-pathway model. How internalization of the receptor affects signaling is explored.

Chapter 2

Sensitivity Analysis on the Basic Model for the Initial Steps of G-protein Coupled Receptor Signaling

2.1 Introduction

The ability to respond to environmental stimuli is one of the hallmarks of life; this characteristic applies not only to organisms as a whole, but equally to the individual cells of a multicellular organism. At the cellular level, this response involves changes in the biochemical state of a cell — changes in the expression level of various genes or in the phosphorylation state of particular proteins, as examples — which may further lead to changes in cellular morphology or motility. These regulated responses are essential to multicellular life, as they govern both cellular differentiation during development and organismal homeostasis, in addition to numerous other functions. Disruptions in the regulation of cellular behavior is the fundamental origin of cancer and additionally underlies many other human diseases.

While some cellular responses result from the diffusion of molecular signals across the cell membrane into the intracellular milieu — where they directly exert an effect by association with intracellular proteins — in many cases, extracellular cues must be specifically transduced into intracellular responses. The molecular mechanisms underlying this signal transduction process can be grouped into a number of fundamental classes; one of these prototypical models is the heterotrimeric-G-protein signal transduction pathway [15, 33, 34]. The outermost components of this pathway are heptahelical, integral membrane proteins, the G-protein-coupled receptors (GPCRs). GPCRs are present in most known eukaryotic genomes and constitute one of the largest families of mammalian

proteins [35, 14]. Various extracellular ligands can stimulate GPCRs to activate heterotrimeric G-proteins, which consist of three subunits (α, β and γ) and are localized to the intracellular face of the membrane through lipid modifications of both the α- and γ-subunits. In turn, the activated G-protein can regulate many downstream signaling processes.

In mammalian genomes, there are multiple variants of each subunit — at least twenty α (sixteen well-characterized, and several putative forms that are less or uncharacterized), seven β (including multiple isoforms coded by a single gene) and twelve γ variants [36, 37]; it is the appropriate combination of these that leads to the correct coupling of a specific GPCR to the cognate cellular response. Based on the primary sequence similarity of the α subunits, G-proteins can be divided into 4 families: G_s, G_i, G_q and G_{12}; variants within a class tend to interact with related downstream components, while those of different classes have more diverse targets of action [15].

In the inactive state, the G-proteins are in a trimeric form, with the α-subunit additionally associated with guanosine-5'-diphosphate (GDP). Activated receptors promote exchange of the GDP bound to G_α with guanosine-5'-triphosphate (GTP); this leads to a conformational change in G_α that results in dissociation from the β- and γ-subunits (which remain as a stable dimer) or in reconfiguration of the trimer geometry [38]. Both G_α and $G_{\beta\gamma}$ are then free to interact with additional cellular-signaling proteins; as both the α- and γ-subunits are lipidated, both components remain membrane associated [39, 40]. G_α is a guanine-nucleotide hydrolase, which catalyzes the conversion of GTP to GDP and pyrophospate; this activity returns G_α to an inactive state, reforming the heterotrimer, and thus resetting the system for subsequent stimulation [11].

(a) Cartoon Model **(b) Reaction Scheme**

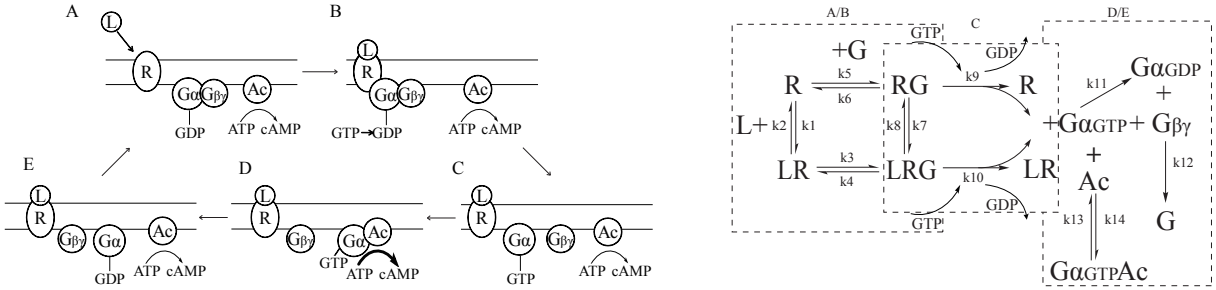

(c) System of Equations

$$\frac{d[L]}{dt} = k_2\,[LR] + k_8\,[LRG] - k_1\,[L]\,[R] - k_7\,[L]\,[RG] \tag{2.1}$$

$$\frac{d[R]}{dt} = k_2\,[LR] + k_6\,[RG] + k_9\,[RG] - k_1\,[L]\,[R] - k_5\,[R]\,[G] \tag{2.2}$$

$$\frac{d[G]}{dt} = k_6\,[RG] + k_4\,[LRG] + k_{12}\left[G_\alpha^{GDP}\right]\,[G_{\beta\gamma}] - k_5\,[R]\,[G] - k_3\,[LR]\,[G] \tag{2.3}$$

$$\frac{d[LR]}{dt} = k_1\,[L]\,[R] + k_4\,[LRG] + k_{10}\,[LRG] - k_2\,[LR] - k_3\,[LR]\,[G] \tag{2.4}$$

$$\frac{d[RG]}{dt} = k_5\,[R]\,[G] + k_8\,[LRG] - k_6\,[RG] - k_7\,[L]\,[RG] - k_9\,[RG] \tag{2.5}$$

$$\frac{d[LRG]}{dt} = k_3\,[LR]\,[G] + k_7\,[L]\,[RG] - k_4\,[LRG] - k_8\,[LRG] - k_{10}\,[LRG] \tag{2.6}$$

$$\frac{d[G_\alpha^{GTP}]}{dt} = k_9\,[RG] + k_{10}\,[LRG] + k_{14}\left[G_\alpha^{GTP}E\right] - k_{11}\left[G_\alpha^{GTP}\right] - k_{13}\left[G_\alpha^{GTP}\right]\,[E] \tag{2.7}$$

$$\frac{d[G_\alpha^{GDP}]}{dt} = k_{11}[G_\alpha^{GTP}] - k_{12}\left[G_\alpha^{GDP}\right]\,[G_{\beta\gamma}] \tag{2.8}$$

$$\frac{d[G_{\beta\gamma}]}{dt} = k_9\,[RG] + k_{10}\,[LRG] - k_{12}\left[G_\alpha^{GDP}\right]\,[G_{\beta\gamma}] \tag{2.9}$$

$$\frac{d[E]}{dt} = k_{14}\left[G_\alpha^{GTP}E\right] - k_{13}\left[G_\alpha^{GTP}\right]\,[E] \tag{2.10}$$

$$\frac{d[G_\alpha^{GTP}E]}{dt} = k_{13}\left[G_\alpha^{GTP}\right]\,[E] - k_{14}\left[G_\alpha^{GTP}E\right] \tag{2.11}$$

Figure 2.1: **The early steps of G-protein-coupled receptor signal transduction. (a) Cartoon representation:** Binding of ligand induces a conformational change in the receptor. The G-protein becomes active when GDP is replaced by GTP in the α subunit, an exchange catalyzed by the activated receptor, with the α subunit dissociating with the $\beta\gamma$ subunits. The α subunit can bind downstream effectors such as adenylyl cyclase, modulating their enzymatic activity; for the G_s subfamily, activity of adenylyl cyclase is enhanced. Finally, due to the intrinsic GTPase activity of the α subunit, GTP will be hydrolyzed to GDP, and the (inactive) trimeric G-protein will be re-formed by association of the α and $\beta\gamma$ subunits. The cycle is completed. **(b) Chemical reaction representation:** k1 through k14 are the reaction rate constants for their corresponding reactions. The reaction scheme is divided to correspond with the process shown in (a). **(c) Mathematical model:** A system of ordinary differential equations (ODEs) are given, based on the chemical reactions from (b) and the law of mass action kinetics. In the system of ODEs, a general effector (E) replaces the specific effector adenylate cyclase (Ac) shown in (a) and (b).

A great deal of insight into how complex biological systems behave and the mechanisms by which they are regulated can be obtained through the use of mathematical models, complementing experimental investigations. Such models can be useful in helping to explain experimental observations, as well in the design of novel experiments. Additionally, detailed models of cellular regulatory networks show promise in the rational design of therapeutics and in the engineering of novel functional pathways for biotechnological applications [41, 42, 43, 44].

A number of applications of simulation to the problem of GPCR-mediated signal transduction have been described in the literature [21]. The seminal work of Bhalla and Iyengar on understanding the emergent properties of biochemical networks included a G-protein module [45]; Linderman and colleagues, as well as Bridge and co-workers, have noted the differences between kinetic and equilibrium responses, as well as the effect of certain parameters on ligand agonism [28, 29, 30, 31, 46], while Katanaev has observed variations in the dynamic system response as a result of regulatory elements [47]. In addition, a number of groups have used computational approaches to consider promiscuity in G-protein signal transduction [48, 49]. While most of these models have involved spatially-uniform systems of conserved mass, extensions to allow for receptor synthesis, degradation and internalization [50], and for spatial organization of signaling have been also been described [51, 52, 53].

An important question regarding such models is the sensitivity of predictions to variations in the model parameters, both in a quantitative and qualitative manner. Sensitivity analysis techniques are well developed for differential-equation-based models and have been applied to a number of biological signaling pathways [54, 55, 56]. Approaches to sensitivity analysis can be classified either as local methods, which focus on the sensitivity at a particular point in the parameter space, or global methods, which use sampling to study the importance of parameters globally. Here, we model the initial steps of GPCR-

mediated signal transduction using a system of ordinary differential equations based on mass-action kinetics; a systematic variation of the parameters of the model was carried out, with a particular focus on the effects of parameter variation on the dose-response of the system.

2.2 Methods

2.2.1 Model description

The system discussed here is a minimal model of a ligand-activated G-protein-coupled receptor linked to the modulation of single downstream element by the α subunit; a cartoon of the cycle of activation/deactivation and a schematic of all chemical reactions involved are shown in Figure 2.1 (panels (a) and (b)) using a stimulatory G_α coupled to adenylate cyclase (Ac) as an example. The reactions include a set of binding equilibria describing the association of ligand, receptor, and G-protein heterotrimer (denoted by steps A/B), activation and dissociation of the G-protein trimer by receptor-catalyzed nucleotide exchange (C), interaction of free G_α^{GTP} with adenylate cyclase (D), and deactivation by GTP hydrolysis and subsequent trimer re-association (E).

The reactions were all modeled according the law of mass action. Dissociation and association were treated as first- and second-order reactions, respectively. Nucleotide exchange was treated as a second-order reaction in the concentrations of GTP and either receptor–G-protein or ligand–receptor–G-protein complexes (with different rate constants), but as cellular GTP concentrations were considered to be invariant, these reactions reduce to pseudo-first order in our model; the rate constants correspond to a GTP concentration of about 200 μM. GTP hydrolysis by G_α was treated as first-order in the concentration of the G_α^{GTP} complex. These result in a system of differential equations shown in Figure 2.1(c), using E to denote a general effector such as adenylate cyclase.

Two initial sets of parameters were used: model 1 was adapted from the glutamate-

receptor model of Iyengar and colleagues [45]; and model 2 was adapted from a stimulatory G-protein pathway described by Bhalla [57]. The specific parameters for these models are listed in Table 2.1; both models are additionally described in the Database of Quantitative Cellular Signaling [58]. It should be noted that the two systems couple to different second messenger systems, with activation of phospholipase C (PLC) in model 1 and activation of adenylyl cyclase (AC) in model 2. However, as our model ends with G_α^{GTP} association with its immediate downstream target, this distinction is largely unimportant. Thus, in the following discussion G_q/PLC and G_s/AC should be considered as arbitrary G_α/effector pairs.

A brief discussion of units is worthwhile to clarify any confusion. Concentration units for cellular signaling models are often defined in terms of numbers of molecules per cell; many *in vivo* experiments characterize expression levels in this manner. However, *in vitro* experiments aimed specifically at characterizing parameters such as equilibrium binding constants and reaction rate constants tend to be cast in molar units of concentration. In order to convert between these units, an assumption of a reasonable cellular volume is typically used — given a cellular volume of 10^{-12} L, 1 μM is roughly equivalent to 6×10^5 molecules per cell. However, this only holds for components that are essentially distributed uniformly through the cytoplasmic volume; for components localized in particular sub-cellular compartments, the appropriate volume of that compartment must be known.

In the context of GPCR-mediated signal transduction an additional complication arises, as many of the components are associated with the cellular membrane. For these molecules, free molecular diffusion is limited to the two dimensional surface, and thus units of a two-dimensional density (such as moles per square meter) are more appropriate than those of molar concentration. Conversion into these units, however, requires a reasonable estimate of the cellular surface area. A perfectly spherical cell with a volume

of 10^{-12} L would have a cellular surface area of $4.8{\times}10^{-10}$ m^2, setting a lower bound on the surface area; few cells are particularly close to spherical, and thus 10^{-9} m^2 may be a reasonable estimate for a "typical" cellular area. Given this value, a cytosolic component present at a concentration of 1 μM would yield the same number of molecules per cell as a two-dimensional density of 1 nmol/m^2. These are the equivalencies that we have chosen to use. Notationally, we define 1 $M_{2D} \equiv 1$ mol/m^2 as , and thus 1 nmol/m^2 = 1 nM_{2D}

We define the measure of signal strength as the concentration of G_α^{GTP} complexed with the primary effector ($G_{\alpha q}^{GTP}$·PLC or $G_{\alpha s}^{GTP}$·AC, accordingly). The underlying presumption for this is that the total quantity of PLC or AC does not change, and thus overall enzyme activity is a monotonic function of the quantity in complex with G_α. While there are certainly non-linearities in the formation of second messengers (DAG and IP3 or cAMP), as well as in their downstream effects, we have chosen to focus this initial analysis on the first steps in signaling.

2.2.2 Starting model parameters

The reference model parameters (listed in Table 2.1) were primarily taken from the work of Bhalla and Iyengar [45, 57], and are additionally available from the Database of Quantitative Cellular Signaling (DQCS) [58]; for model 1 initial concentrations were not published, and thus these were set to the values recorded in DQCS. The published description of model 2 does not include any activity for unliganded receptor [57]; the base model for parameter variation was thus set to have an intrinsic receptor activation rate 100-fold less than the activated rate; this is consistent with the parameters of model 1.

Table 2.1: Reference Model Parameters

	Molecules per cell			Concentrations		
	Model			Model		
Parameter	**1**	**2**	**Units**[a]	**1**	**2**	**Units**[a]
k1: L+R→LR	28	0.167	$(\mathrm{M}\#)^{-1}/\mathrm{s}$	16.8	0.1	$\mu\mathrm{M}^{-1}/\mathrm{s}$
k2: L+R←LR	10	0.1	/s	10	0.1	/s
k3: LR+G→LRG	0.01	16.7	$(\mathrm{M}\#)^{-1}/\mathrm{s}$	0.006	10	$(\mathrm{nM}_{2D})^{-1}/\mathrm{s}$
k4: LR+G←LRG	0.1	100	/ks	0.1	100	/ks
k5: R+G→RG	1.0	0.33	$(\mathrm{M}\#)^{-1}/\mathrm{s}$	0.6	0.2	$(\mathrm{nM}_{2D})^{-1}/\mathrm{s}$
k6: R+G←RG	1.0	0.1	/s	1.0	0.1	/s
k7: L+RG→LRG	28	8.33	$(\mathrm{M}\#)^{-1}/\mathrm{s}$	16.8	5.0	$\mu\mathrm{M}^{-1}/\mathrm{s}$
k8: L+RG←LRG	0.1	0.1	/s	0.1	0.1	/s
[b]k9: $\mathrm{RG}\rightarrow\mathrm{R}+\mathrm{G}_{\alpha}^{\mathrm{GTP}}+\mathrm{G}_{\beta\gamma}$	0.1	0.25	/ks	0.1	0.25	/ks
k10: $\mathrm{LRG}\rightarrow\mathrm{LR}+\mathrm{G}_{\alpha}^{\mathrm{GTP}}+\mathrm{G}_{\beta\gamma}$	10	25	/ks	10	25	/ks
k11: $\mathrm{G}_{\alpha}^{\mathrm{GTP}}\rightarrow\mathrm{G}_{\alpha}^{GDP}$	13.3	66.7	/ks	13.3	66.7	/ks
k12: $\mathrm{G}_{\alpha}^{GDP}+\mathrm{G}_{\beta\gamma}\rightarrow\mathrm{G}$	10	10	$(\mathrm{M}\#)^{-1}/\mathrm{s}$	6.0	6.0	$(\mathrm{nM}_{2D})^{-1}/\mathrm{s}$
k13: $\mathrm{G}_{\alpha}^{\mathrm{GTP}}+\mathrm{E}\rightarrow\mathrm{G}_{\alpha}^{\mathrm{GTP}}\mathrm{E}$	4.2	833	$(\mathrm{M}\#)^{-1}/\mathrm{s}$	2.52	500	$(\mathrm{nM}_{2D})^{-1}/\mathrm{s}$
k14: $\mathrm{G}_{\alpha}^{\mathrm{GTP}}+\mathrm{E}\leftarrow\mathrm{G}_{\alpha}^{\mathrm{GTP}}\mathrm{E}$	1.0	1.0	/s	1.0	1.0	/s
R_0: Total Receptor	180	50	k#	0.3	0.083	$\mathrm{nmol/m}^2$
G_0: Total G-protein	600	600	k#	1.0	1.0	$\mathrm{nmol/m}^2$
E_0: Total Effector[b]	480	9	k#	0.8	0.015	$\mathrm{nmol/m}^2$

[a] # indicates number of molecules per cell, and the two-dimensional density units are defined as 1 M_{2D}=1 $\mathrm{mol/m}^2$.; [b] Effector is phospholipase C (PLC) for model 1, and adenylyl cyclase (AC) for model 2.

2.2.3 Simulation methodology

The system of ordinary differential equations described above were integrated using Matlab v.7.1.0 (Mathworks, Natick, MA). As varying the model parameters can significantly alter the dynamic behavior of the system, numerical integration algorithms differ in efficiency and accuracy for different systems. Systems were primarily solved using the ode15s and ode23s solvers with default options; in the vast majority of cases, these gave results that were identical within machine precision. If one solver failed to generate a stable solution, other solvers were used and/or the thresholds of the absolute and relative tolerances were adjusted to achieve stable behavior. In all of these cases, consistency between at least two methods was ensured.

For each set of parameters, the system was pre-equilibrated by setting the unbound

G-protein, GPCR and effector (AC or PLC) concentrations equal to the total species concentration, then integrating the dynamics of the system until a converged, steady-state solution was reached. These steady-state concentrations were then used in a second simulation where a given concentration of free ligand was also included in the initial conditions; again, these systems were simulated to convergence. Convergence was assessed by considering the derivative of the response with respect to time at the end of the simulation, as well as by comparison of the response at simulation times of 10^5 and 10^8 s; see Appendix Table A1 for more details.

Parameter variation consisted of multiplying a given rate or pair of rates in each model by a scaling factor, α. α was sampled evenly in the logarithmic domain, with 10 points per log-unit (this was reduced to about 3 points per unit for visibility in the figures).

2.3 Results & Discussion

2.3.1 Dose response of two models

Computer simulations (involving integration of a system of biochemical kinetic equations over time) were performed to generate the dose response curves for two previously-published models of G-protein-coupled receptor (GPCR) activation. Given a set of initial concentrations, the system was first equilibrated in the absence of ligand to mimic a pre-existing biological system; in this stage, resting-state concentrations of free receptor and receptor–G-protein complex are formed. Following pre-equilibration, the total concentration of ligand was stepped from zero to a particular value, and the the system again allowed to reach equilibrium. The equilibrium concentration of $G_s^{GTP}{\cdot}AC$ following ligand addition was then taken as the response for the given input ligand concentration. This procedure was repeated for a range of ligand concentrations from 0.1 pM to 10 M, thus covering all possible biologically-relevant values.

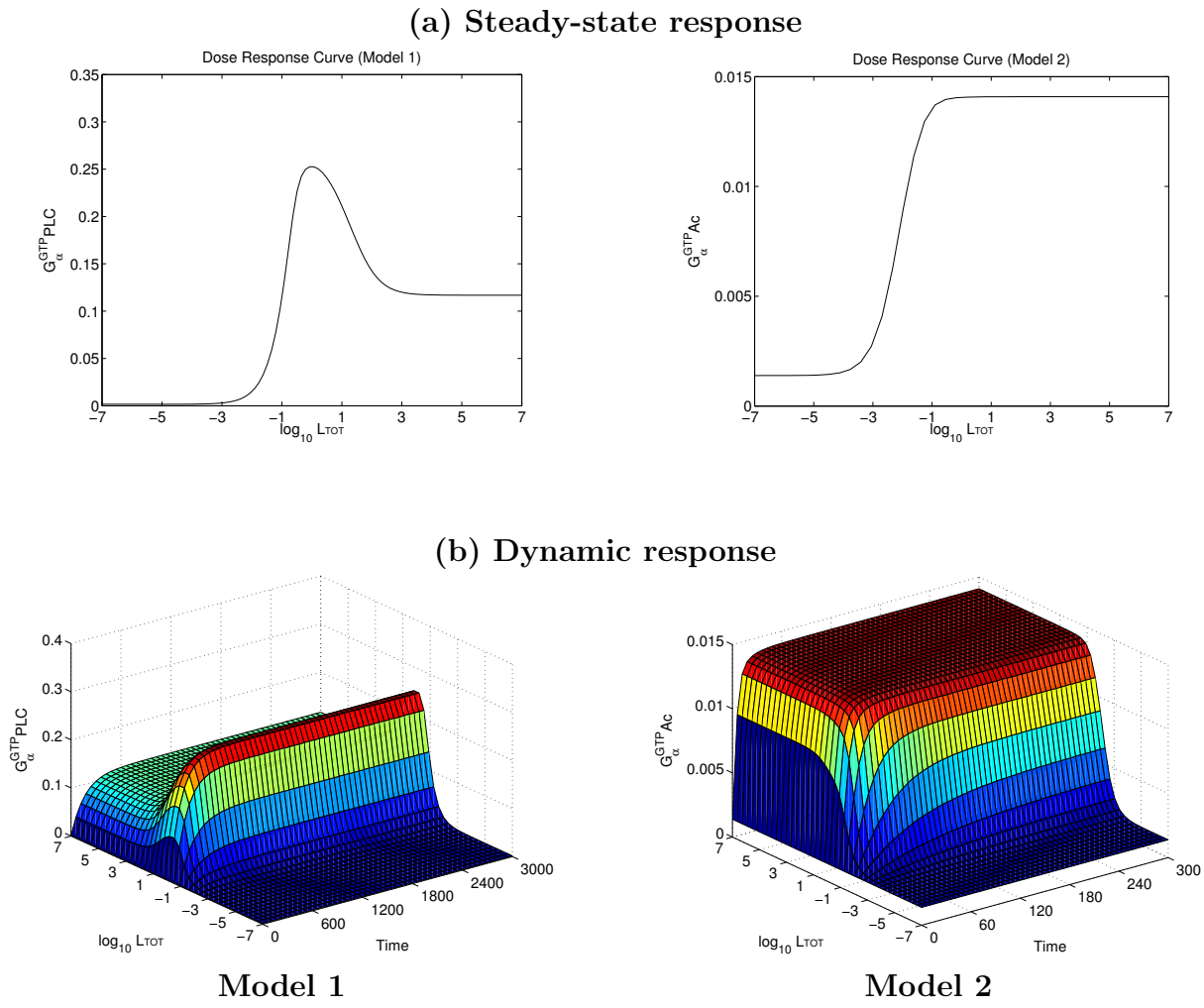

Figure 2.2: **Dose response of base models.** The equilibrium concentration of G_α^{GTP}·E is plotted as a function of added ligand concentration (L_{TOT}). Model 1 is shown on the left and model 2 on the right.

The results for each of the two models are shown in Figure 2.2; the dynamic variation of all components of the system can be found in Appendix. Pre-equilibration results in a low level of activity as a result of the constitutive activity of the receptor, described by a non-zero rate of nucleotide exchange by the receptor–G-protein complex in absence of ligand. This activity was not present in the published parameters of model 2, but was added (with the rate of unliganded-receptor activation of the G-protein set to 100-fold less than the ligand-activated rate) for consistency with model 1. With this modification,

both models reach similar basal levels of activity (of about 1.5 pmol/m^2, or 1000 molecules per cell of G_α complexed to effector).

In both cases, addition of ligand results in a monotonic increase in response over time, leveling off to a constant equilibrium value, at all input ligand concentrations (Figure 2.2(b)). At ligand doses giving maximal response, the time scale of reaching steady state is longer in model 1 (by roughly 20-fold) but the equilibrium value is larger by a similar factor; both systems reach the activity level of model 2 on roughly the same time scale. These differences can easily be understood in the context of total effector concentration, which is slightly less than 50-fold higher in model 1 than in model 2. While both models are qualitatively similar in their dynamic response at a single ligand concentration, the dose-response curves of the two are dramatically different. In particular, while model 2 exhibits a sigmoidal dose response (on a logarithmic dose scale), model 1 exhibits a peaked dose response; that is, the system response reaches a maximal value at moderate ligand concentrations, and falls to lower values both at low and high concentrations of ligand. Naïve intuition about how signaling systems might be expected to work would suggest the behavior seen in model 2, and thus understanding the origins of the behavior in model 1 is of great interest.

2.3.2 Systematic variation of parameters

To answer the question of why the two dose-response curves have different behaviors, a systematic variation of the parameters of each model was carried out. This sensitivity analysis was geared towards understanding the degree to which each system parameter affects the system response, both qualitatively and quantitatively. For each parameter, a scaling factor, α, was applied; α was sampled uniformly in the log-domain, with a range of $\alpha \in [10^{-6}, 10^{6}]$.

The binding reactions between the ligand, receptor, and G-protein form a square of

reactions on the left-hand side of the schematic in Figure 2.1(b); the rates along each side of the square (k1 to k8) were first varied as pairs, with both association and dissociation rates scaled equally. This variation does not change the equilibrium binding constants (the relative energies of each complex are unchanged) but rather affects the rate at which equilibrium would be achieved in an isolated system. Additionally, variations of pairs of these rates that change the equilibrium binding constants were also considered; variations were chosen such that the equilibrium constant of the first reaction increases with increasing α, while the second is adjusted to preserve thermodynamic consistency within the binding cycle. When rates of two reactions that connect to the same corner of the binding square are varied, the variation can be considered as a perturbation of the stability of the corresponding state. When rates of reactions on opposing sides of the binding square are varied, the change can be interpreted as an adjustment of the stability of the two states on one side relative to the other.

The rates for G-protein activation, either by free receptor (k9) or ligand-receptor complex (k10) were varied individually. The rates for GTP hydrolysis (k11) and the subsequent re-association of the G-protein heterotrimer (k12) were also varied individually. Changes to the rates of association and dissociation of the G_{α}^{GTP}·E complex (k13/k14) were done in a coupled manner so as not to change the equilibrium binding constant, as was done initially for binding equilibria involving the ligand, receptor and G-protein heterotrimer. Finally, the effects of changing the total concentrations of receptor, G-protein and effector were also considered.

Surfaces showing the dose-response across all parameter variations (see Appendix, Figures A5–A11), show that most parameters had effects that are quite easily described. Overall, several possible effects were identified. First, some parameters led to no (or very low) signal response at low values; these may be described as "required for signal". Secondly, some variations led to changes in signal response in at least one of three regimes:

the basal (low ligand) state, the high ligand concentration state, and/or the maximal response; only parameters that affect the high ligand signal level independently of the maximal response can switch the system from a sigmoidal to a peaked response. Finally, variation of certain parameters was able to modulate the ligand concentration at which the onset of signaling occurs and/or (in the case of a peaked response) the concentration at which the response drops off.

Table 2.2 provides a summary of the behaviors each parameter was seen to be associated with. A number of parameters were involved only in modulating the basal signal level, or the sole effect of their variation was a lack of response at very low rates; these variations are not discussed further. Other parameters were seen to have more complex effects, including modulating the existence of a peaked response, the width of such a peak, or allowing for any response only over a fairly narrow window of parameter values; each of these variations is considered in more detail in the following sections.

2.3.3 Control of peaked or sigmoidal dose response

In a very striking result, we found the rate constants of the binding of the G-protein heterotrimer to a preformed ligand–receptor complex (k3/k4) to play a critical in controlling the behavior of the dose-response curve (Figure 2.3). In Figure 2.3 (and in subsequent figures for other parameter variations), the parameter scaling factor, α,is plotted on the left-hand axis, the total ligand concentration on the right-hand axis, and the equilibrium system response (G_α^{GTP}·PLC or G_α^{GTP}·Ac level) on the vertical axis; thus, individual traces followed from left to right along the ligand concentration axis correspond to dose-response curves for a particular scaling.

In both models, simultaneous variation of k3 and k4 leads to profound differences in the qualitative system response, promoting a transition between a sigmoidal and peaked dose-response curve. Both models are affected by the parameters in a very similar way,

Table 2.2: Observed effects of parameter variation.[a]

Values Varied	**Required**[b]	**Basal Signal**	**Maximal Signal**	**High [L] Signal**	**Onset [L]**	**Offset [L]**
Concentrations of key species						
R[c]	+	+			+	
G[c]	+	+				
E[c]	+	+				
Binding-square perturbations that do not affect equilibrium constants						
k1/k2			+			
k3/k4				+		
k5/k6		+	+			+
k7/k8			+			
Stability of the ligand–receptor complex						
k1/k3[c]	+					
k2/k4	+					+
Stability of the ligand–receptor–G-protein complex						
k7/k3[c]	+					
k8/k4	+					
Stability of the uncomplexed state						
k1/k5		+	+		+	
k2/k6		+	+		+	+
Stability of the (unliganded) receptor–G-protein complex						
k5/k7		+	+		+	+
k6/k8		+	+		+	
Stability of G-protein-bound states						
k1/k7					+	+
k2/k8			+		+	+
Stability of ligand-bound states						
k5/k3[c]	+	+				
k6/k4	+	+				
G-protein activation rates						
k9		+				
k10	+					
Post-activation processes						
k11[c]	+					
k12	+					
k13/k14[d]	+					

[a] A '+' sign indicates that variation of the parameters listed in a given row was observed to have an effect on the property listed for a given column over the range considered (a twelve order of magnitude range centered on the base parameters); an effect was not necessarily observed with both base models. [b] "Required" indicates that low parameter values eliminated a ligand-induced signal response. [c] These parameters were additionally seen to have a small range over which more complex variations were observed. [d] These rates have no effect at steady-state, but can have a strong effect on how quickly steady-state is reached; a minimal value is needed for steady-state to be accessible on a reasonable time scale.

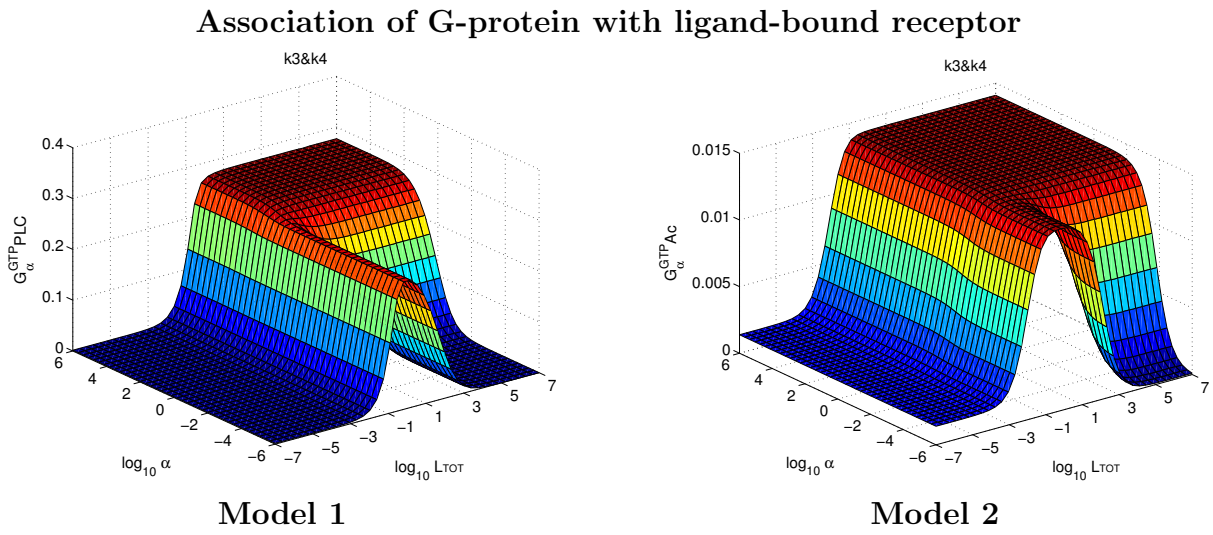

Model 1 **Model 2**

Figure 2.3: **Control of peaked or sigmoidal dose response.** The equilibrium concentration of G_α^{GTP}·E is plotted as a function of both added ligand concentration (L_{TOT}) and the parameter scaling factor (α); the on and off rates for G-protein association with ligand-bound (k3 and k4) receptor were simultaneously multiplied by α, preserving the equilibrium binding constant. Low rates result in a peaked response (and high rates a sigmoidal response) for both models.

with a sigmoidal response seen with fast rates and a peaked response observed when the reaction rates are slowed. There is a very slight drop in the maximal response that is coupled to the shift from a sigmoidal to the peaked response; this is somewhat greater for model 1, but measurable in both cases. In the regime of a peaked response, the activation at high ligand concentration is near zero, and is, in fact, below the basal response with no ligand present. Transitions from peaked response to sigmoid response were also observed with the variation of other parameters in model 1, but no other perturbation induced a peaked dose response in model 2.

2.3.4 Control of dose-response peak width

In model 1, where a peaked dose response is observed, the width of the peak is further shown to be controllable by other rates within the binding square of ligand, receptor and G-protein (Figure 2.4).

k5 and k6 describe the rates of the binding reaction between (unliganded) receptor and the G-protein heterotrimer; these were varied together so as not to affect the equilibrium binding constant of this reaction (Figure 2.4(a)). In the context of model 1, there is a transition from a moderate-strength sigmoidal dose-response curve to one that shows peaked behavior (but with a moderate response at high ligand concentrations) as the reaction rates become faster. More significantly, increasing k5 and k6 leads to an increase in the concentration at which the fall-off in system response occurs; the concentration at which the peak first rises is unchanged, as is the magnitude of the response, and thus this results simply in a widening of the response peak with this rate. In model 2, the only effect is on the response at low ligand concentration — as the rate constants are reduced by roughly a thousand-fold, a shift is observed from a low, but measurable, level of intrinsic activity to essentially no basal activity. Neither the maximal response nor the consistently sigmoidal shape of the response curve is affected .

A similar effect was observed with variation of k2 (the dissociation rate of the ligand–receptor complex) and k4 (the rate of dissociation of the ligand–receptor dimer from the ternary ligand–receptor–G-protein complex). In Figure 2.4(b), k2 is divided by α while k4 is multiplied by the same amount. The result is an increase in the equilibrium constant for the binding of ligand and receptor with increasing α, coupled with a corresponding decrease in the equilibrium constant for association of the ligand–receptor complex with G-protein; thus, this perturbation can be considered a variation in the stability of the ligand–receptor complex (uncoupled to G-protein, the lower-left corner of the binding square), where the stability is high for a large α and low for a small α.

With model 1, no response is seen when the ligand-receptor complex is extremely stable, while a peaked response is seen throughout the lower-stability regime. Again the ligand concentration for signal onset is unperturbed by variation of these rates, but the offset concentration increases as α decreases; a widening of the response peak is thus

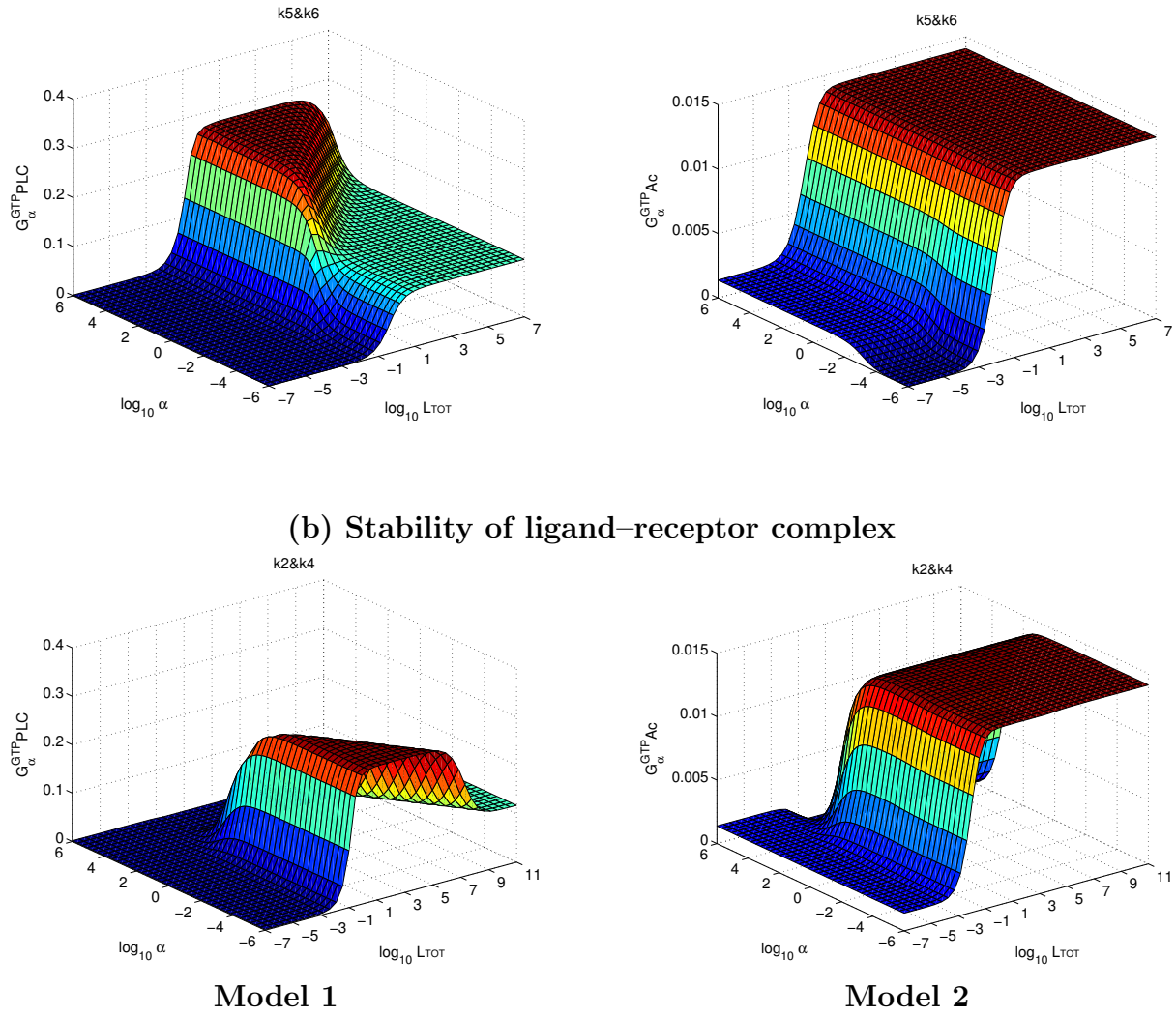

Figure 2.4: **Control of dose-response peak width.** The equilibrium concentration of G_α^{GTP}·E is plotted as a function of both added ligand concentration (L_{TOT}) and the parameter scaling factor (α). **(a)** The on and off rates for G-protein association with unliganded receptor (k5 and k6) were simultaneously multiplied by α, preserving the equilibrium binding constant. Increasing the rates results in an increase in peak width. **(b)** The rate of ligand dissociation from the ligand–receptor complex (k2) was divided by α, while the rate of ligand–receptor dissociation from the ternary ligand–receptor–G-protein complex (k4) was multiplied by α. Decreasing α (corresponding to a decrease in the stability of ligand–receptor complex) results in an increase in peak width.

seen as the stability of the ligand–receptor complex is decreased. For model 2, reducing the stability of this state has no effect on the response; neither the maximal response nor the transition midpoint vary. At very high stabilities, a shift to an inverse-sigmoidal

response is seen, albeit with very low magnitude; the low ligand-concentration response is unaffected by these variations, while the high-concentration response drops to near zero.

2.3.5 Signaling observed only over restricted parameter range.

Some parameters are shown to have a qualitatively different impact on signaling, with a differential response occurring only over a relatively small range of parameter values. One of these is the rate at which G_α is able to hydrolyze bound GTP, while another is the total effector density; both are highlighted in Figure 2.5.

When the GTP hydrolysis rate (k11) is low, the response remains high even at low (or zero) input ligand concentrations, while at high hydrolysis rates, the response is uniformly zero (Figure 2.5(a)). The switch from low to high basal (low ligand concentration) activity occurs at slightly higher hydrolysis rate than does the switch from low to high stimulated (high ligand concentration) activity, and it is only in between these values that a ligand-dependent dose response is seen. The total concentration of effector has a similar impact — both models give uniformly high responses at high protein levels and no response at low levels (Figure 2.5(b)). Again, the transition from low to high output occurs at slightly different concentrations under basal and ligand-stimulated conditions, and thus differential signal is observed over this small range of concentrations. In both cases, model 1 generally gives a peaked response over the active range, although as a uniform high response is approached, the difference between the peak and high ligand-concentration responses becomes negligible. Conversely, model 2 displays a sigmoidal response throughout the transition regime.

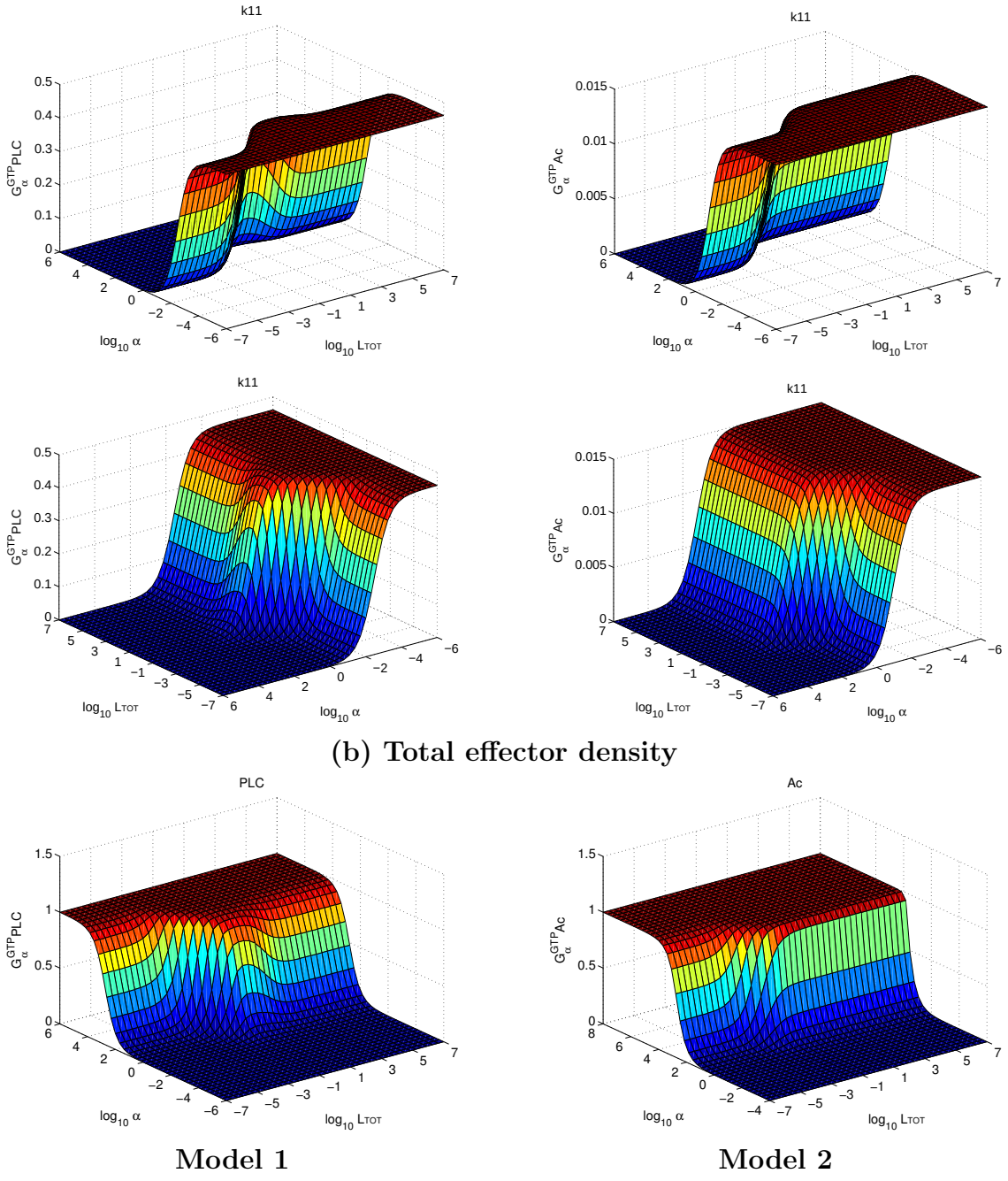

Figure 2.5: **Signaling observed only over restricted parameter range.** The equilibrium concentration of G_α^{GTP}·E is plotted as a function of both added ligand concentration (L_{TOT}) and the parameter scaling factor (α). **(a)** k11 describes the GTP hydrolysis rate, and model 1 is shown on the left and model 2 on the right. The second row contains the same data as the first, but is rotated 90° for clarity. **(b)** The total concentration of effector was varied by multiplying α. Here, the range of α was adjusted so that the minimum corresponds to roughly 1 molecule per cell. In both cases, signaling is only observed in a small range of the parameters.

2.3.6 Dynamics of peaked dose-response

In order to help understand the origins of the peaked dose response, we additionally considered the dynamics of the signal response under with variations in k3 and k4 (the rate constants of the binding of the G-protein heterotrimer to a preformed ligand–receptor complex), which were shown in Figure 2.3 to be the primary determinants of this response.

As the major effect of this variation was on the response at high ligand concentrations, we first considered the time evolution of the signal upon addition of a high (1 mM) dose of ligand (Figure 2.6(a)). In both models, under conditions results in a sigmoidal dose response (a high response at high ligand concentrations) the signal increases monotonically with time towards the steady-state value, while under conditions that yield a peaked (steady-state) dose response the signal peaks early then decays towards zero with increasing time. In both cases, this early peak is of lower magnitude than the maximal signal seen under sigmoidal response conditions, but only slightly so for model 2. For model 1, where the maximal signal is more than an order of magnitude larger than that of model 2, the difference is much more pronounced.

We next considered the time-dependent dose-response curves of variants of both model 1 and 2 with pronounced peaked behavior (k3 and k4 both scaled by 10^{-6}, Figure 2.6(b)). Again both models behave qualitatively the same; for moderate ligand concentrations (*i.e* the peak of the steady-state response) the signal increases monotonically towards steady-state, while for high ligand concentrations, the signal again displays an early peak followed by decay towards zero. When the dynamics display such a peak its magnitude is the same as that seen in Figure 2.6(a).

(a) Time-dependent responses at high ligand concentration.

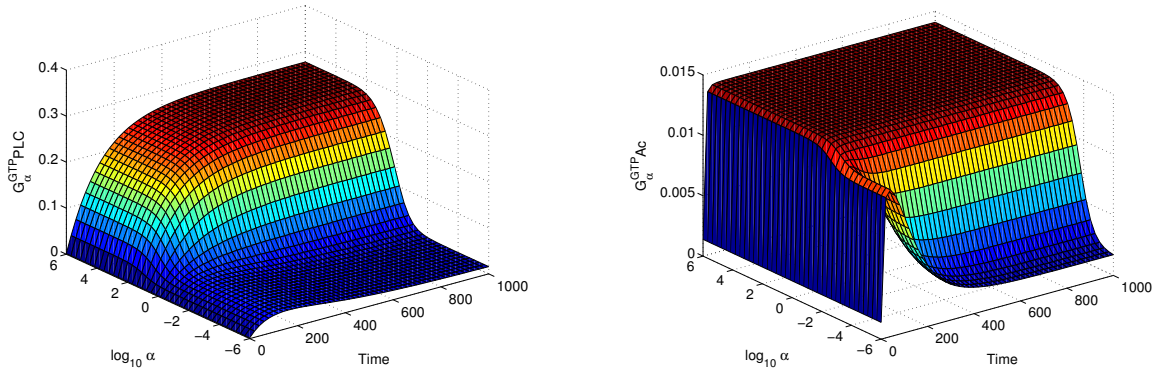

(b) Time-dependent dose response in peaked regime.

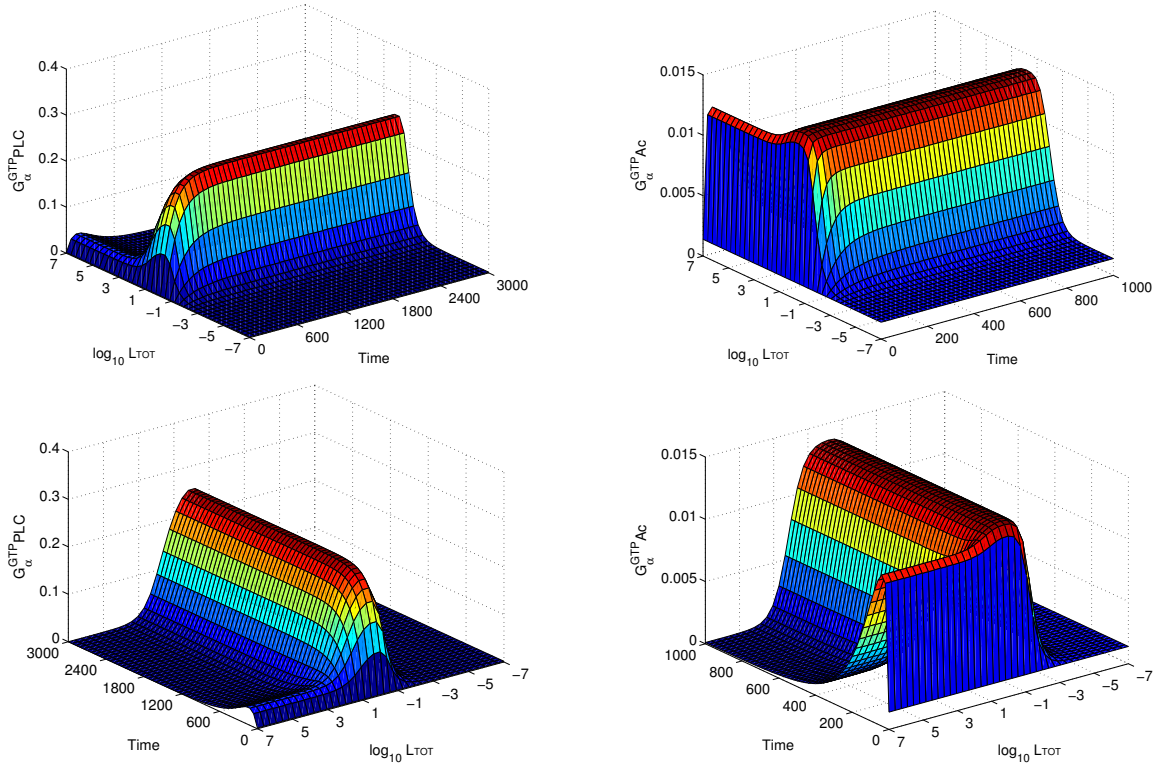

Model 1 **Model 2**

Figure 2.6: **Dynamic variations underlying peaked steady-state response.** The time-dependence of the concentration of $G_\alpha^{GTP}{\cdot}E$ is plotted as a function of either the scaling factor for k3 and k4 or ligand concentration. **(a)** The on and off rates for G-protein association with ligand-bound (k3 and k4) receptor were simultaneously multiplied by α, preserving the equilibrium binding constant, and a ligand concentration of 1 mM was applied to the system. **(b)** Using either model 1 or 2 with both k3 and k4 scaled by 10^{-6}, input ligand dose was varied. The second row contains the same data as the first, but is rotated 90° for clarity.

2.3.7 Discussion

In the absence of ligand, the equilibrium state of both base models has the majority of receptors associated with inactive G-protein trimers; a small level of G_α^{GTP} bound to effector (AC or PLC) results from intrinsic receptor activity. Upon initial exposure of the system to ligand, these pre-associated complexes are stimulated, yielding a sharp rise in $G_\alpha^{GTP}{\cdot}E$ levels. Prolonged stimulation lowers the concentration of inactive G-protein trimers which acts in conjunction with elevated ligand concentrations to cause a redistribution of receptor states; a steady-state response is then achieved. The magnitude of this steady-state response is affected by many factors, including the total concentrations of the species involved, the fundamental activation rates of the G-protein and the G_α-effector binding constant, as well as on more subtle factors, such as the details of how deactivated G_α is recycled for re-activation.

The primary determinant of a peaked steady-state response is the rate at which preformed ligand–receptor dimers complex with inactive G-protein heterotrimers (to form the ternary complex). When the rate of association is low (even if the corresponding rate of dissociation is equally reduced), a peaked response is observed, and when the rate is high a sigmoidal response is seen. For any signal above the basal level, the ternary ligand-receptor-G-protein complex must be formed; this can happen either by the binding of a G-protein to a preformed ligand–receptor complex or by the binding of ligand to a preformed receptor–G-protein complex. At high ligand concentrations, the receptor will be saturated, existing almost exclusively in a ligand-bound state. For prolonged stimulation of a response, free G-protein (recycled from activation of the effector) must thus bind to the ligand–receptor complex, and if this rate is low, prolonged signal strength is dramatically reduced. At more moderate ligand concentrations, however, there is a balance of both free and ligand-bound receptors, and thus free G-protein can be reactivated through a pathway that involves initial binding to an unliganded receptor which

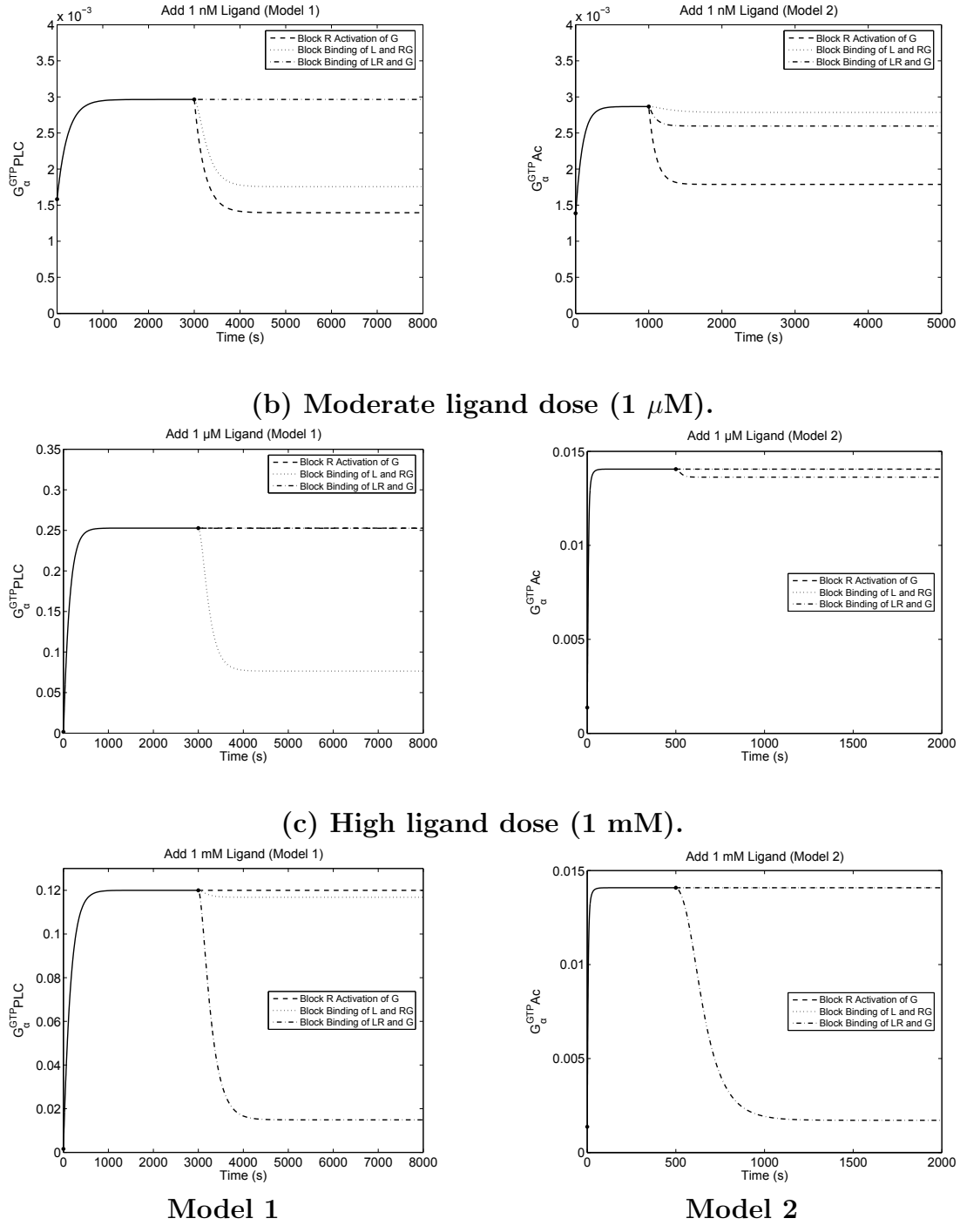

Figure 2.7: **Formation of peaked response.** Each model system was allowed to reach equilibrium (solid line), followed by individual inhibition of either: (i) activation of G-protein by unliganded receptor (dashed); (ii) binding of ligand to preformed receptor–G-protein complex (dotted); or (iii) binding of G-protein to preformed ligand–receptor complex (dash dotted).

is subsequently activated by ligand.

The effect of these pathways can be directly assessed by an experiment in which the system is allowed to reach steady state, following which a single path is blocked. How the system responds to this perturbation provides direct evidence of the role of that path in formation of the signal. The result of such a perturbation is illustrated in Figure 2.7 where the binding of ligand to the receptor–G-protein, the binding of G-protein to the ligand–receptor complex, as well as the intrinsic receptor activation were individually blocked. Blocking association of the G-protein with ligand–receptor complex leads to a dramatic reduction in signal level under high ligand-concentration for both models; blocking the alternative route under the same conditions has no effect, supporting the importance of the $\mathrm{LR} + \mathrm{G} \rightarrow \mathrm{LRG}$ route to the ternary complex under high-ligand conditions. Under moderate ligand concentrations, blocking association of the G-protein with ligand–receptor complex has negligible effect on either model, while blocking association of ligand with the receptor–G-protein complex leads to a reduction in response only for model 1. This suggests that in model 1, the alternative route dominates under moderate ligand concentrations, although since the residual activity is well above basal, the $\mathrm{LR} + \mathrm{G} \rightarrow \mathrm{LRG}$ route is still accessible. In model 2, neither route is essential, suggesting that the flux through either route is at or above another rate limiting step. Under low ligand conditions, where stimulated activity is less than two-fold above basal levels, the conclusions for moderate ligand concentrations are recapitulated, although the effects of blocking either route to the LRG trimer are less significant than blocking the ability of unligand-bound receptor to activate the G-protein.

When the rate of ligand–receptor dissociation is increased and the rate of ligand–receptor–G-protein dissociation is decreased (corresponding to a destabilization of the ligand–receptor state), the ligand concentration at which the receptor approaches saturation increases. Correspondingly, the concentration at which the signal drops in a peaked

response shifts to a higher value (see Figure 2.4(b)). As signaling at low and moderate ligand concentrations is dominated by the alternate route to the ternary complex, the onset concentration is unaffected.

Similarly, as the rate of association of the G-protein with unliganded receptor increases (even when balanced with an increase in the dissociation rate of the complex), lower concentrations of free receptor are needed to give the same flux through the alternate path. Again, this results in an upwards shift of the offset concentration for the peaked response, as seen in Figure 2.4(a). The onset concentration is unaffected by this variation, as it is a primarily a function of the binding affinity of receptor for the ligand.

Most parameter variations had limited impact on the overall system response over very large ranges of parameters; a transition between two types of general behavior may be seen, but each types is stable over several orders of magnitude of variation. This suggests that, in general, these systems are robust to perturbation, which is a hallmark of many biological networks [41, 59, 60].

However, the system was seen to be quite sensitive to a small number of parameters. For example, in both models considered, no signaling was observed unless the rate constant for GTP hydrolysis by G_α was held within regime spanning only two orders of magnitude; GTPase activity below this regime gives uniform (ligand-independent) high levels of output while high GTPase activity leads to no output under any conditions. Both of these behaviors make sense, as an overly active GTPase would result in deactivation of the G_α before association with effector, while an under active enzyme would lose the ability to reset system to an inactive state.

A similar effect is seen with effector density, with high levels resulting in a constitutively active system and low levels losing the ability to signal. It is certainly reasonable that a minimal concentration of effector is needed for a response, but the saturation of the system by overexpression of effector is somewhat less intuitive. When effector is

present in excess, the equilibrium of G_α^{GTP}–effector binding will shift towards the complexed state, which is our measure of output. However, this should be limited by the overall amount of G_α^{GTP} present, which one might expect to be ligand-dose dependent. This discrepancy originates in the effect of effector binding on the GTPase activity of G_α; in the models considered here, G_α is active as a GTPase only in the unbound state (indicating that the effector acts as a potent inhibitor of the enzymatic activity). As a result, a shift towards increased formation of the active complex additionally reduces the rate at which G_α^{GTP} is returned to the inactive (GDP-bound) state. While this choice was made based on the published details of the two models we started with, the biological relevance of this is less clear; as a counter example, phospholipase C-β1 has long been known to enhance the GTPase activity of G_αq [61].

Over the past decade, there has been a increasing interest in the development of quantitatively predictive models of the biochemical systems involved in cellular signaling and regulation. However, detailed experimental data can not feasibly be obtained for all possible biological systems, and thus the ability to transfer results between related systems is essential. While it is easy to understand that some quantitative details can be lost in such a transfer, it is less intuitive that the fundamental qualitative response of a system may change with relative small changes in the system details. However, that is precisely what we have observed here. These results indicate a need to take particular care in the transfer of quantitative measurements between systems, even when those systems seem closely related. Additionally, one must be especially careful in the estimation of values that can not easy be directly measured. Another issue relating to the effect of varying concentrations of different components is the interpretation of experiments involving the over-expression of a particular G-protein or GPCR. Variation of these concentrations can have dramatic effects on the system response, with high concentrations of either component uniformly resulting in a sigmoidal dose-response curve.

Additionally, the results presented here may have interesting ramifications for the emerging field of synthetic biology. When engineering novel biochemical networks, a common approach is to consider a set of functional modules, or network motifs, each with specific properties. If one thinks of the network described here as a module for the initial response of a signaling cascade, we must keep in mind the non-trivial result that quantitative variations to the module can lead to qualitative variations in system output. As some of the parameters (such as cellular concentrations of different species) may not be directly controllable, understanding these variations is essential to assessing the robustness of an engineered network. However, while this diversity of response adds challenges to synthetic biology, it also may open up new opportunities as well. For example, a peaked dose-response provides a very different set of signal processing capabilities than does a sigmoidal response, yielding an output only over a finite range of input amplitudes; the width of this band seems to be tunable as well. While the ability to engineer modules with a specific set of parameters is beyond the current state of the art in molecular engineering, it is entirely possible that a set of diverse modules may be identified from various natural networks.

2.4 Conclusions

We have shown that qualitatively different signaling patterns can result in the initial steps of G-protein signaling, solely due to quantitative variation of the model parameters. Most notably, we have characterized a switch between a sigmoidal and peaked dose response that can be tuned with the variation in the kinetics of a single binding equilibrium step. The width of this transition is additionally tunable by an additional pair of kinetic parameters.

These results are not meant to directly describe a specific biological system, but rather provide an important guide for the interpretation of both experimental and computational

results. In particular, the profound differences we observe raise significant concerns about the transferability of observations from one system to a related system. Additionally, the results may have interesting future applicability to the engineering of novel signaling pathways.

Chapter 3

Modeling Nonspecific Interactions between Two Signaling Pathways

3.1 Introduction

G-protein-coupled receptors form the largest family of membrane receptors and play an essential role in cellular sensing. The spectrum of ligands that they can detect ranges from natural endogenous molecules such as hormones and neurotransmitters to pharmaceutical drugs treating various diseases[62][63]. A map of interactions between GPCRs and their ligands is provided in the GPCR-Ligand Database (GLINDA) [64]. As recorded in the database, interactions between ligands and GPCRs are mostly not exclusive. For example, dopamine receptors expressed in human cells can interact with hundreds of other ligands besides its natural ligand dopamine, while dopamine can as well bind with other receptors such as the β-adrenergic receptor. As a consequence, GPCR signaling pathways may interact with each other from the very beginning of the signaling processes. The interactions between GPCRs and G-proteins are also not exclusive. Many receptors have the ability to signal through multiple G-proteins. For example, cannabinoid receptor can interact with both Gs and Gi to regulate the intracellular cAMP level [65]. On the other hand, it is even more common for multiple receptors to signal trough the same G-protein due to the relatively small number of G-proteins [15]. Because of such interconnectivity, the activation of one pathway may regulate other pathways in a cell expressing multiple GPCRs or G-proteins.

Models containing more than one ligand, receptor or G-protein have been described in several studies with different focuses. Chen et. al. built a model in which a receptor has 3 active states and each couples to a distinct G-protein, then studied the effect

of pathway-dependent ligand potency and efficacy [51]. Patrick et. al. developed a Bayesian approach for estimating parameters and applied it to a model containing C5a receptor activating Gi protein and P2Y6 receptor activating Gq protein [49]. Bridge et al. presented a model containing two ligands and examined the effect of their competition for the same receptor [46]. Asymptotic analysis was also carried out to measure the importance of parameters in different time scales. Although all models can be considered as multiple pathways with interactions to some extent, none of them systemically studied the effect of such interactions on the signaling processes.

Despite the fact that signaling pathways are often connected to each other, specificity from the signaling cue to responses can still be maintained. For example, the pheromone pathway, filamentous growth pathway and osmolarity glycerol pathway in yeast share the components of the MAPK signaling pathway, but respond to their own stimulus independently. A framework to analyze specificity in a signaling network was developed by Komarova et. al. Several following studies applied this concept to measure the specificity in MAPK signaling network or to examine possible mechanisms to maintain specificity [66][67][68][69].

In this chapter, we have expanded the basic model to include two signaling pathways and studied the effect of interactions on signaling. First, we defined 6 basic interactions and used 3-D dose response surfaces to provide a direct illustration of signal levels activated at combinations of ligand concentrations for these interactions. The metrics for specificity proposed by Komarova et. al. [70] were adapted and specificity scores were calculated for steady state responses. For each type of interactions, relative changes in signal level, changes in shape similarity and the specificity of signaling were measured at various strengths of interactions. The presence of the ligand from the other pathway was also considered. Then, shape similarity and specificity were calculated for all combinations of the 6 basic interactions. Finally, the effect of the concentration of receptor on

signaling specificity was also examined.

3.2 Methods

3.2.1 Defining Interactions

A model describing two signaling pathways was built and different types of interactions were considered. Each pathway was modeled in the same way as we did previously for the single pathway. For simplicity, we named them Pathway 1 and Pathway 2, and used Signal 1 and Signal 2 to refer the signals of the two pathways in the rest of the thesis. L1, R1, G1 and E1 were used to represent the ligand, receptor, G-protein and effector in Pathway 1, and correspondingly, L2, R2, G2, E2 were used for the ones in Pathway 2. Interactions within the same pathway are considered as specific, while interactions between two molecules from different pathways are considered as nonspecific. A full model containing all possible interactions between ligand, receptor and G-protein was built and a scaling factor was added to control the forward rate constants of all nonspecific interactions. The initial rate constants for the nonspecific bindings were adapted from the specific bindings involving the same receptor. For example, the parameters for the binding of L1 and R1 were used initially for the binding of L2 and R1. When the scaling factor is 0, the two pathways do not interact with each other and behave independently as the previous single pathway. We started from 6 basic interactions and named them based on the new pathway generated due to the nonspecific interactions between ligand and receptor or between receptor and G-protein (Figure 3.1). There are 6 of them: L1R1G2E2, L1R2G1E1, L1R2G2E2, L2R1G1E1, L2R1G2E2, and L2R2G1E1. For the nonspecific interactions between the two pathways, if two molecules can bind with each other, all forms of the two molecules were considered to interact with each other. For example, in the systems containing nonspecific interaction between R1 and G2, L1R1 was also considered to be able to bind with G2. Both the rates are controlled by the

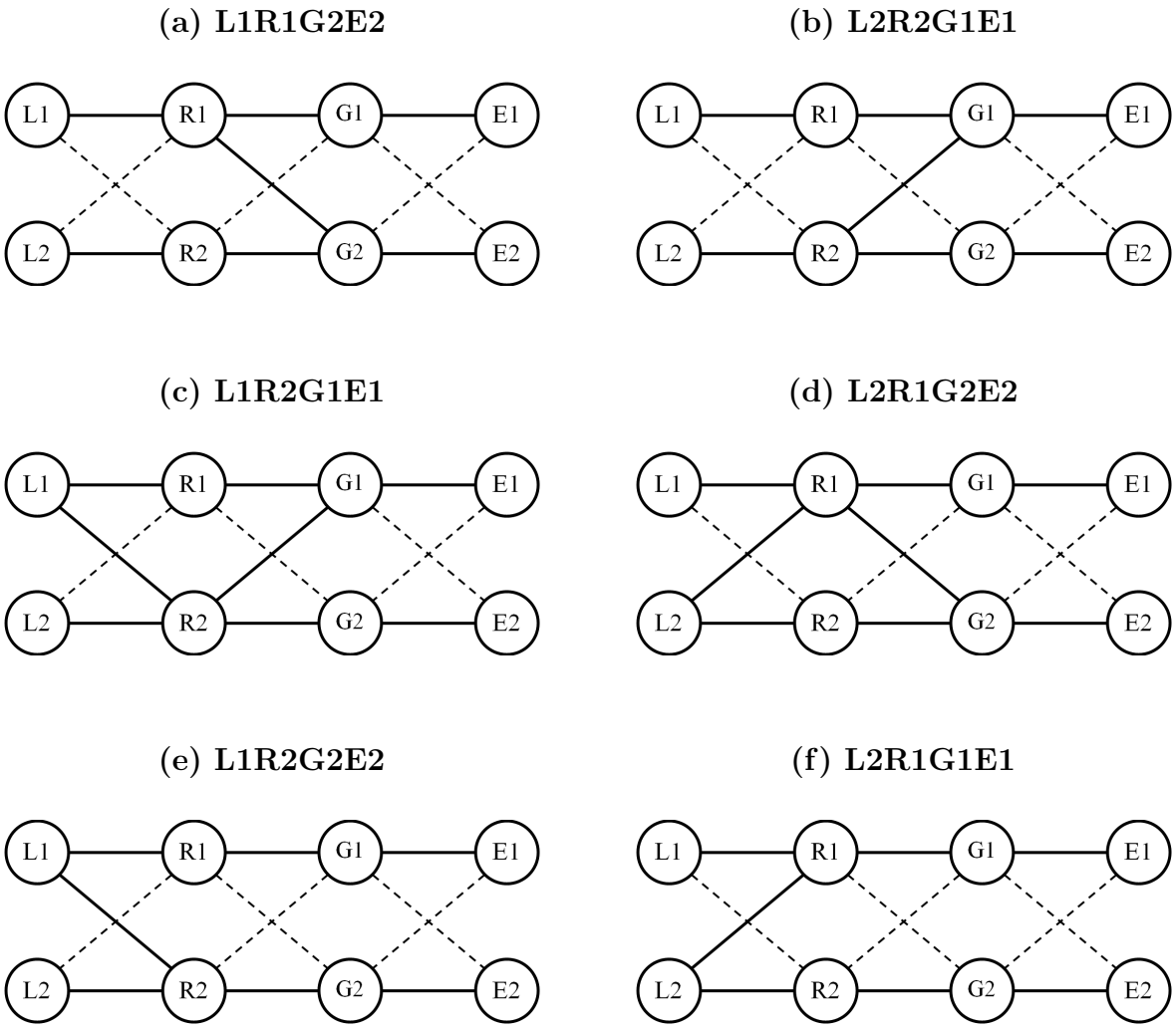

Figure 3.1: **Cartoons for the six basic interactions.** In each figure, interactions existing in the system are label using solid lines. The two original pathways always exist and the new pathways generated due to the interactions between the two pathways are used for the names the six basic interactions.

same scaling factor.

3.2.2 Metrics for measuring the effect of interactions

We first examined the responses of the two pathways as the two ligands were simultaneously added to the system. 3-D dose response surfaces were obtained, with the concentrations of the two ligands on the x and y axes. We then studied the effect of

interactions on the signaling of each pathway, in presence or absent of the other ligand. The effects of interactions between two signaling pathways were considered in 3 aspects:

1) Relative change in signal level.

Since a dose response curve is comprised of signal induced at various ligand concentrations, a weighted relative change was used to describe the change of the dose response curves. If X and Y are vectors containing all the points in a dose response curve, whether it is a single dose response curve or a 3-D dose response surface, the formula used to describe the relative change from X to Y is defined as

$$\sum_i \frac{x_i}{X_{max}} \frac{y_i - x_i}{x_i} = \sum_i \frac{y_i - x_i}{X_{max}} \tag{3.1}$$

Where x_i and y_i are elements of X and Y, respectively.

2) Shape similarity of dose response curves.

The shape of the dose response curves can also be changed by the interactions between the two pathways and the formula below was used to calculate the shape similarity between two dose response curves.

$$1 - \frac{\left\| \frac{X}{\|X\|} - \frac{Y}{\|Y\|} \right\|}{\sqrt{2}} \tag{3.2}$$

The two vectors are first normalized, and then the distance between two normalized vectors are calculated. Since the maximum distance between them is $\sqrt{2}$, the distance divided by $\sqrt{2}$ then subtracted from 1 was used as our similarity score. The range of the similarity score is in [0,1], where 1 means the two dose response curves have the same shape.

3) Signaling specificity of the two pathways.

The concept of the specificity metric proposed by Komarava et. al. [70] were adapted and applied for the steady state signal level. It essentially compares the two signals

induced by the same ligand. The change in the signal level normalized by the total concentration of effector was used to reflect the amount of signal triggered by one ligand. The formula to calculate the specificity of Pathway 1 in the presence of L2 is shown below

$$S1_{L1|L2} = \frac{\frac{|Signal1([L1],[L2]) - Signal1(0,[L2])|}{E1}}{\frac{|Signal1([L1],[L2]) - Signal1(0,[L2])|}{E1} + \frac{|Signal2([L1],[L2]) - Signal2(0,[L2])|}{E2}} \tag{3.3}$$

In this formula, Signal1([L1],[L2]) is the steady state Signal 1 level as L1 and L2 of particular concentrations added. Since signal levels are obtained by numerical simulation, round-off error may cause inaccurate specificity scores. Thus, we applied a cutoff and the specificity score is only calculated when at least one signal changes above the cutoff. Otherwise the specificity score is recorded as NaN. 1% was used for the rest of study. Since the specificity score calculated using the above formula varies with the concentration of L1, we examined both the maximum and minimum specificities among the whole range of the concentration of L1. When L1 only activates Signal 1, the specificity score of Pathway 1 is equal to 1. A specific score of 0.5 indicates both signals are activated to the same extent by the same ligand.

3.2.3 Simulation

The system contains 44 variables and 72 rate constants. Models were built in C and the system of differential equations were solved using the cvode solver in SUNDIALS (SUite of Nonlinear and DIfferential/ALgebraic equation Solvers).

3.3 Results & Discussion

3.3.1 3-D dose response surface for the basic interactions

3-D dose response surfaces were first plotted to provide a direct illustration of the signal levels of the two signaling pathway induced by various combinations of the two ligands.

(a) L1R2G2E2.

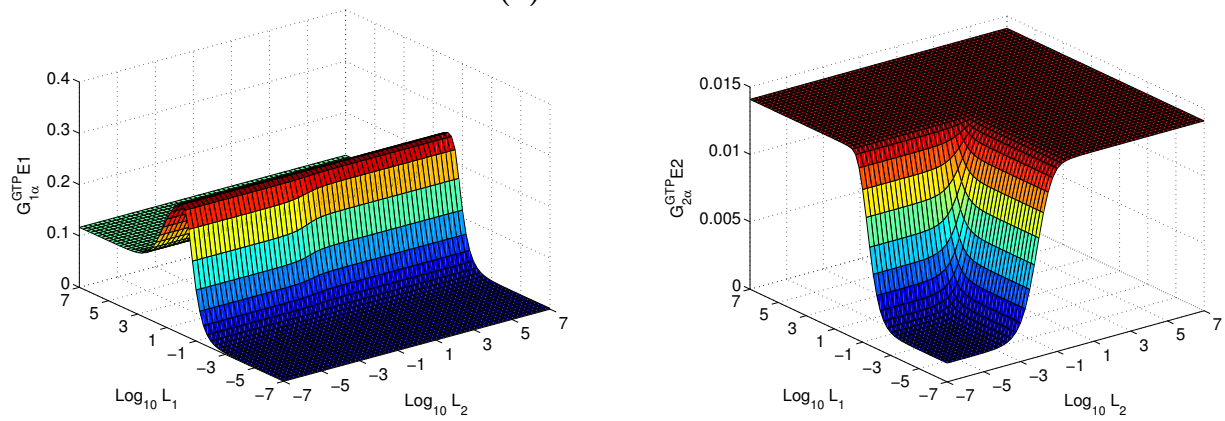

(b) L2R1G1E1.

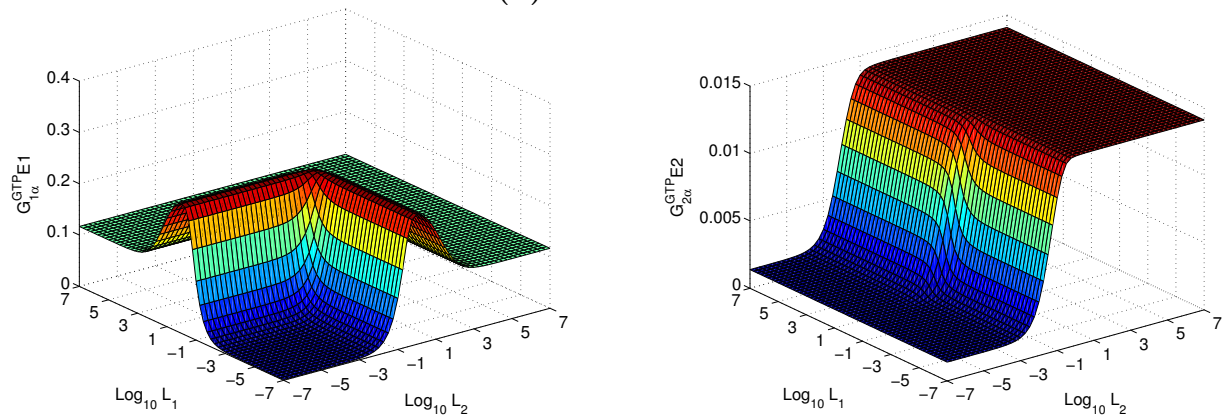

Figure 3.2: **Interaction L1R2G2E2 & L2R1G1E1.** Steady state levels of Signal 1 (left) and Signal 2 (right) are plotted at different combinations of L1 and L2 for interaction L1R2G2E2 and L2R1G1E1. (a) When L1 directly interacts with R2, L1 and L2 behave in the same way and Signal 2 is symmetric with respect to the two ligands. Signal 1 is only slightly affected by L2. (b) Similarly, Signal 1 is symmetric with respect to L1 and L2 when L2 directly interacts with R1.

The 6 basic interactions were separated into 3 groups; each contains 2 basic interactions with the same structure but started from different pathways (Figure 3.2-3.4). For all figures shown here, 1 is used as the scaling factor for the nonspecific interactions. In other words, ligand and G-protein from one pathway that bind the receptor from the other pathway behave the same as the ones in the other pathway. When the two pathways do not interact with each other, they behave independently and only respond to their own ligands.

(a) L1R1G2E2.

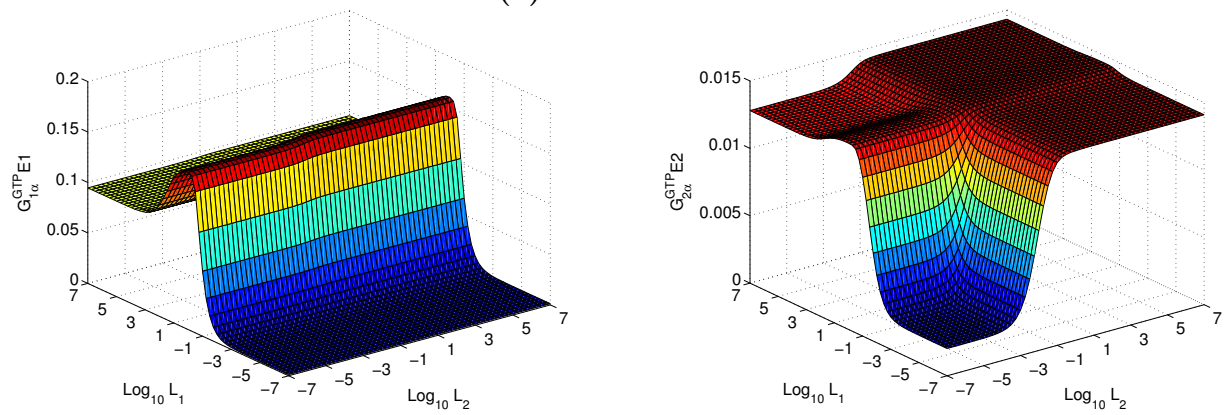

(b) L2R2G1E1.

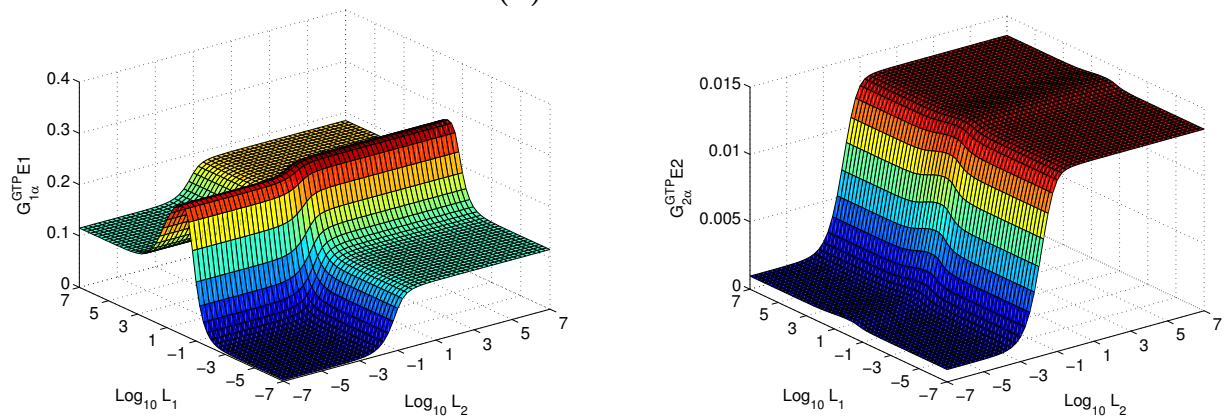

Figure 3.3: **Interaction L1R1G2E2 & L2R2G1E1.** Steady state levels of Signal 1 (left) and Signal 2 (right) are plotted at different combinations of L1 and L2 for interaction L1R1G2E2 and L2R2G1E1. (a) When R1 activates both G-proteins, L1 can affect Signal 2 even when R2 is saturated with L2. However, the overall Signal 1 level is decreased. (b) For interaction L2R2G1E1, it is even more noticeable that Signal 1 is increased by L2 even the concentration of L1 is high.

In Figure 3.2, the two basic interactions in which ligands directly interact with the receptor from the other pathway are shown. For interaction L1R2G2E2 (Figure 3.2(a)), since L1 behave the same as L2, the 3-D dose response surface is symmetric with respect to L1 and L2. At low concentrations of L2, Signal 2 can still be activated by L1. From the direction of L2, at high concentrations of L1, R2 is saturated and Signal 2 is not affected by L2. Increase the concentration of L2 can slightly increase Signal 1, because more L1 are free to interact with R1 instead of R2. Interaction L2R1G1E1 shows the

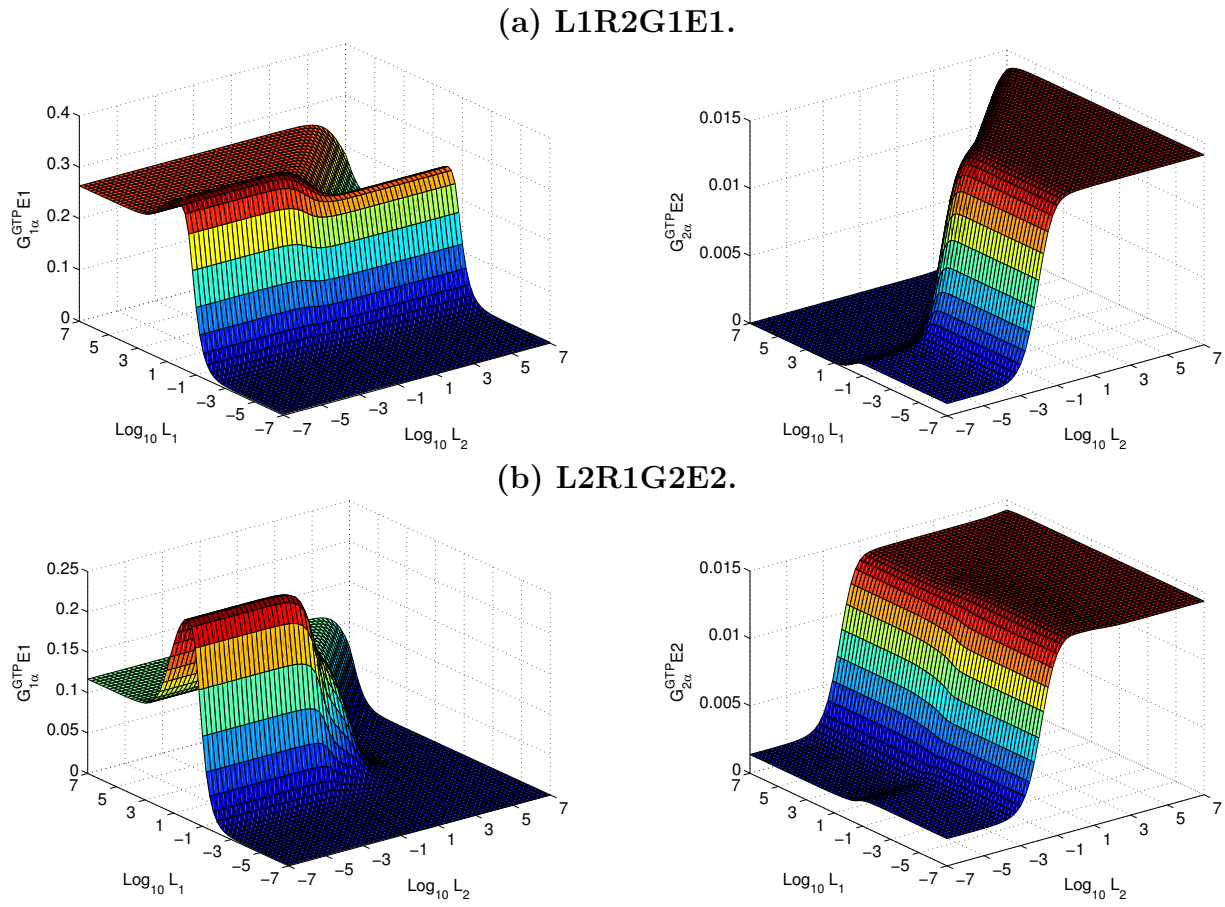

Figure 3.4: **Interaction L1R2G1E1 & L2R1G2E2.** Steady state levels of Signal 1 (left) and Signal 2 (right) are plotted at different combinations of L1 and L2 for interaction L1R2G1E1 and L2R1G2E2. (a) At high concentration of L2, Signal 1 induced by L1 shows a biphasic behavior, when L1 can interact with both R1 and R2 to activate G1. Shifts in Signal 2 is observed as increasing the concentration of L1. (b) For interaction L2R1GL2, Signal 1 is also shifted by L2 and its peak level is reduced.

same effect: Signal 1 is symmetric with respect to L1 and L2, and Signal 2 is increased as increasing the concentration of L1.

Interactions started from the nonspecific bindings between receptors and G-proteins are shown in Figure 3.3. Similar to L1R2G2E2, Signal 2 can be activated by L1 at low concentrations of L2 when R1 interacts with G2 (Figure 3.2(a) right). However, even at high concentrations of L2, L1 can still slightly increase Signal 2. For interaction L2R2G1E1 (Figure 3.3(b) left), it is more clear that L2 is able to regulate Signal 1

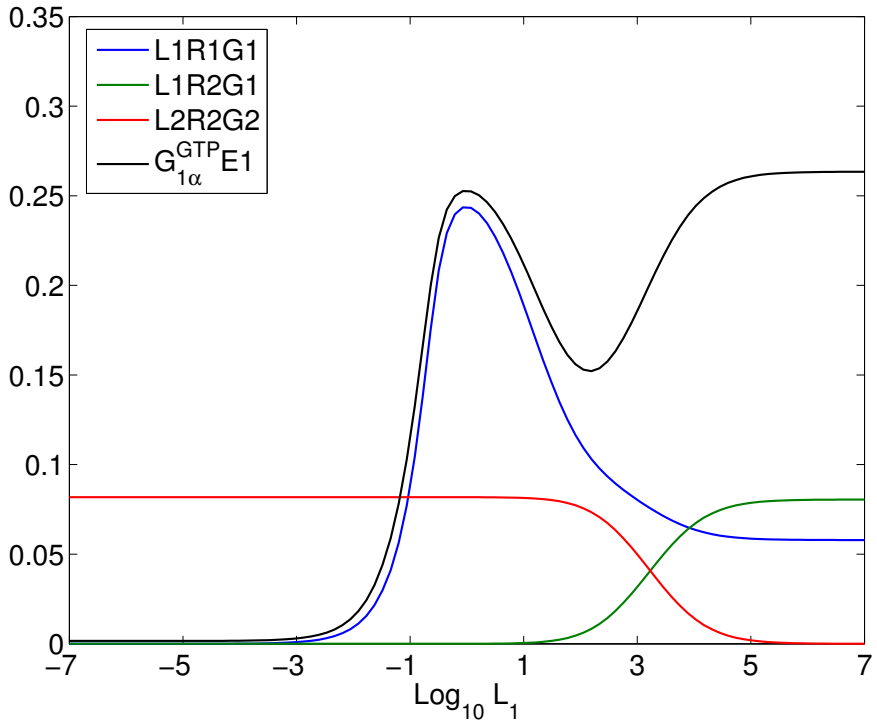

Figure 3.5: **Explanation of the biphasic steady state response.** The concentration of LRG complex is used to demonstrate the formation of the biphasic response. The initial activation of Signal 1 is through the activation of R1, while the second increase is caused by the activation of R2.

even at high concentrations of L1. Signal 1 for interaction L1R1G2E2 is not affected by L2, although the overall signal level is lower compared with no interactions. A slight decrease in the overall Signal 2 level is also observed for interaction L2R2G1E1 (Figure 3.3(b) right).

When a ligand can interact with both receptors to activate the G-protein in its own pathway, the signals of the two pathways are controlled by the two ligands in a more complicated manner (Figure 3.4). For interaction L1R2G1E1, an interesting biphasic response is observed for Signal 1 at high concentrations of L2 (Figure 3.4(a) left). Signal 1 is increased in the beginning and dropped to a lower level as increasing the concentration of L1. However, instead of staying at a particular level, as seen previously in Model 1, Signal 1 is increased again as further increasing the concentration of L1. An explanation for this behavior is provided in Figure 3.5. Since the total concentration of receptors

that can be used by L1 is higher, Signal 1 becomes greater at high concentrations of L1. Due to the competition between L2 and L1 for R2, Signal 1 is decreased as increasing the concentration of L2. Signal 2 is also affected by L1. Along the L1 direction, Signal 2 is decreased by L1. Along the L2 direction, increasing the concentration of L1 shifts the concentration of L2 at which Signal 2 starts to increase to a higher value. For interaction L2R1G2E2, a transition from peaked response to sigmoidal response is observed as increasing the concentration of L2 (Figure 3.4(b) left). A shift of the concentration of L1 to raise Signal 1 is also seen. Signal 2 is not affected much by this interaction, since the concentration of R2 is high enough to activate G2 originally.

The biphasic response is a result of combined activation of R1 and R2, and the concentration of ligand-receptor-G-protein complex is used as an indicator to explain this behavior (Figure 3.5). At high concentration of L2, R2 is primarily bound with L2 (red line) and only R1 is used for L1 to activate G1. Thus, as increasing the concentration of L1 initially, Signal 1 (black line) is increased by the activation of R1 (blue line). The ability of R1 to activate Signal 1 is hindered when L1 is further increased, as seen in Model 1. In the meanwhile, higher concentration of L1 causes a higher occupancy of R2 by L1 (green line) and Signal 1 is again increased due to R2 activation (black line).

3.3.2 The effect of the strength of interactions on signaling

In the next step, we examined the effect of the strength of interactions on signaling. We first compared the dose response curves for the 6 basic interactions at various strengths with the ones generated without interactions, in the presence of different concentrations of the ligand from the other pathway. The relative changes in signal levels and the shape similarity scores are calculated as described in the method section and shown in Figure 3.6 and Figure 3.7, respectively.

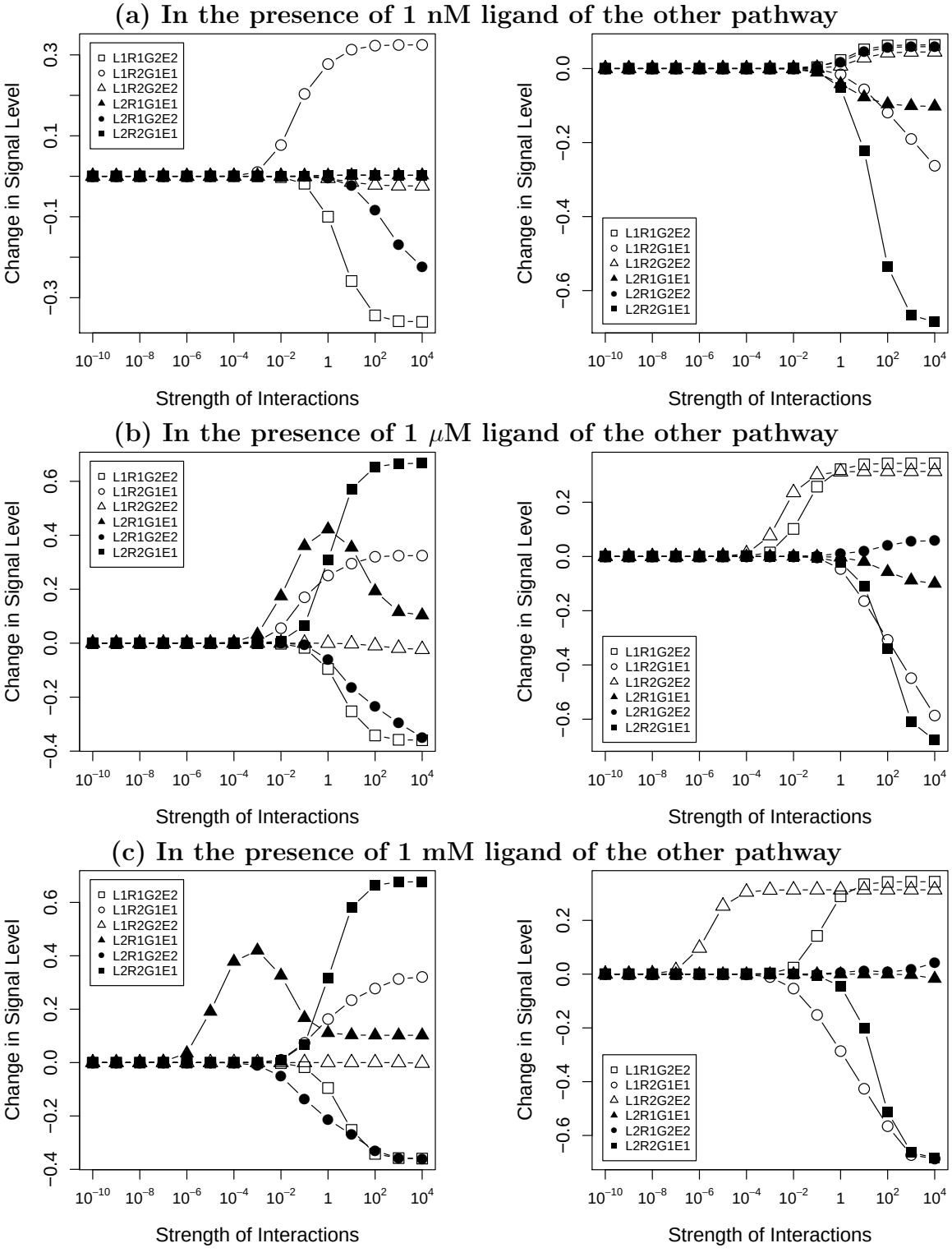

Figure 3.6: **Relative changes in the signal level.** For the 6 basic interactions, relative changes in the dose response curves compared with the dose response curves in two independent signaling pathways are plotted at various strengths of interactions and concentrations of the ligand from the other pathway.

In general, the overall signal level is increased when a ligand can interact with both receptors to activate the G-protein in its pathway (Figure 3.6, L1R2G1E1○ for Signal 1 and L2R1G2E2● for Signal 2) when the strength of interactions is strong. On the opposite, when the receptor from one pathway also interact with the ligand of the other pathway, the overall signal level is decreased (L2R1G2E2● for Signal 1 and L1R2G1E1○for Signal 2). A more dramatic decrease in signal level is observed when a receptor directly activates the G-protein from the other pathway (L1R1G2E2□ for Signal 1 and L2R2G1E1■ for Signal 2). Due to the interactions between the two pathways, the signal of one pathway can also be affected by the other pathway. When a ligand can signal through its own receptor to activate the G-protein from the other pathway, the signal of the other pathway can be increased only when the strength of interactions is high enough (L2R2G1E1■ for Signal 1 and L1R1G2E2□ for Signal 2 in Figure 3.6(b)(c)). However, if the ligand directly interacts with the receptor in the other pathway, its signal can be increased even when the strength of the interaction is weak. A shift in the curve of relative changes to a weaker strength of interactions is also observed as increasing the concentration of the other ligand (L2R1G1E1▲ for Signal 1 and L1R2G2E2△ for Signal 2 in Figure 3.6(b)(c)). More interestingly, the relative change for Signal 1 as increasing the strength of L2R1G1E1 in the present of a relatively high concentration of L2 shows a peaked behavior. The relative change is high when the activation of Signal 1 by L2 is maximized at low concentration of L1 (Figure 3.2(b) left). The relative change is smaller if all R1 are occupied and L1 has no effect on Signal 1.

(a) Shape similarity between single dose response curves

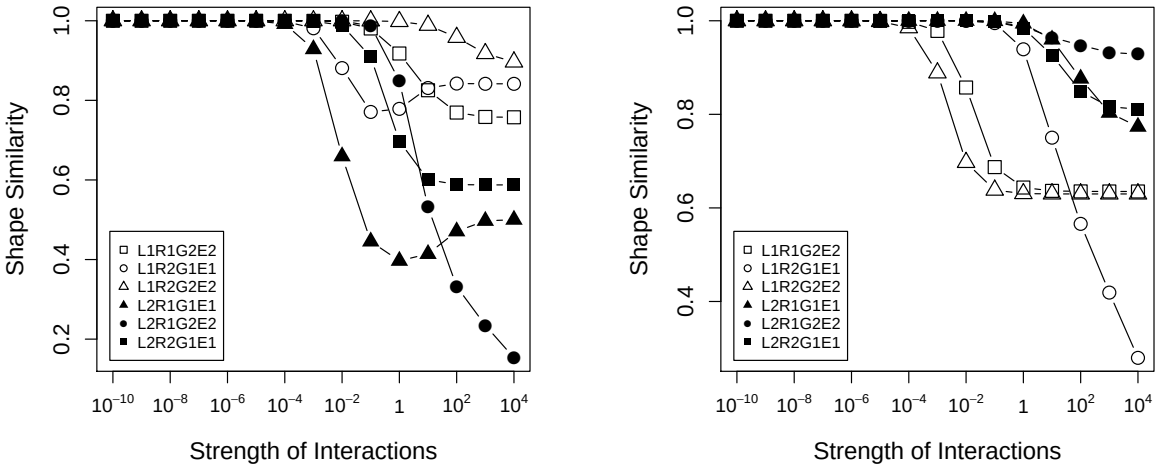

(b) Shape similarity between 3-D dose response surfaces

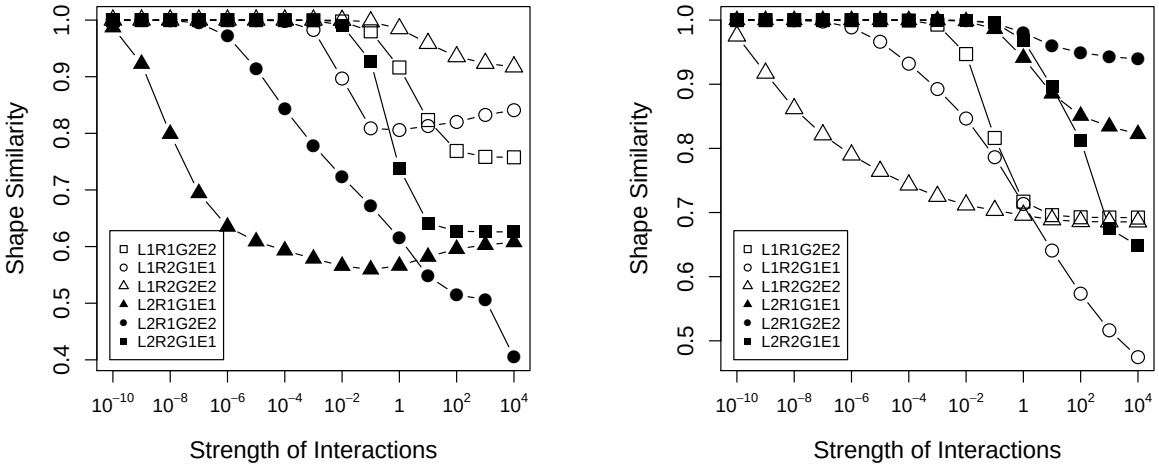

Figure 3.7: **Shape changes in the dose response curve.** Shape similarities between the dose response curves obtained from systems with basic interactions and without interactions are calculated.**(a)** Comparisons between single dose response curves in the presence of 1 μM ligand from the other pathway are made. Non-monotonic change is observed as increasing the strength of interactions for interaction L2R1G1E1 and L1R2G1E1. **(b)** Comparisons between 3-D dose response surfaces are shown. Shape of the 3-D dose response surfaces is affected dramatically when a ligand directly interacts with the receptor in the other pathway, even when the strength of interactions is weak.

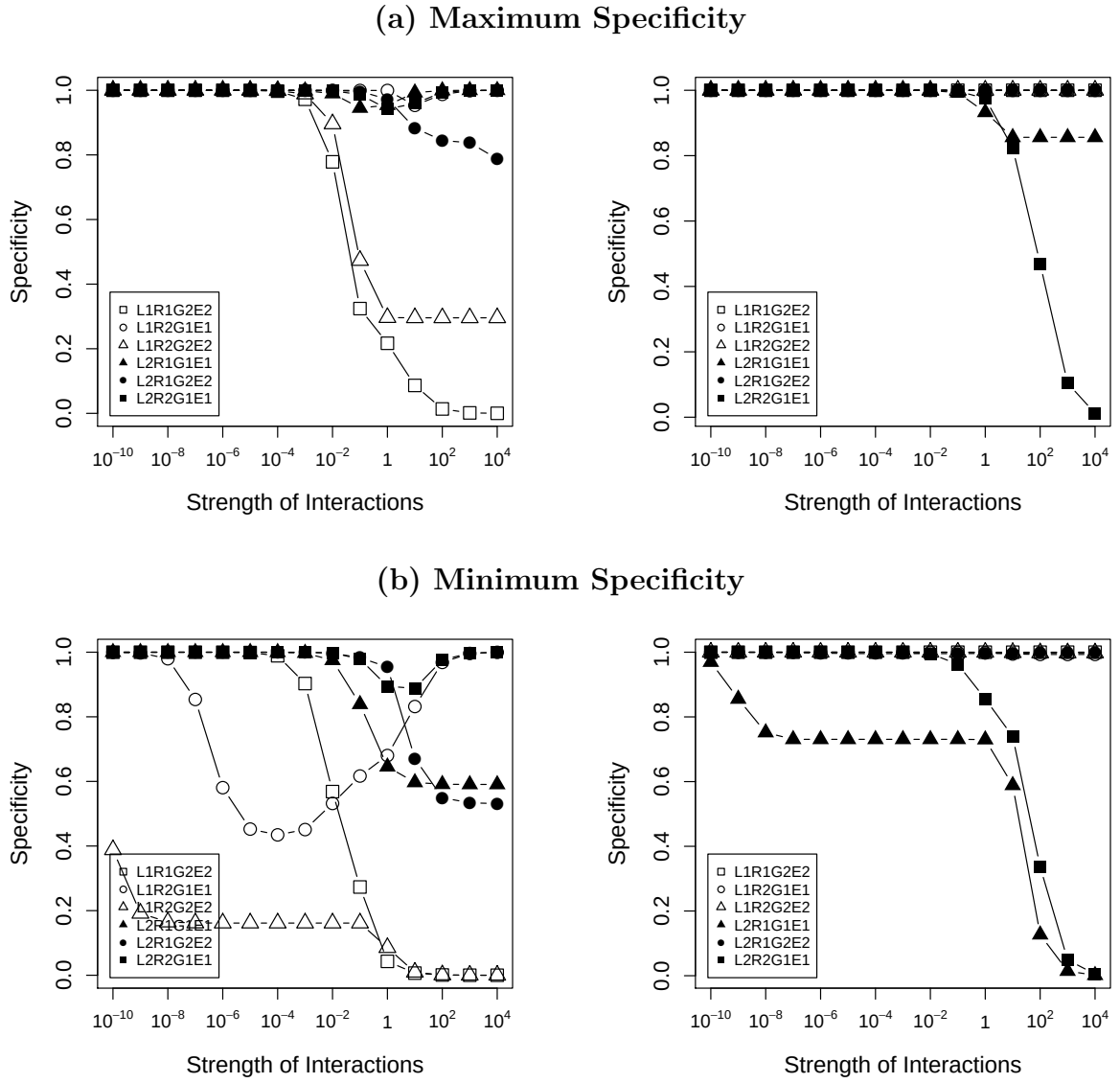

Figure 3.8: **Maximum and minimum specificities in the presence of 1 nM ligand from the other pathway.(a)** The maximum specificity of one pathway can be affected dramatically when its ligand directly interact with the receptor in the other pathway or its receptor actives the G-protein in the other pathway. For Pathway 1, even when the nonspecific interactions are 100-fold weaker, the maximum specificity is lower than 1. **(b)** The minimum specificity is more easily affected by the nonspecific interactions between the ligand from one pathway and the receptor from the other pathway. Even when the rates for the nonspecific bindings are really weak, the specificity of one pathway can be low since the other pathway can be activated when the concentration of the ligand is high. The specificity of Pathway 1 shows a inverse peaked behavior for interaction L1R2G1E1 as increasing the strength of interactions.

Shape of the dose response curves obtained when the two pathways interact with each other are compared with the original ones. The shape similarity between single dose response curves obtained from systems with the basic interactions and without interactions are calculated in the presence of 1 μM ligand of the other pathway and shown in Figure 3.7(a). Shape similarity and relative changes in the signal levels carry similar information since changes in the shape and signal level occur concurrently. Since the relative change is measured over a range of ligand concentrations and averaged both positive and negative changes while shape similarity neglects the magnitude of signal, the two do not behave exactly the same. For example, Signal 1 is increased about 18% when the scaling factor of interaction L2R1G1E1 is 10^{-2} or 10^{2} (Figure 3.6, left), while the shape similarities between the two dose response curves and the original ones differ.

Shape similarities of the 3-D dose response surfaces compared with the ones without interactions were also calculated at various strengths of the basic interactions (Figure 3.7(b)). The shape of the dose response surface can be dramatically changed when the signal is regulated by the ligand from the other pathway. The nonspecific interactions between ligand and receptor have the most dramatic effect on the shape of the dose response curve. Even when the strength of interactions is weak, the shape of the 3-D dose response surface can be significantly changed.

Specificity scores were calculated as described in the Methods section for the 6 basic interactions in the presence of different concentrations of the other ligand (Figure 3.8-3.9). Since different concentrations of ligand can result in distinct specificity scores, we examined both the maximum and minimum specificity scores a ligand can achieve over a range of concentrations. For interaction L1R2G2E2, although the highest specificity for Pathway 1 is 1, lowest specificity is 0.2 even when the strength of interactions is low. Similarly, the specificity of Pathway 2 is also low for interaction L2R1G1E1 when the two pathways only weakly interact with each other. For interaction L1R1G2E2, the maximum

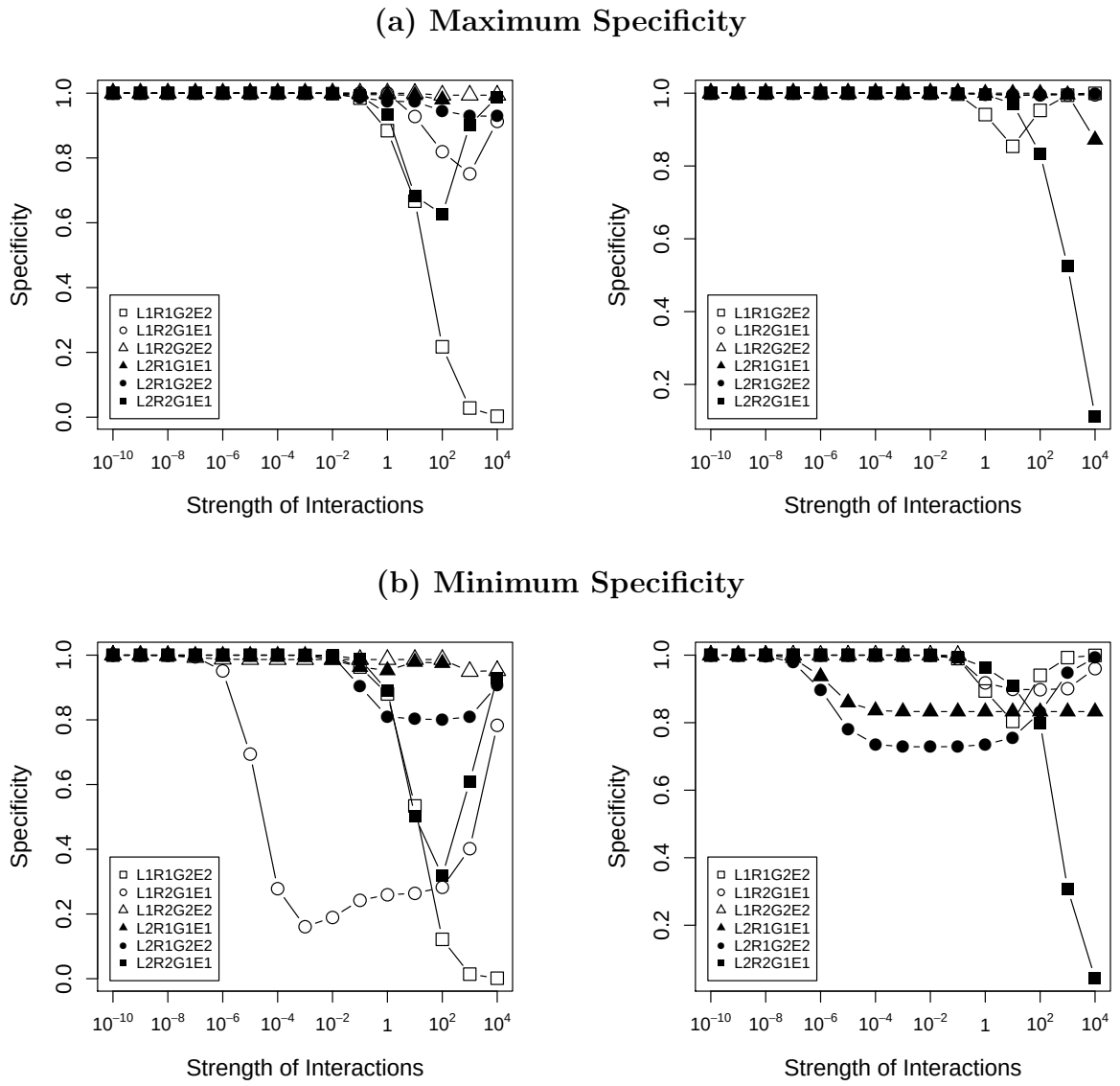

Figure 3.9: **Maximum and minimum specificities in the presence of 1 μM ligand from the other pathway.(a)** The specificity of one pathway is affected when the concentration the other ligand in the system is increased. When a ligand from one pathway directly interacts with the receptor in the other pathway, specificity of pathway is increased since the receptor in the other pathway is occupied with its own ligand. **(b)** The minimum specificity of Pathway 1 is also increased to 1 for interaction L1R2G2E2 when the strength is weak. The specificity of Pathway 2 for interaction L2R1G2E2 has an inverted bell shape as increasing the strength of interactions.

specificity of Pathway 1 is high when the strength of interactions is weak, however, it cannot be maintained as increasing the strength of interactions. The effect of interaction

L2R2G1E1 on the specificity of Pathway 2 is similar. For interaction L1R2G1E1, the maximum specificity of Pathway 1 is always high. However, the minimum specificity shows a inverse peaked behavior. The reason for this is that the specificity is considered to compare the outputs after ligand addition and before ligand addition. It may have a negative effect on signaling. As shown in Figure 3.4, initial signal level is high when the concentration of L2 is high and it can be decreased by L1.

Signaling specificity is affected by the amount of other ligands existed in the system. When the concentration of L2 is increased from 1nM to 1μM (Figure 3.9), the minimum specificity of Pathway 1 is increased from below 0.5 to 1 for interaction L1R2G2E2. The effect of the other ligands on signaling specificity is primarily exerted by saturating their own receptors. For example, if the concentration of L2 is high for interaction L1R2G2E2, R1 is not able to interact with R2, so the specificity of Pathway 1 is increased. Specificity can also be decreased by other ligands. The specificity of Pathway 1 is reduced due to the competition between L1 and L2 for R1 for interaction L2R1G2E2.

3.3.3 Combinations of the basic interactions

In next step, we considered the effect of all combinations of the basic interactions on signaling. First, we calculated the shape similarities between 3-D dose response surfaces of all types of interactions. Figure 3.10 shows the similarity scores when the strengths of interactions are weak (the scaling factor is 10^{-3}). The color bar on the left of the heat map shows which basic interactions in the system. Each column represents one of the basic interactions and from left to right (or rows from up to down in other figures) they are L1R1G2E2, L1R2G1E1, L1R2G2E2, L2R1G1E1, L2R1G2E2 and L2R2G1E1. The existence of a basic interaction is colored by red. The shape of the 3-D dose response surfaces is dominated by the nonspecific interaction between ligand and receptor. As long as it exists, other interactions do not change the dose response curve significantly

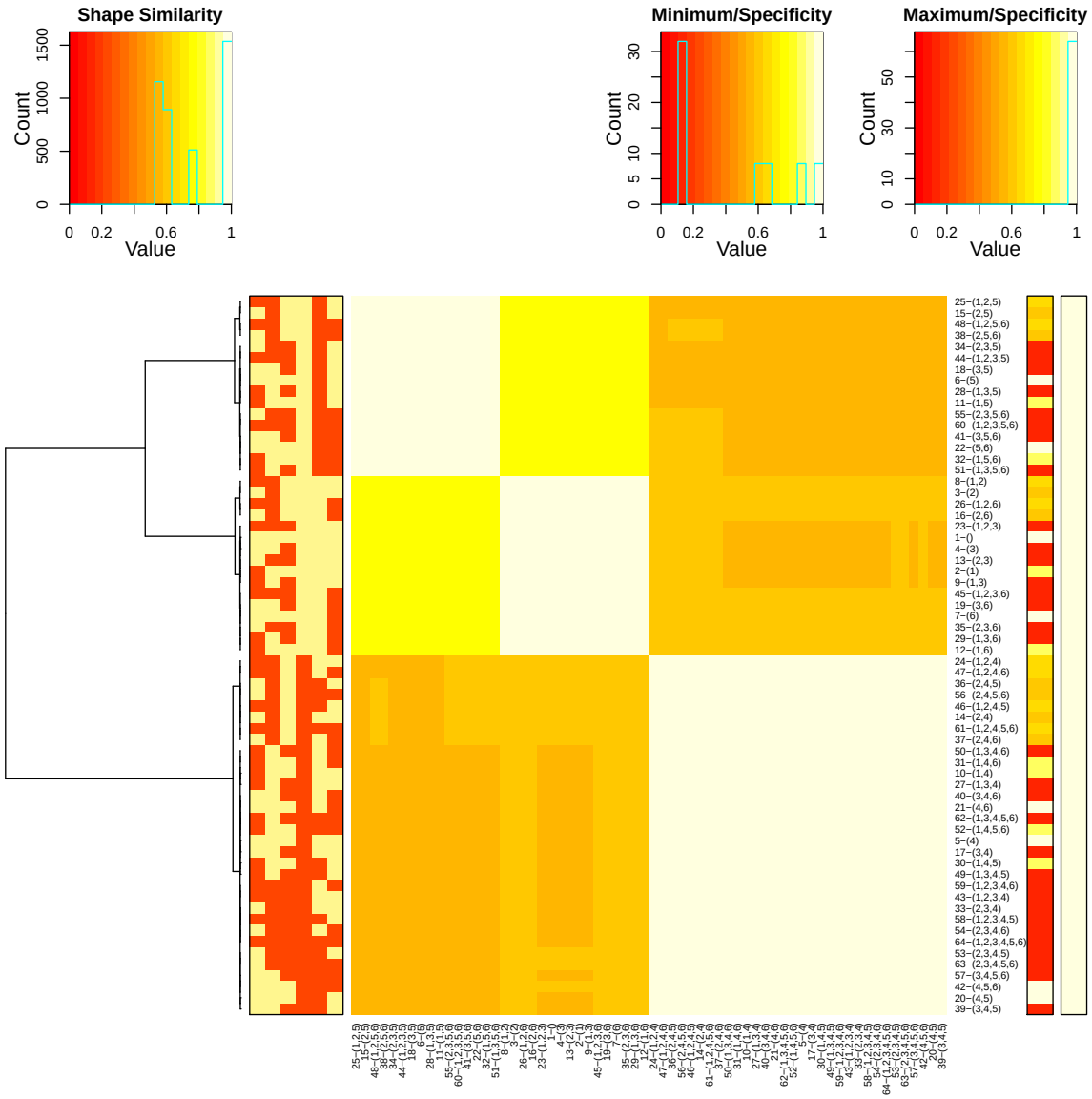

Figure 3.10: **Shape changes in the 3-D dose response surfaces for Signal 1.** Shape similarities between the 3-D dose response surfaces obtained from systems with all different combinations of the 6 basic interactions and without interactions are calculated. Existences of interaction L1R1G2E2, L1R2G1E1, L1R2G2E2, L2R1G1E1, L2R1G2E2 or L2R2G1E1 are colored in red in the color bar on the left of the heat map. When the strengths of interactions are weak (10^{-3} is used for the scaling factor) , the nonspecific interaction between the ligand from one pathway and the receptor from the other pathway has a dominant effect on the shape of the 3-D dose response surface.

and they all have similar shapes.

The maximum and minimum specificities of Pathway 1 are calculated for all combi-

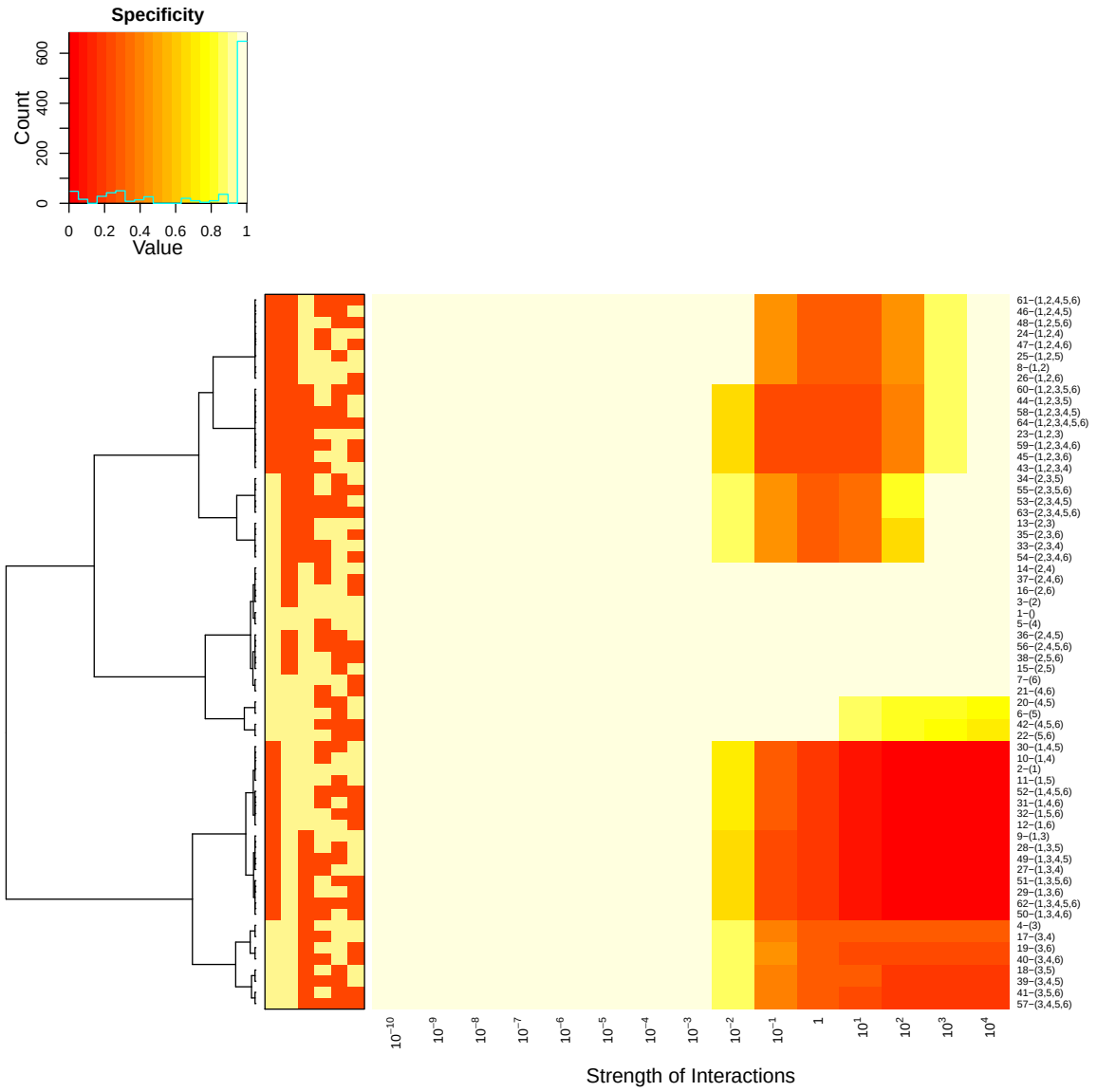

Figure 3.11: **Maximum specificity of Pathway 1 for all different combinations of the 6 interactions as varying the strengths of interactions.** Maximum and minimum specificity of Pathway 1 under all different combinations of the 6 basic interactions are calculated. Existences of interaction L1R1G2E2, L1R2G1E1, L1R2G2E2, L2R1G1E1, L2R1G2E2 or L2R2G1E1 are colored in red in the color bar on the left of the heat map. Interaction L1R1G2E2 and L1R2G2E2 have a dominant effect on the maximum specificity over other interactions.

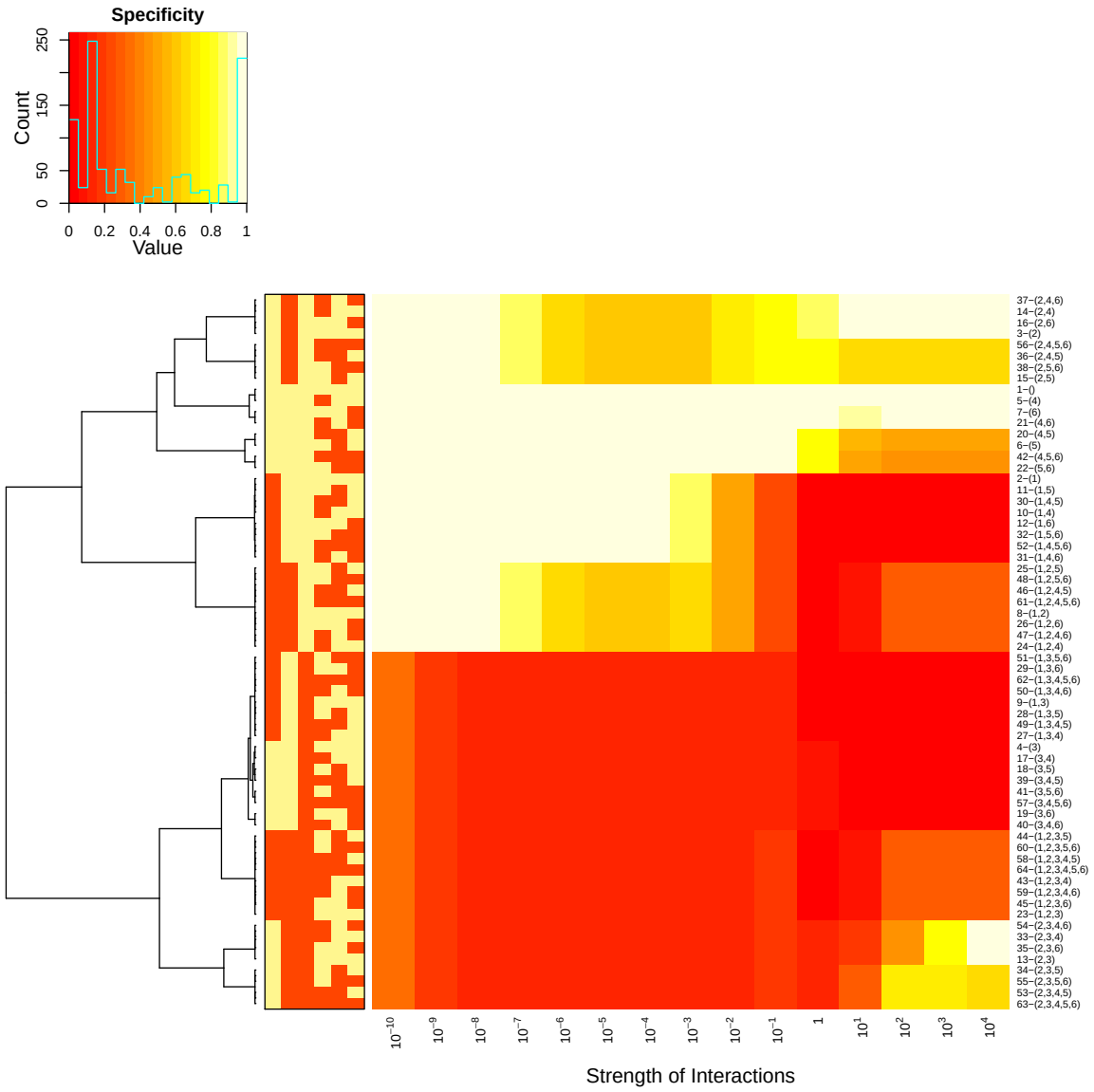

Figure 3.12: **Minimum specificity of Pathway 1 for all different combinations of the 6 interactions as varying the strengths of interactions.** Maximum and minimum specificity of Pathway 1 under all different combinations of the 6 basic interactions are calculated. Existences of interaction L1R1G2E2, L1R2G1E1, L1R2G2E2, L2R1G1E1, L2R1G2E2 or L2R2G1E1 are colored in red in the color bar on the left of the heat map. The minimum specificity is low as long as interaction L1R2G2E2 exists even when the strengths of interactions are weak.

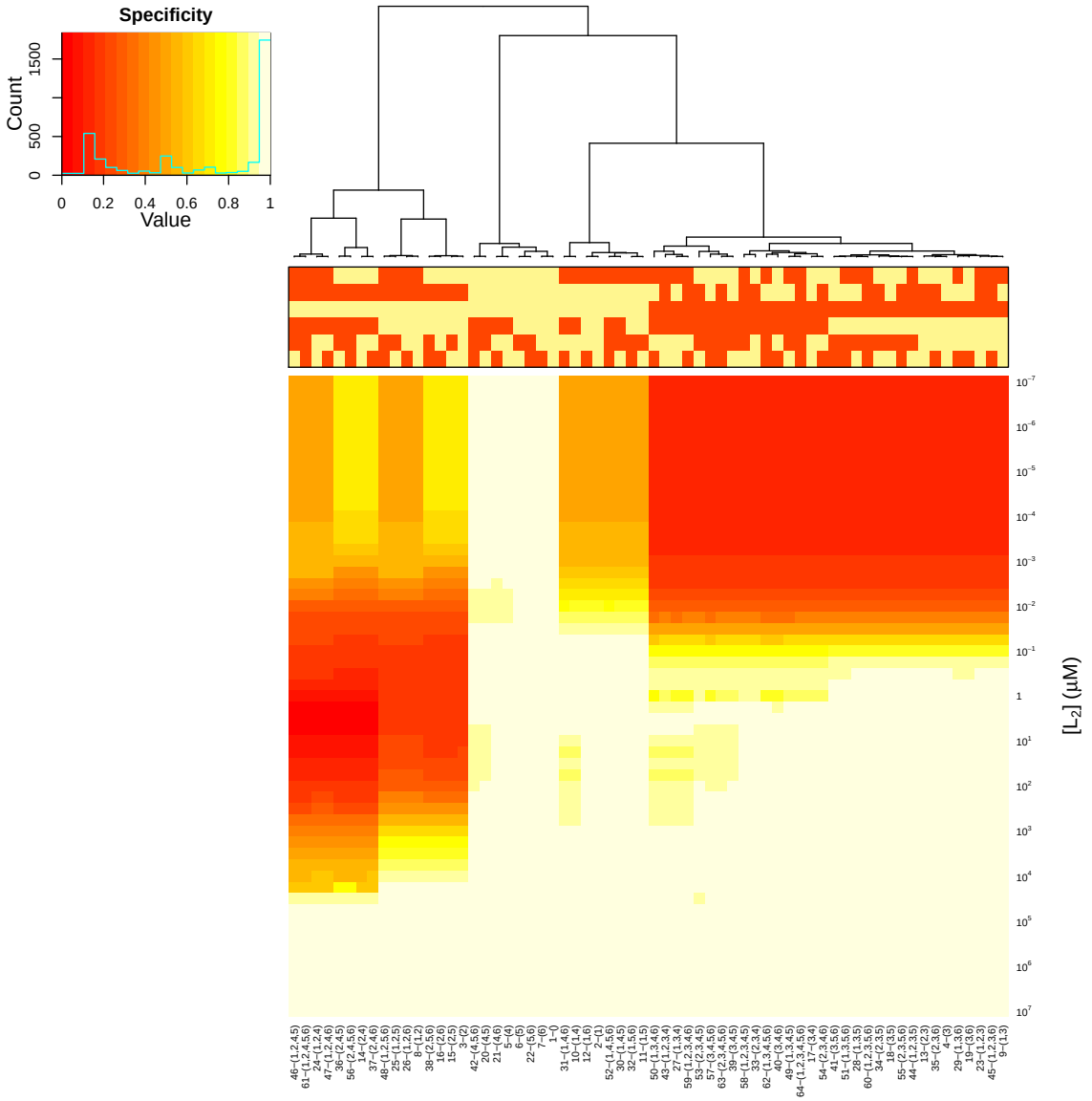

Figure 3.13: **Minimum specificity of Pathway 1 for all different combinations of the 6 interactions as varying the concentration of L2.** Minimum specificity of Pathway 1 under all different combinations of the 6 basic interactions are calculated (10^{-2} is used for the scaling factor). Existences of interaction L1R1G2E2, L1R2G1E1, L1R2G2E2, L2R1G1E1, L2R1G2E2 or L2R2G1E1 are colored in red in the color bar on top of the heat map. L2 can have an non-monotonic effect when interaction L1R2G1E1 exists but interaction L1R2G2E2 does not.

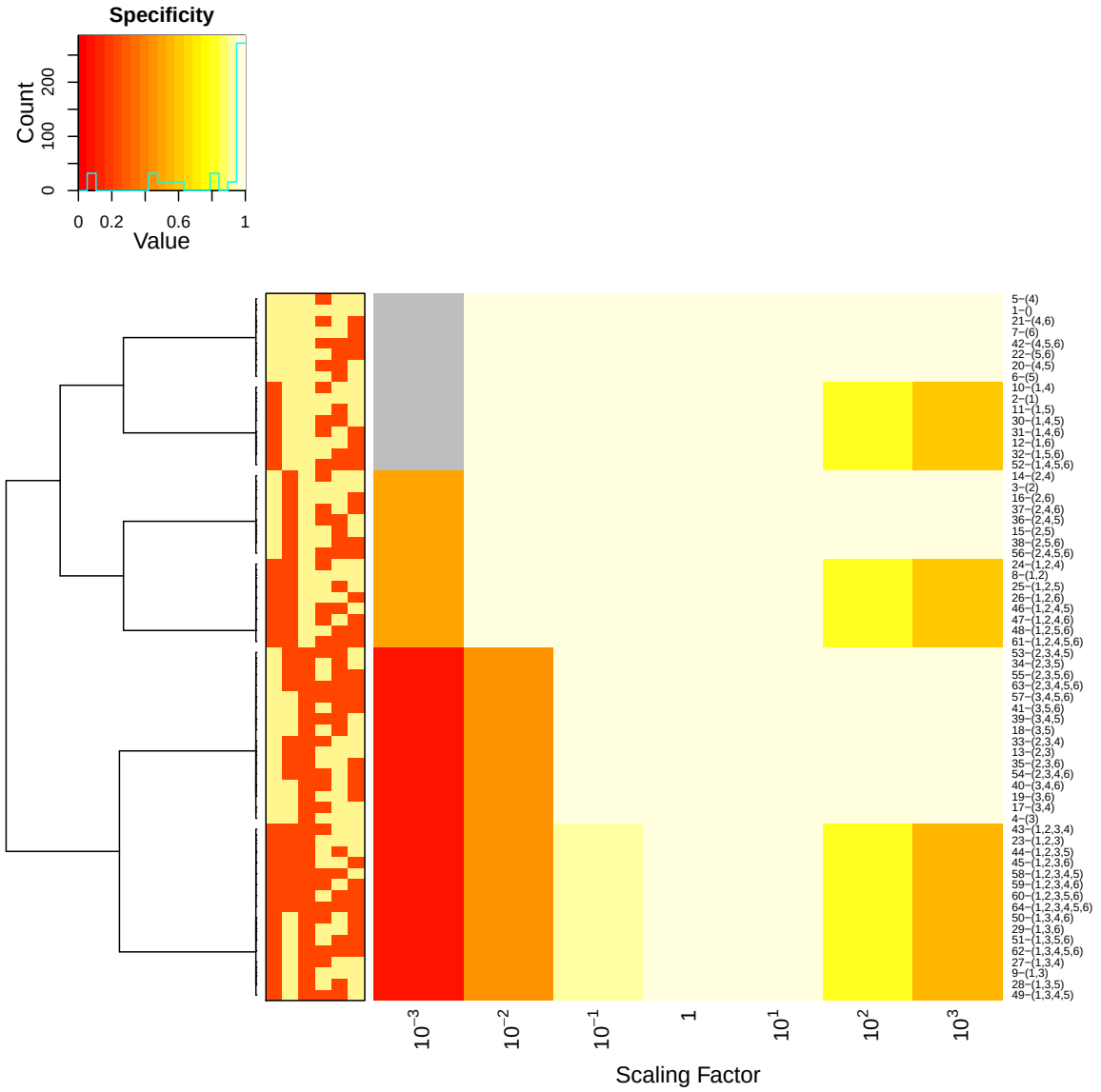

Figure 3.14: **Maximum specificity of Pathway 1 for all different combinations of the 6 interactions as varying the concentration of R1.** Maximum specificity of Pathway 1 under all different combinations of the 6 basic interactions are calculated (10^{-3} is used for the scaling factor). Existences of interaction L1R1G2E2, L1R2G1E1, L1R2G2E2, L2R1G1E1, L2R1G2E2 or L2R2G1E1 are colored in red in the color bar on the left of the heat map. The concentration of R1 has an non-monotonic effect on the maximum specificity of Pathway 1.

nations of the basic interactions at various strengths, in the absence of L2 (Figure 3.11 and Figure 3.12). Maximum specificity and minimum specificity have similar trends. Non-monotonic changes in specificity are observed for interactions containing interaction

L1R2G1E1 and at least one of interaction L1R2G2E2 and L1R1G2E2. Specificity of Pathway 1 is decreased either due to the binding of L1 with R2 or the binding of R1 with G2 when their interaction is relatively strong. However, if R2 strongly favors binding with G1 rather than G2, the specificity of Pathway 1 is high. Interaction L1R2G2E2 has a dominant effect on the minimum specificity. All interactions containing L1R2G2E2 has a low specificity score, even when the strength of interactions is weak.

The effect of the other ligand on specificity for all different combinations of the basic interactions were also examined. The minimum specificity of Pathway 1 is dominated by interaction L1R2G2E2 when the strength of interactions is weak (Figure 3.13(b)). All interactions containing L1R2G2E2 result in similar scores and can be alleviated by increasing the concentration L2. L2 has an non-monotonic effect on the specificity of Pathway 1 for all interactions containing L1R2G1E1 but not L1R2G2E2. Because L1 has a negative effect on Signal 2 due to the binding with R2 for interaction L1R2G1E1, specificity of Pathway 1 is low at intermediate L2 concentration since initial Signal 2 level is high and can be largely inhibited by L1. When R2 is fully occupied by L2, specificity of Pathway 1 is increased.

Finally, we also examined the effect of the concentration of receptors on signaling specificity (Figure 3.14). For systems containing interaction L1R1G2E2 and L1R2G1E1 or L1R2G2E2, specificity of Pathway 1 is decreased at both high and low receptor concentrations. It is the result of combined effect of different interactions. Interaction L1R1G2E2 can result in low specificity at high concentrations of R1 since more G2 can be easily activated. When L1 can also interact with R2, low concentration of R1 caused a low activation of G1, thus reduces the specificity of Pathway 1.

3.4 Conclusions

In summary, we studied in details of the interactions between two GPCR signaling pathways in the initial steps. Signaling can be affected by the strength of interactions, the presence of other ligands, as well as the expression level of the molecules in the signaling pathways. A biphasic response curve is observed as an effect of combined activation by two receptors. Both changes in the signal level and signaling specificity can be affected by the presence of ligands for other pathways. Signaling specificity can also have non-monotonic changes as varying the strength of interactions, the concentration of the other ligand as well as the concentration of the receptors.

Interactions between the two signaling pathways can either have direct or indirect effect on signaling. One ligand can directly interact with the receptor in the other pathway, or its receptor can directly activate the G-protein in the other pathway. The impact of direct effect is usually strong and changes the behavior of signaling dramatically as we can see in interaction L1R2G2E2 (Figure 3.2(a) left) or L1R2G2E2 (Figure 3.3(a) left). Signaling can also be affected indirectly due to the competition for the same molecule. Indirect effect is often subtle, but can still be noticeable (Figure 3.2 (b) Right).

Here, we mainly focused on the nonspecific interactions between signaling pathways, the rates for the specific interactions between molecules in the original pathways are kept unchanged. Considering one ligand activating two receptors (L1R2G2E2 or L2R1G1E1), even if the ligand interacts with the two receptors exactly in the same way, differences in the bindings of other molecules can still affect signaling specificity. Since the activities of the ligand on the two pathways are largely independent, the variation of parameters in the previous chapter can generally demonstrate the changes in specificity. Signaling specificity is 0.5 for all ligand concentrations when the two pathways are identical, and it can be increased or decreased as varying particular parameters due to changes in the

magnitude or shifts of the whole dose response curve.

Chapter 4

Modeling Dimerization of Receptors in GPCR Signaling Pathways

4.1 Introduction

Over the past few decades, more and more evidence suggests G-protein-coupled receptors can form dimers and higher-order oligomers within the cell membrane [71][72][73][74][75]. They can either form homodimers or interact with other types of GPCRs to form heterodimers. The ability of GPCRs to dimerize has been extensively reviewed [76][77][78][79] [80][81]. Due to the critical role of GPCRs in drug discovery, a better understanding of dimerization may enhance our ability to design selective drugs that minimize side effects [82][83].

It has been shown that GPCR dimers can play a role in receptor trafficking. When coexpressed with α_{1B}-adrenergic receptors, the surface expression of α_{1D}-adrenergic receptors can be significantly increased [84]. When δ opioid receptors and β_2-adrenergic receptors are coexpressed, internalization of both receptors can be triggered by either of their ligands [85]. Signaling can also be affected by dimerization. When α_2-adrenergic receptors and μ opioid receptors are coexpressed, they form heterodimers and the stimulus effects of morphine on μ opioid receptors are enhanced [86]. More information about the effects of dimerization is provided in [76].

Dimerization of GPCRs provides the opportunity for allosteric regulation. GPCRs can serve as allosteric modulators for each other. For example, coexpression of μ opioid receptor and δ opioid receptor alters the binding affinities of their ligands [87]. Similarly, the presence of ligand can also alter the dimerization status [88]. Ligands and G-proteins can also serve as allosteric modulators, where ligand or G-protein binding on one side of

the dimer affects the binding of ligand or G-protein on the other side of the dimer. Ligands can have either positive cooperativity or negative cooperativity when binding to the dimer [89]. Binding of G-proteins to the receptors may also be affected by dimerization [90].

Dimerization and oligomerization of GPCRs have been studied using mathematical models elsewhere [91, 92, 93, 94, 95, 96, 97, 98, 99]. Most of the models are limited to the level of the binding of ligands and receptors, and focused on the allosteric effects of ligand binding [92, 93, 94, 95, 96, 97]. Some other studies focused on the organization of receptors on the cell membrane, and how it is affected by parameters in the model as such the rate for dimerization [91, 98, 99]. To our knowledge, the effects of dimerization on signaling specificity has not been systematically studied using mathematical models.

In this chapter, we extended the two-pathway model by considering heterodimerization between the two receptors. The model contains all possible binding reactions of the ligands and G-proteins to the dimer. Scaling factors are included in the model for exploring possible allosteric effects associated with dimerization. 3-D dose response curves were plotted and a double-peaked dose response curves are observed under certain conditions. The effects of dimerization on signaling specificity were also examined.

4.2 Model description

4.2.1 Structure of the model.

The model containing two GPCR signaling pathways was further enriched by considering dimerization between the two receptors. The reaction scheme for the system is shown in Figure 4.1. Receptors of different forms, whether bound with ligand or G-protein or not, were considered to be able to dimerize. The bindings between L1, R1 and G1 are shown in the top of Figure 4.1(a). A_1 and B_1 are used for the dissociation constants for the binding of L1 with R1 and the binding of R1 with G1, respectively. A scaling factor k_1 is applied to the two reactions in the other corner of the binding square to maintain

thermodynamic stability. The bottom of the reaction scheme contains all dimer states and reactions describing the bindings of ligands and G-proteins to the dimer in different orders. Between the top and the bottom are the dimerization reactions in the model. Dimerization with R, LR complex, RG complex and LRG complex are indicated by black, red, blue and green, respectively. The dissociation constant for the dimerization of R1 and R2 is indicated by C, and rates for the dimerizations of receptors bound with ligands or G-proteins can be adjusted by scaling factors. All reactions in the system are contained in the reaction scheme in Figure 1(a). If the binding square of L1, R1 and G1 on the top are replaced by the binding square of L2, R2 and G2, dimerization reactions connecting the top and bottom will be shifted in the figure, but the rate constants are described exactly in the same way. Details of the bottom of the reaction scheme are further demonstrated in Figure 1(b). The center of the figure is the R1/R2 dimer without ligand or G-protein bound. In the original model, ligands and G-proteins were assumed to only interact with the receptor in their own pathway. An underscore connecting R1 and R2 is used to represent the dimer and ligand or G-protein bound to a receptor is put on the same side of the underscore as the receptor. For example, L1R1G1_L2R2 indicates R1 in the dimer is bound with L1 and G1, while R2 is only bound with L2. The binding of L1 and L2 to the apo dimer can happen in two orders. From the middle row of the reaction scheme, binding of L1 first is shown in the bottom and the top shows binding L2 before L1. Despite the order of bindings, the dimer reaches the same states and the species and reactions in the first row and the last row are exactly the same. Similar for the binding of G-proteins, the left part and right part divided by the column in the middle show different orders of the bindings of the two G-proteins. The same final states are reached in the leftmost and rightmost columns.

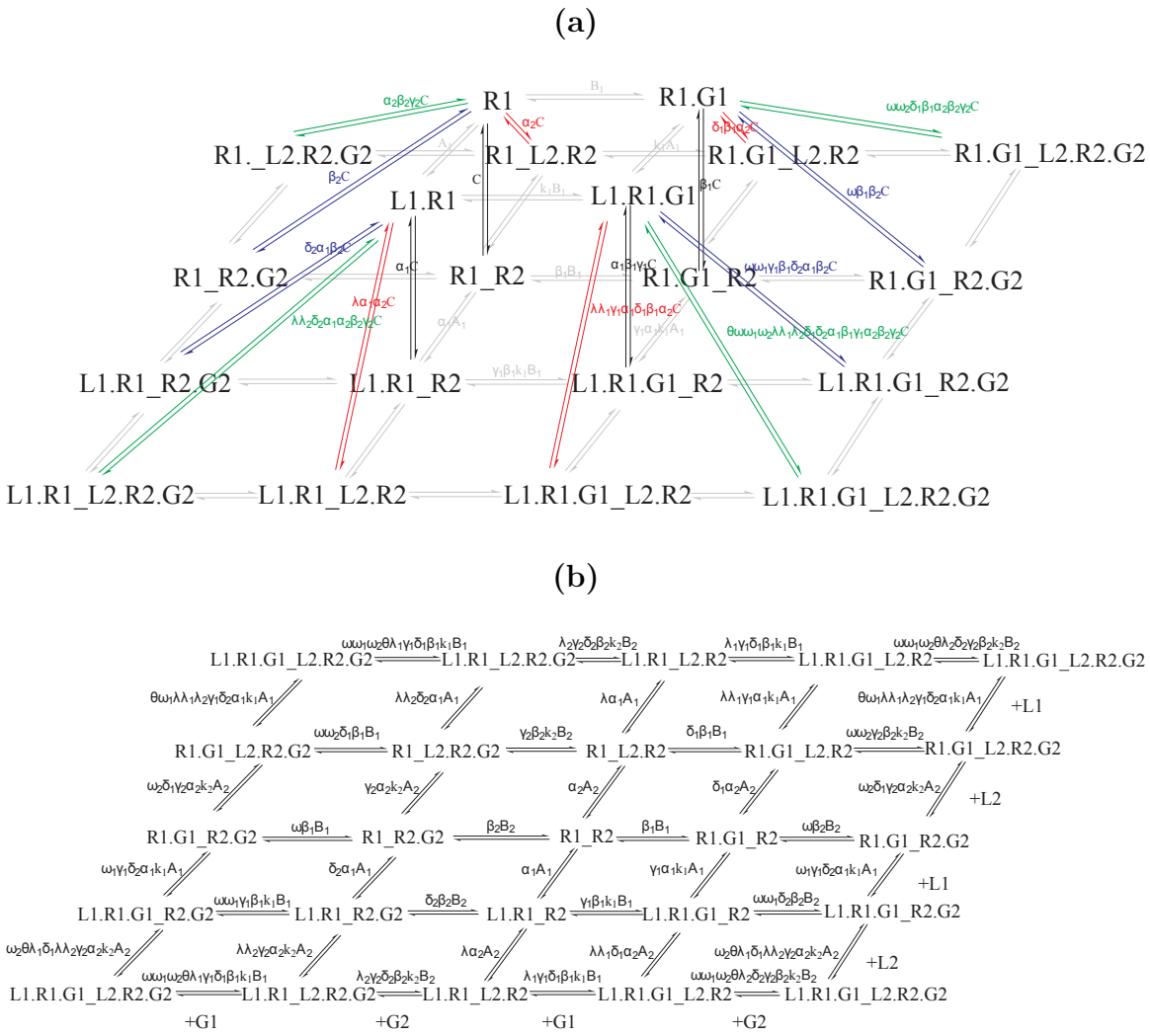

Figure 4.1: **Reaction Scheme for the Dimerization Model.** (a) The interactions between L1, R1 and G1 are shown on the top, and the bindings of ligands and receptors to the dimer are shown in the bottom. Dimerization reactions are indicated by the arrows between the top and bottom. Dissociation rate constants are shown along reactions and Greek letters are the scaling factors that can be used to control the effects of dimerization. (b) A detailed description of the bottom of the reaction scheme in (a). The dimer R1_R2 is shown in the center. Interactions of ligands and G-proteins to the dimer can have different orders, but only to their own receptor in the original model. The scaling factors are the same with the ones in (a).

4.2.2 Parameters in the model.

The forward and backward rate constants incorporated in the dissociation constants A_1, A_2, B_1, B_2 and C are maintained across all reactions. k_1 and k_2 are split and multiplied

to the forward and backward rate constants the same way as in the basic model. For example, the dissociation rate constant for the binding of L1 and R1G1_R2 is $\gamma_1\alpha_1 k_1 A_1$. $k_1 A_1$ was considered as an entity, and the forward and backward rate constants for the binding of L1 and R1G1 were used. The rate for dimerization was obtained from a study carried out by Kasai, R. S et. al. [100]. In their work, the forward and backward rate constants on a 2-D surface for the dimerization of N-formyl peptide receptors were measured using a single fluorescent-molecule imaging method. The forward rate constant $3.1(1/\mu m^2)^{-1}$/s was converted to 1.86×10^3(nM2D)$^{-1}$/s to be consistent with the units we used in the basic model.

The effects of scaling factors are carried over from reactions involving simpler species to reactions involving more complex species. For example, scaling factor $\alpha 1$ was first used to control the effect of dimerization on the binding of L1 and R1 and vice versa. As a result, the dissociation constant for the binding of R1_R2 dimer and L1 is $\alpha_1 A_1$. When R2 is pre-bound with G2 in the dimer, scaling factor α_1 is preserved in the binding of L1 to the R1_R2G2 complex, and the effect of G2 is described by an additional scaling factor $\delta 2$, resulting in a dissociation constant $\delta 2\alpha_1 A_1$. All scaling factors besides k_1 and k_2 in the reaction scheme are set to 1 initially. In other words, the binding of ligand or G-protein to the receptor is not affected by dimerization and dimerization of the receptor is not affected by the binding of ligand or G-protein in the initial model.

4.2.3 Simulation.

The full model contains all specific interactions as shown in the reaction scheme as well as nonspecific interactions. Species formed by nonspecific interactions are also considered to be able to dimerize. For example, L2R1 and L1R2 are considered to form the dimer in which R1 is bound with L2 and R2 is bound with L1 (L2R1_L1R2). The strength of nonspecific interactions was treated in the same way as described in Chapter 3. The

system contains 115 variables and 770 rate constants. Models were built in C and the systems of differential equations were solved using the cvode solver in SUNDIALS (SUite of Nonlinear and DIfferential/ALgebraic equation Solvers).

4.3 Results & Discussion

When all scaling factors are equal to 1, the bindings of ligand and G-protein to a receptor are not affected when the receptor is part of a dimer. Although two receptors form a dimer, the dimer behaves like two independent receptors. No matter whether non-specific interactions exist or not, the system acts like the two-signaling-pathways system that has been discussed in Chapter 3. We examined the effects of all scaling factors on signal level and signaling specificity at various dimer stabilities.

4.3.1 Double-peaked steady state response in the dimerization model.

First, we examined the effects of scaling factors on the 3-D steady state dose response curves when dimer stability is high. Double-peaked responses are observed as increasing the concentration of L1 for Pathway 1 for scaling when factor $\alpha 1$ and λ are small (Figure 4.2). Scaling factor $\alpha 1$ controls how dimerization and the binding of L1 and R1 affect each other. Scaling factor λ controls the effects of the binding of L1 and R1 and the binding of L2 and R2 on each other. Figures on the right are the same with the figures on the left, but rotated 90° for clarity. In Figure 4.2(a), since $\alpha 1$ only affects dimerization and the binding of L1 with R1, Signal 1 is not affected by the presence of L2. For all concentrations of L2, the dose response curves for Signal 1 as increasing the concentration of L1 contain two local peaks. For scaling factor λ, at low concentrations of L2, Signal 1 is not affected by L2 and shows a peaked behavior as previously seen in the basic model. However, a second peak appears at high concentrations of L2, while the height of the

(a) The effect of scaling factor $\alpha 1$

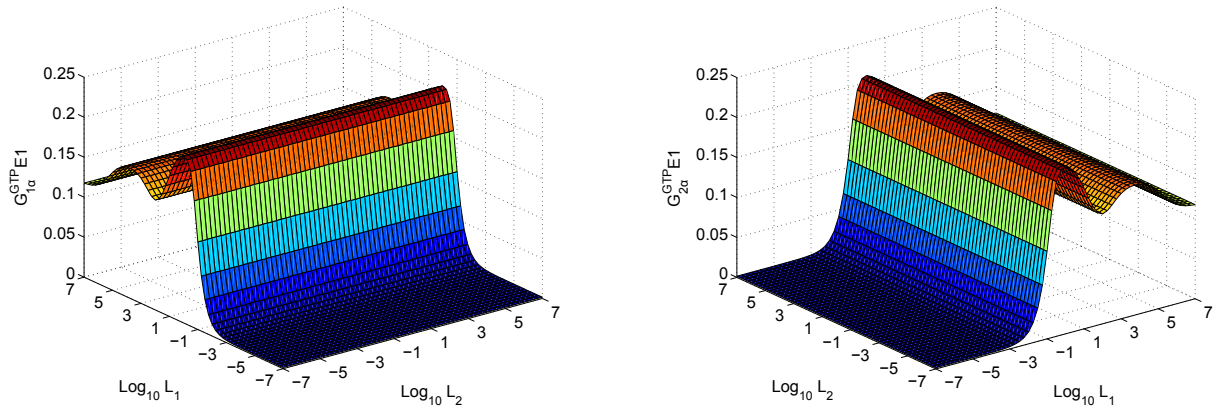

(b) The effect of scaling factor λ

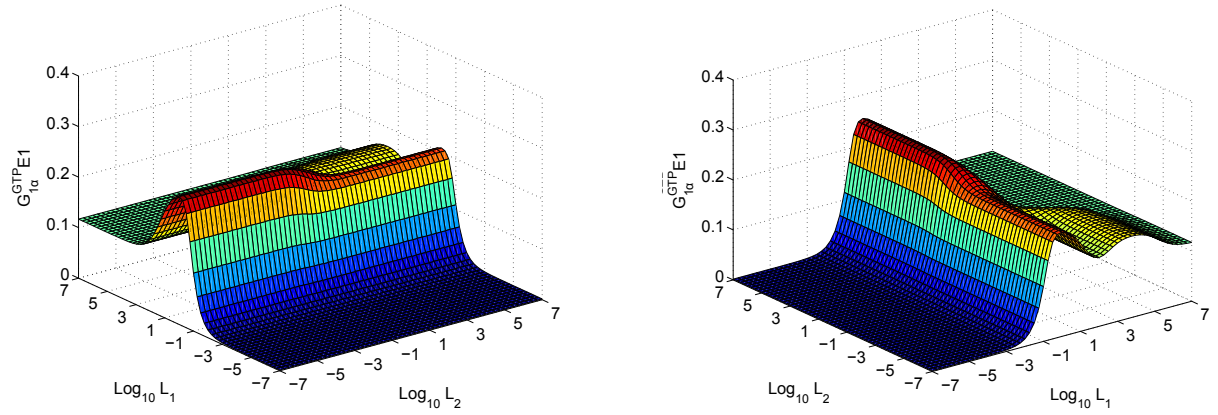

Figure 4.2: **Double-peaked steady state dose response curve.** (a) Scaling factor $\alpha 1$ controls the effects of dimerization and the binding of L1 and R1 on each other. A double-peaked dose response curve appears for Signal 1 when they inhibit each other. In addition, the double-peaked dose response curve is not affected by L2. (b) Scaling factor λ controls the cooperativity of ligand binding to the dimer. Double-peaked dose response curves are also seen for Signal 1 when the two ligands inhibit each others binding to their receptors. Unlike scaling factor $\alpha 1$, the double-peaked dose response curve is controlled by the concentration of L2 and it only appears when the concentration of L2 is high. Both figures are generated when dimer stability is increased from the origianl model (backward rate constant for the dimerization is scaled by 10^{-4}), and values for both $\alpha 1$ and λ are 10^{-4}.

first peak is reduced.

Species containing L1R1G1 complex are used to explain the double-peaked steady

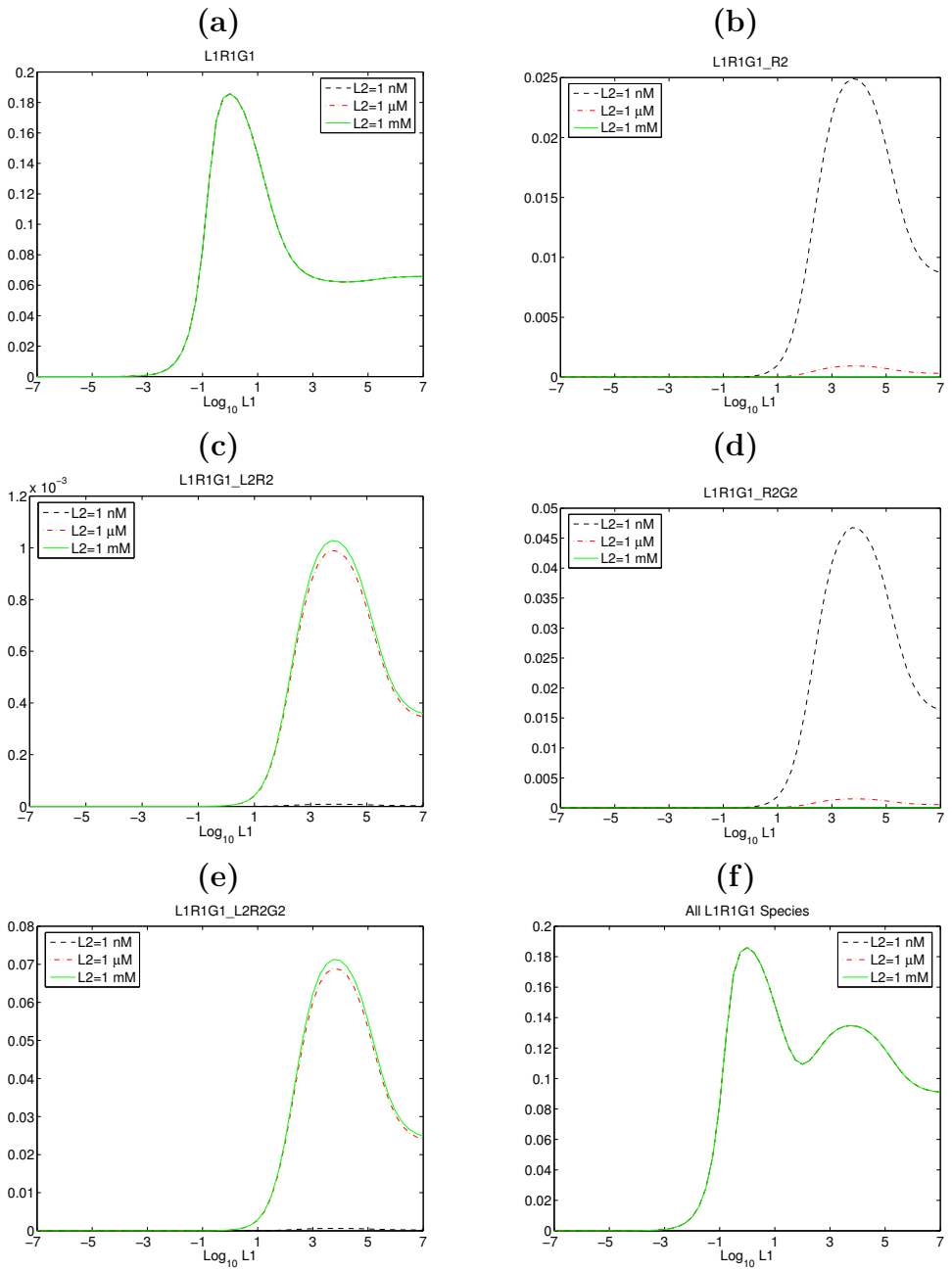

Figure 4.3: **Explanation for the effect of scaling factor $\alpha 1$.** The concentrations of all species containing L1R1G1 at various concentrations of L1 are plotted in (a)-(e) and their sum is shown in (f). Dimerization increases the concentration of L1 needed to maximize the concentration of L1R1G1 (b)-(d). Double-peaked dose response curve appears due to the combined effects of the activation by free L1R1 and the activation by L1R1 in dimer states.

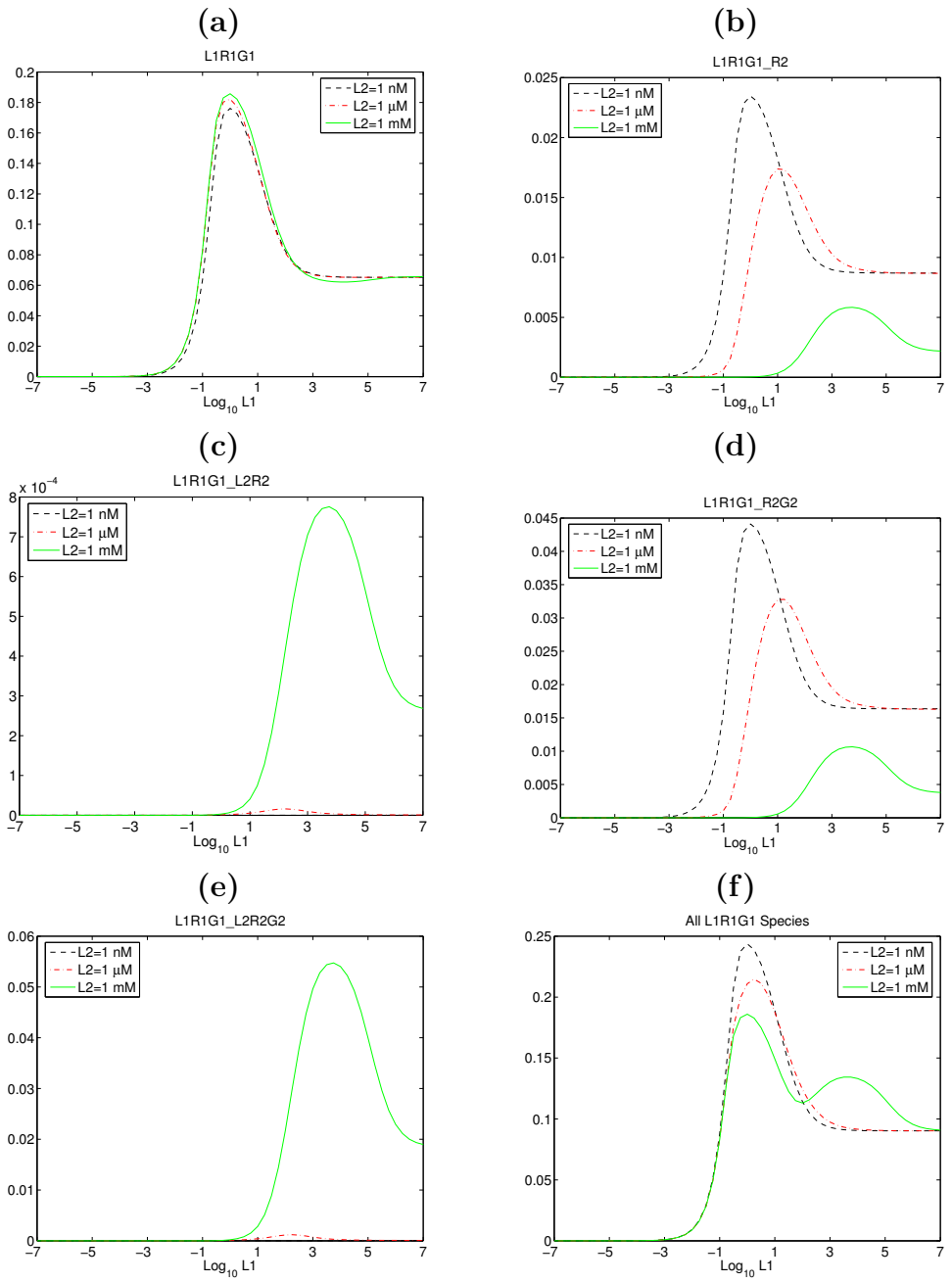

Figure 4.4: **Explanation for the effect of scaling factor λ.** The concentrations of all species containing L1R1G1 at various concentrations of L1 are plotted in (a)-(e) and their sum is shown in (f). Double- peaked dose responses appear due to the combined effects of the activation by free L1R1 and the activation by L1R1 in dimer states. It only appears at high concentrations of L2 when the binding of L1 to the R1 in the dimer is inhibited.

state dose response curve for scaling factor $\alpha 2$ and plotted in Figure 4.3. The concentration change of L1R1G1 complex without dimerization is shown in Figure 4.3(a). The receptor in L1R1G1 complex can dimerize with R2, L2R2, R2G2 and L2R2G2, and the resulting species are shown in (b)-(e), respectively. The effect of the presence of L2 is also examined, and 1 nM, 1 μM and 1 mM L2 were used for illustration. Since L2 does not affect the dimerization of R1 and R2, the ratio between free L1R1G1 and L1R1G1 dimerized with R2 is not changed by L2. However, L2 changes the distribution of R2 among different binding states. When the concentration of L2 is low, R2 is either in its free state or pre-coupled with G-protein, resulting in a relatively high concentration of L1R1G1_R2 and L1R1G1_R2G2 (Figure 4.3(b)(d)). At high concentrations of L2, R2 is occupied by L2 and in consequence, the concentrations of L1R1G1_L2R2 and L1R1G1_L2R2G2 are high. All LRG species show peaked behavior as increasing the concentration of L1 in the presence of different concentrations of L2. However, the concentrations of L1 at which the peaks are reached are not exactly the same. About 1 μM L1 maximize the concentration of free L1R1G1 complex. The concentrations of L1 needed for other species containing L1R1G1 complex to reach the maximum are significantly higher, but all around 10 mM. This is due to the negative effect of dimerization on the binding of L1 to R1. Since G-protein activation is assumed not to be affected by dimerization, the direct sum of all LRG species can reflect the signal level to some extents (Figure 4.3(f)). The first peak in the dose response curve of Signal 1 comes from the activation by LR complex without dimerization, while the activation by the dimer contributes to the second peak.

The same species are plotted in Figure 4.4 to explain the double-peaked steady state response resulted at high concentrations of L2 for scaling factor λ. The concentrations of LRG complex without dimerization at different concentrations of L1 are not dramatically affected by the presence of L2 (Figure 4.3(a)). However, when R1 in the L1R1G1 complex is dimerized with R2, both the magnitude of the peak and the concentration of L1 at

which the peak is reached are affected (Figure 4.3 (b)-(e)). Since the binding of L2 to R2 has a negative effect on the binding of L1 and R1, more L1 is required to reach the peak when the concentration of L2 is high. The shape of the dose response curve is determined by the sum of all L1R1G1 species. When the concentration of L2 is low, the peak of the dose response curve is caused by the activation by L1R1 complex without dimerization. The shape of the curve resulted from summing two bell-shaped curves depends on the distance between the two peaks. At low concentrations of L2, the two peaks are close to each other and the final curve only has one peak, although the height and the concentration of L1 at which the peak is reached may be affected. However, when the concentration of L2 is large, two peaks are well separated and the resulting curve has two peaks.

4.3.2 The effect of dimerization on signaling specificity.

In the next step, we examined how signaling specificity can be affected by dimerization. In Figure 4.5 - Figure 4.8, each column represents a different type of basic interactions and the dimer stability is varied across rows. In each panel, specificity scores are shown at various strengths of interactions. The values of interested scaling factors are labeled using different symbols. The specificities of Pathway 1 and Pathway 2 are shown in black and red, respectively. The dimer stability decreases from the top row to the bottom row. When the dimer stability is low, R1 and R2 primarily stay as monomers and the system should behave in the same way as the two-pathways systems described in Chapter 3. For each column, when the scaling factor is 1, the dimer behaves like two independent monomers no matter of its stability. Thus, curves labels with "+" in each panel containing the same data and can serve as a reference to show the effect of dimerization.

Scaling factor $\alpha 2$

The effect of dimerization on specificity depends on how ligand binding and G-protein

binding are affected by dimerization, as well as the nonspecific bindings existing in the system. The maximum and minimum specificities considering the effect of scaling factor $\alpha 2$ are shown in Figure 4.5 and Figure 4.6. $\alpha 2$ controls how the binding of L2 to R2 and dimerization affect each other. The effects of dimerization are also applied to the nonspecific interactions. For example, if L1 can interact with R2, their binding is also affected by the scaling factor $\alpha 2$.

Specificity scores for interaction L1R1G2E2 are not affected by dimerization since dimerization only affect the binding of ligands to R2 and L1 does not directly interact with R2 (1^{st} column in Figure 4.5 and Figure 4.6). For interaction L2R2G1E1, L2 does not directly interact with R1 and both G1 and G2 are activated by L2R2. Although dimerization hinders the binding of L2 and R2, same L2R2 can be reached at a higher concentration of L2 and both G1 and G2 are still activated in the same way as before. As a result, specificity scores are not affected by dimerization (6^{th} column in Figure 4.5 and Figure 4.6). For these two interactions, the only factor affects the specificity of the two pathways is the strength of interactions.

For interaction L1R2G1E1, the effect of L1 on Pathway 2 is exerted by binding with R2 and inhibits its signaling. When the stability of the dimer is high, signaling specificity of Pathway 1 is affected by scaling factor $\alpha 2$. If dimerization enhances the binding of L1 and R2, Signal 2 is more easily affected and specificity of Pathway 1 will be reduced. On the opposite, if the binding of L1 with R2 is hindered by dimerization, specificity of Pathway 1 will be increased (2^{st} column in Figure 4.6). For interaction L2R1G2E2, although the binding of L2 to R2 is hindered by dimerization, specificity of Pathway 2 is not affected since both of R1 and R2 activate G2 (5^{th} column in Figure 4.5 and Figure 4.6).

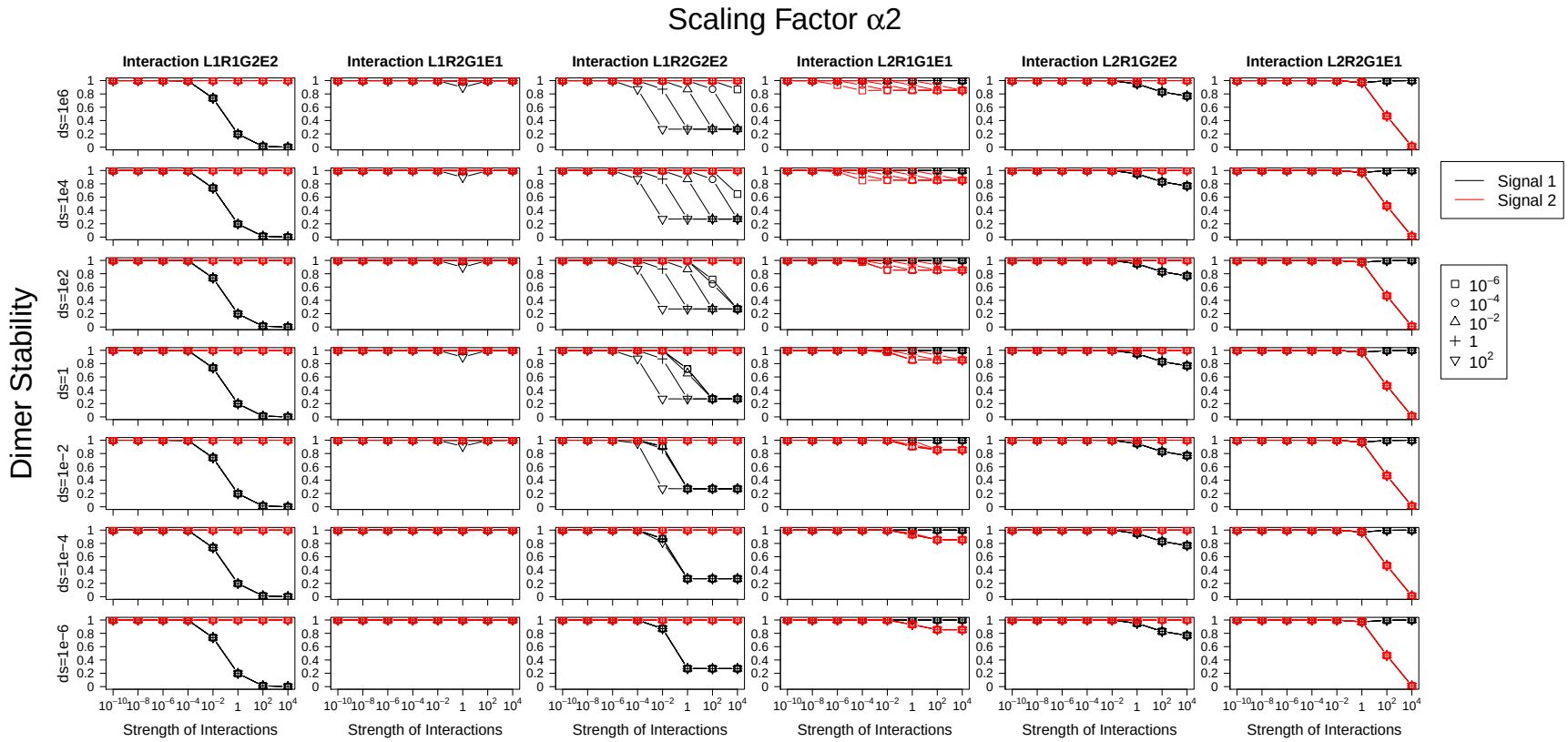

Figure 4.5: **The effects of dimerization on the maximum signaling specificity when scaling factor $\alpha 2$ is considered.** Each column represents a basic interaction and the dimer stability is varied across rows. In each panel, the strengths of interactions are plotted along the x axis and the values of the scaling factor are shown using different symbols. $\alpha 2$ controls the effects of the binding of R1 and R2 and the binding of L1 and R1 on each other.

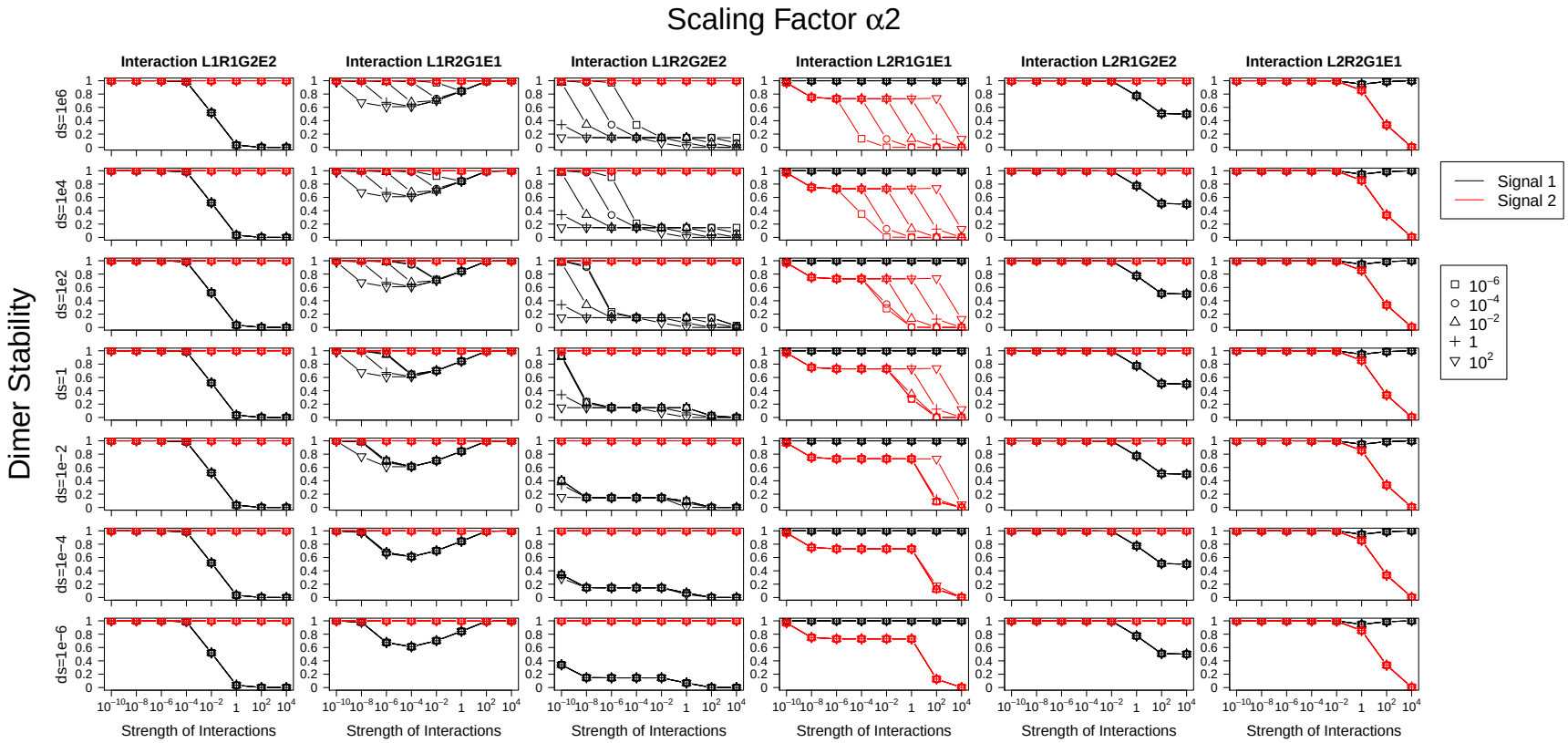

Figure 4.6: **The effects of dimerization on the minimum signaling specificity when scaling factor $\alpha 2$ is considered.** Each column represents a basic interaction and the dimer stability is varied across rows. In each panel, the strengths of interactions are plotted along the x axis and the values of the scaling factor are shown using different symbols. $\alpha 2$ controls the effects of the binding of R1 and R2 and the binding of L1 and R1 on each other.

For interaction L1R2G2E2, when dimer stability is high, specificity of Pathway 1 is decreased if the binding of L1 and R2 is enhanced by dimerization. If the binding of L1 and R2 is inhibited by dimerization, specificity of Pathway 1 is increased (3^{th} column in Figure 4.5 and Figure 4.6). Opposite effects are observed for interaction L2R1G1E1. Since the binding of L2 and R1 is not affected by dimerization, specificity of Pathway 2 is decreased if the binding of L2 and R2 is inhibited. If dimerization facilitates the binding of L2 and R2, specificity of Pathway 2 can be increased (4^{th} column in Figure 4.5 and Figure 4.6).

Scaling factor λ has a similar effect as scaling factor $\alpha 2$ does. Instead of being controlled by the dimerizations of any forms of receptors, the binding of a ligand to a receptor in a dimer is only affected when the other receptor in the dimer is also bound with a ligand. One difference between λ and $\alpha 2$ is that for interaction L1R2G2E2, specificity is not significantly affected by λ since dimerization has the same effect on the binding of L1 and R1 and the binding of L1 and R2.

Scaling factor $\delta 2$

The binding of ligand and the receptor on one side of the dimer may also affect the binding of G-protein and the receptor one the other side, and vice versa. This effect is controlled by scaling factors $\delta 1$ and $\delta 2$ in the model. Figure 4.7 and Figure 4.8 show the maximum and minimum specificity scores under the controls of scaling factor $\delta 2$, which adjust the effects of the binding of L1 and R1 and the binding of R2 and G2 on each other.

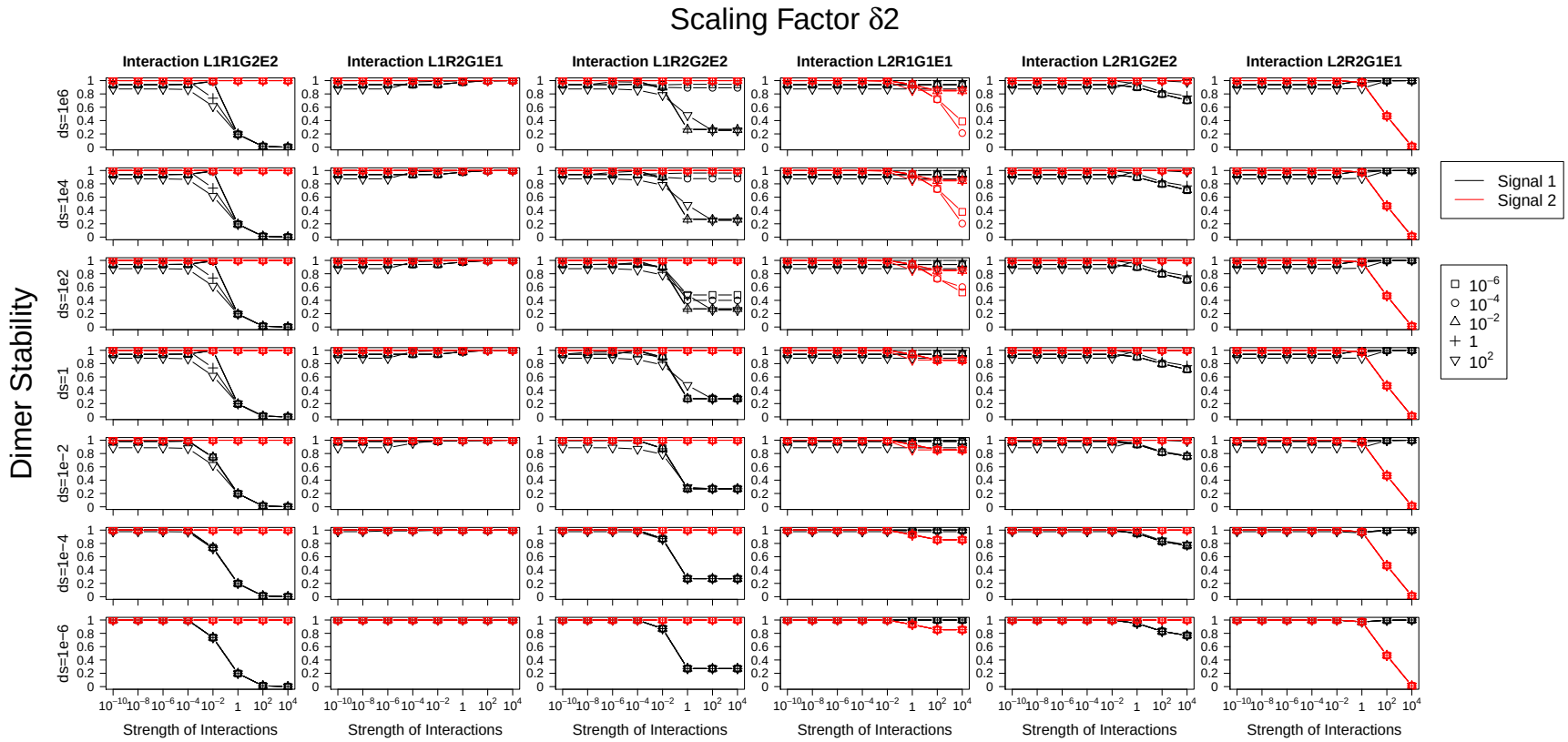

Figure 4.7: **The effects of dimerization on the maximum signaling specificity when scaling factor $\delta 2$ is considered.** Each column represents a basic interaction and the dimer stability is varied across rows. In each panel, the strengths of interactions are plotted along the x axis and the values of the scaling factor are shown using different symbols. $\delta 2$ controls the effects of the binding of L1 and R1 and the binding of R2 and G2 on each other.

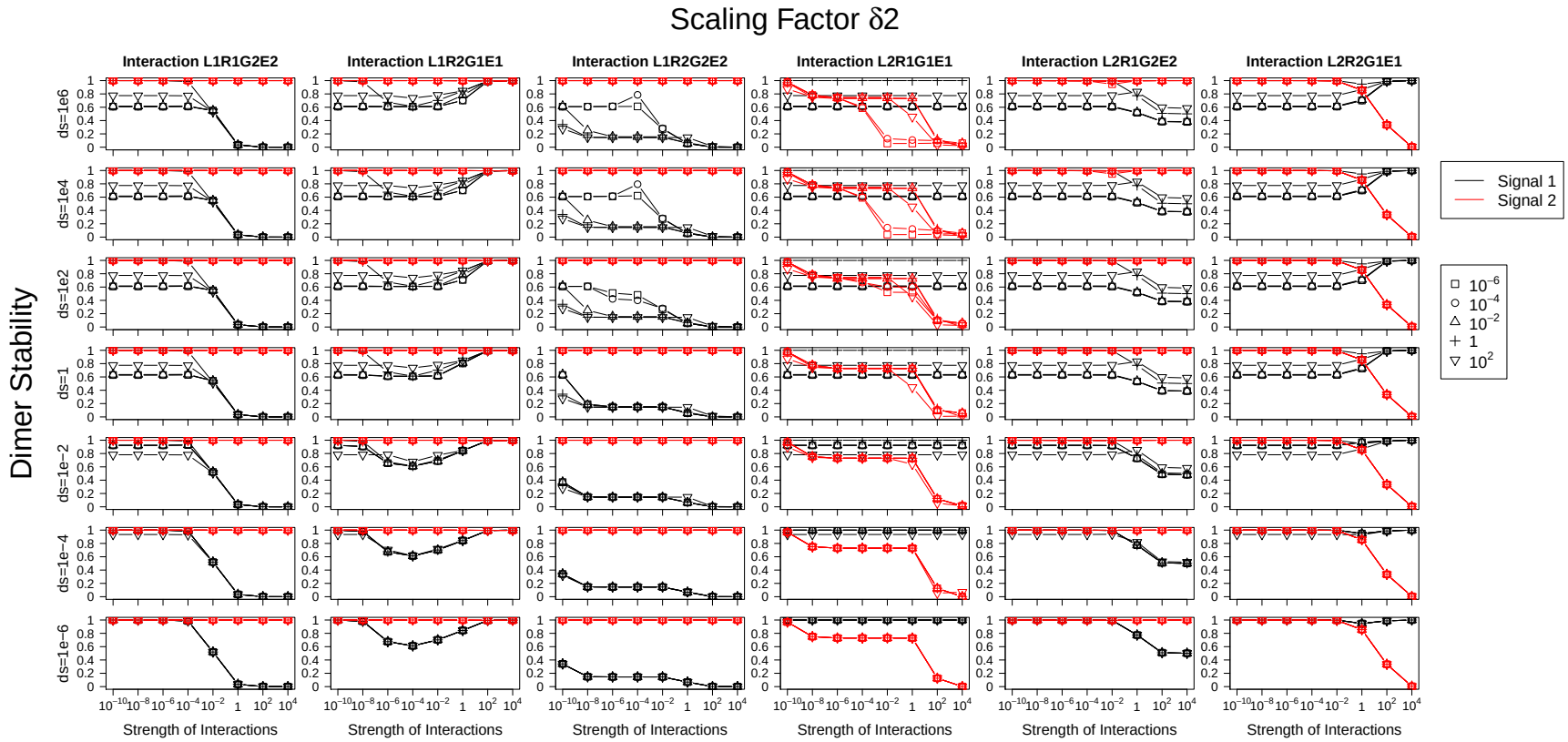

Figure 4.8: **The effects of dimerization on the minimum signaling specificity when scaling factor $\delta 2$ is considered.** Each column represents a basic interaction and the dimer stability is varied across rows. In each panel, the strengths of interactions are plotted along the x axis and the values of the scaling factor are shown using different symbols. $\delta 2$ controls the effects of the binding of L1 and R1 and the binding of R2 and G2 on each other.

For all nonspecific interactions shown in Figure 4.7 and Figure 4.8, when the dimer stability is high (1^{st} row), the specificity of Pathway 1 is affected even when the strengths of interactions are weak. This is because L1 can be considered as an allosteric modulator for the binding of R2 and G2. Signal 2 can be affected when G2 binding to the R2 in the dimer is regulated by L1. The specificity can be changed even without nonspecific interactions.

For interaction L1R1G2E2, when the dimer stability is high (1^{st} row, 1^{st} column in Figure 4.7 and Figure 4.8), specificity of Pathway 1 can be decreased by both increasing and decreasing $\delta 2$. Perturbations of $\delta 2$ away from 1 causes either increases or decreases in Signal 2. Since the effect of L1 on Signal 2 is measured as changes compared to the basal level of Signal 2, no matter Signal 2 is increased or decreased, the specificity of Pathway 1 is decreased. When the strength of interactions is increased (greater than 10^{-2} for the minimum specificity), the effects of L1R1 activating G2 becomes the major effects of L1 on Signal 2, so the specificity of Pathway 1 is unchanged when $\delta 2$ is varied. For interaction L2R2G1E1, specificity of Pathway 1 has a similar behavior for the same reason. Specificity of Pathway 2 is basically not affected.

For interaction L1R2G2E2, specificity of Pathway 1 can be increased by decreasing scaling factor $\delta 2$ when the dimer stability is high and the strength of interactions is weak (1^{st} row, 2^{nd} column in Figure 4.7 and Figure 4.8). Direct activation of R2 by L1 can have a strong negative effect on the specificity of Pathway 1. However, the effect is alleviated if the binding of R2 and G2 are inhibited by L1 and specificity of Pathway 1 is increased. For interaction L2R1G1E1, the specificity of Pathway 2 is reduced by decreasing $\delta 2$. Since L2 is considered the same as L1, the binding of R2 can G2 can also be inhibited by the binding of L2 and R1. The decrease in the specificity of Pathway 2 is caused by the reduction in the activation of Signal 2.

4.4 Conclusions

In summary, we have established a model containing heterodimerization between the receptors in the two signaling pathways. A double-peaked dose response curve is observed due to the combined activation of the monomer and the dimer. Signaling specificity can also be affected when the dimer stability is high and allosteric regulations exist.

In this study, we primarily focused on the effects of dimerization on the binding reactions. G-protein activation is assumed not to be affected by dimerization. For example, binding of L1 to R1 in the dimer is assumed not to change the rate of G-protein activation by R2. There is a possibility that R2 in the dimer undergoes a conformation change due to the binding of L1 and R1, and accelerates or decelerates G-protein activation. Changes in specificity may also be observed without non-specific interactions, similar as for scaling factors $\delta 1$ and $\delta 2$.

The relative concentrations of the two receptors also play a role in controlling signaling when dimerization exists. For the double-peaked dose response curve we observed, one requirement is that the concentration of R1 is greater that the concentration of R2. R1 will primarily stay in the dimer state if its concentration is much smaller than the concentration of R2. Since the first peak is generated due to the activation by free L1R1 complex, Signal 1 will only have one peak which is caused by the activation of L1R1 in dimer state.

The model described here is for heterodimerization, where the two receptors are different. A homodimerization model can be derived directly by considering that the two receptors are the same. Nonspecific interactions should be considered in the model and the final product can be obtained by summing up the two receptor species. For example, the concentration of LR complex in a homodimerization model can be obtained by summing up L1R1 and L1R2 in the heterodimerization model. However, the rate

constants for homodimerization needs to be adjusted since the two receptors are the same, and [R1][R2] in the original model does not describe the frequency of collisions accurately.

Chapter 5

Modeling Internalization of Receptors in GPCR Signaling Pathways

5.1 Introduction

G-protein-coupled receptor signaling can be down-regulated by the desensitization and internalization of the active receptors [101, 102, 103, 104, 105]. A series of steps are involved in this process and illustrated in Figure 5.1 (Figure adapted from the work of Nagi and Pieyro [106]). The down-regulation of signaling starts from the phosphorylation of the receptor and it is usually mediated by the G-protein-coupled receptor kinases (GRKs) (Figure 5.1 ①). Phosphorylation of the receptor promotes the interaction between the receptor and β-arrestins (Figure 5.1 ②). The receptor is desensitized and signaling is hampered. The binding of β-arrestins then initiates the internalization of the receptor via clathrin-coated pits (Figure 5.1 ③). Once inside the cell, receptor is either degraded (Figure 5.1 ⑤) or recycled back to the cell membrane (Figure 5.1 ④).

The desensitization and internalization of different receptors can be regulated differently due to specific regulations by GRKs or β-arrestins. GRKs can be divided into 3 main families [107]. Although both GRK2 and GRK3 belong to the β-adrenergic receptor kinases family, α_1-adrenergic receptor is preferentially regulated by GRK3 in cardiac myocytes [108]. β-arrestin2 can regulate β2-adrenergic receptor signaling. However, knockout of β-arrestin2 has no effects on muscarinic receptor signaling and prostaglandin E_2 receptor signaling in human airway smooth muscle [109].

Desensitization and internalization of GPCRs have been studied using mathematical models previously. In an early work of Riccobene et. al. [110], the desensitization of the receptor was considered in an extended ternary complex model (eTCM) and the effects

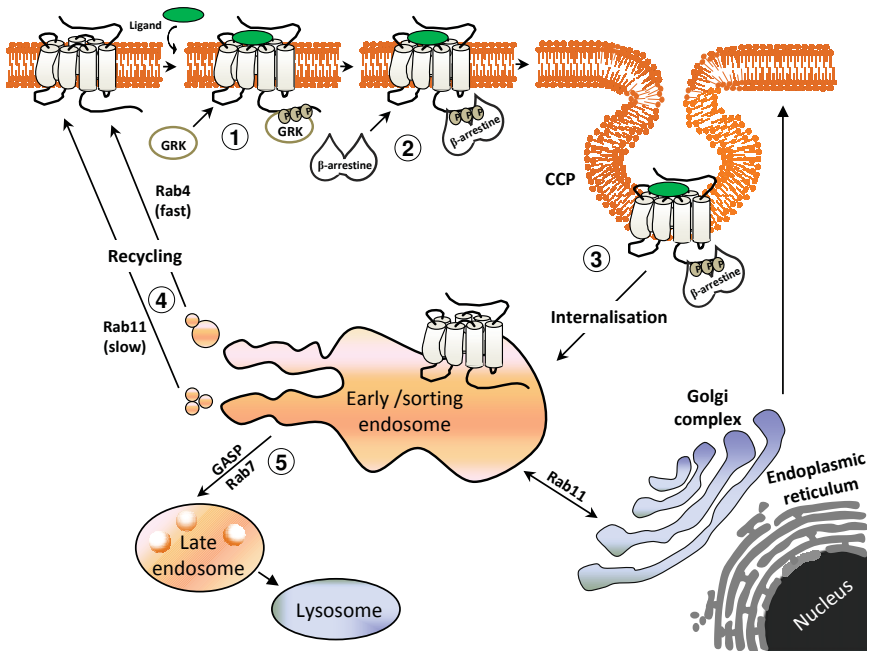

Figure 5.1: **Desensitization and internalization of GPCRs.** GPCR signaling can be down-regulated by the desensitization and internalization of the receptor. The active receptor can first be phosphorylated by GRKs (1), followed by the binding of β-arrestin (2) and clathrin-mediated endocytosis (3). Internalized receptors will either recycle back to the membrane (4) or traffic towards degradation (5). This figure is taken from [106].

of ligand-specific parameters on the activation and desensitization of the receptor were studied. Vayttaden et. al. built a model for the trafficking of β2-adrenergic receptors and demonstrated that receptor desensitization induced by previous stimulations can be memorized for subsequent stimulations [111]. Internalization was incorporated in a model combining ordinary differential equations and stochastic equations developed by Fallahi-Sichani et. al. for investigating the distributions of receptors on the cell membrane [53]. In two consecutive papers of Maurya and Subramaniam, a kinetic model for calcium dynamics in RAW 264.7 cells stimulated by the C5a ligand was developed and effects of the knockdowns of molecules in the system was investigated. Receptor desensitization and internalization are included in their model and the knockdown of GRKs were shown to be able to increase the peak and the duration of the signal [112, 113]. Heitzler et. al. used a mathematical model to demonstrate the negative effect of GRK2 on β-arrestin-

dependent signaling due the competition with GRK5/6 for receptor phosphorylation [114]. To the best of my knowledge, no model has been built to understand the effects of receptor cycling on signaling specificity.

In this chapter, we first extended the basic model by adding the internalization of the receptor to the model. A double-peaked dynamical response is observed and explanations are provided. The trafficking of the receptor on and off the cell membrane plays a critical role in controlling this behavior. Internalization was then added to the two-pathways model and its effect on signaling specificity is investigated.

5.2 Model description

The basic model was first extended by considering the internalization of the receptors. In this Chapter, we will mainly focus on a simplified model in which receptor inside the cell is explicitly modeled and receptor phosphorylation, arrestin binding and internalization are lumped together and described by a single reaction. The reaction scheme for the model is shown in Figure 5.2. In the absence of ligand, a basal rate for the internalization of the receptors is considered (k16). When the receptor is bound with ligand, the rate of internalization is increased and modeled using a first order equation with respect to the concentration of LR complex on the cell membrane (k17). Rin in the reaction scheme describes all receptors inside the cell, and its concentration is increased in the same rate as the internalization. Receptor degradation and production are not explicitly modeled, assuming they are balanced and the total concentration of the receptor is not changed. The rate for the trafficking of receptors to the cell membrane is also described using a first order equation and proportional to the concentration of Rin (k15). The rate constants for the new reactions were adapted from the work of Vayttaden et. al. [111]. Variations of the rates for the new reactions were carried out and their effects on the dynamics of the signal were investigated.

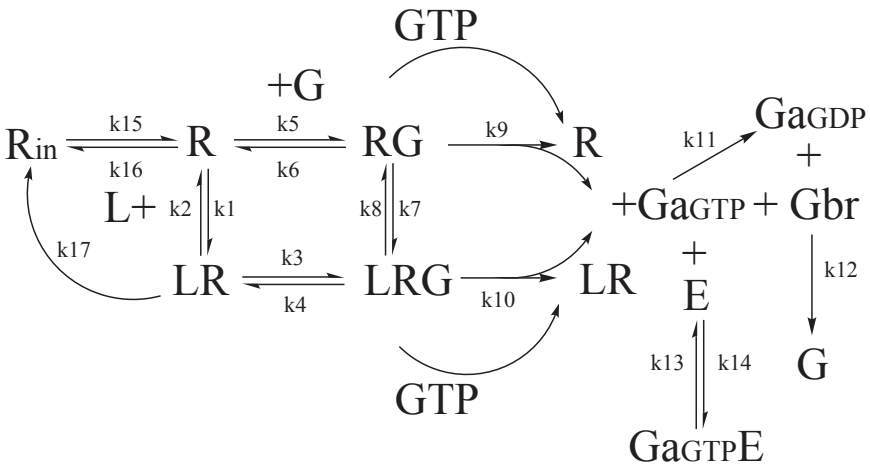

Figure 5.2: **The reaction scheme for the internalization model.** Constitutive and ligand-induced internalization of the receptors are added to the basic model, as well as the recycling of the receptor. Rate constants were adapted from [111] (k15=3.67×10^{-3}/s, k16=1.42×10^{-4}/s, k17=1.5×10^{-3}/s))

In the next step, internalization of the receptors is added to the two-pathways model. In the initial model, internalization of the receptor from one pathway induced by the ligand from the other pathway is considered to have the same rate constant as by its own ligand. Specificities of the two pathways were calculated and how they are affected by the rates of the internalization of two receptors was examined. Same formula for calculating specificity described in Chapter 3 was used. However, instead of the steady state signal, the area under curve of the dynamics of the signal is used as the measure of signal level. The area under the curve is estimated using a trapezoidal rule. Same cutoff as used in calculating the specificity based on the steady state signal level (1%) was applied and calculations were performed only when the change of the signal is above the cutoff. The trafficking of receptors usually takes place on a minutes to hours time scale [105, 115]. Since parameter variations may affect this time scale, we used a longer time (10 days) was used the total time for all simulations. If the system restores back on a short time scale, the amount of signal will not be affected as extending the total simulation time. We also checked that the specificity score calculated using the current total simulation

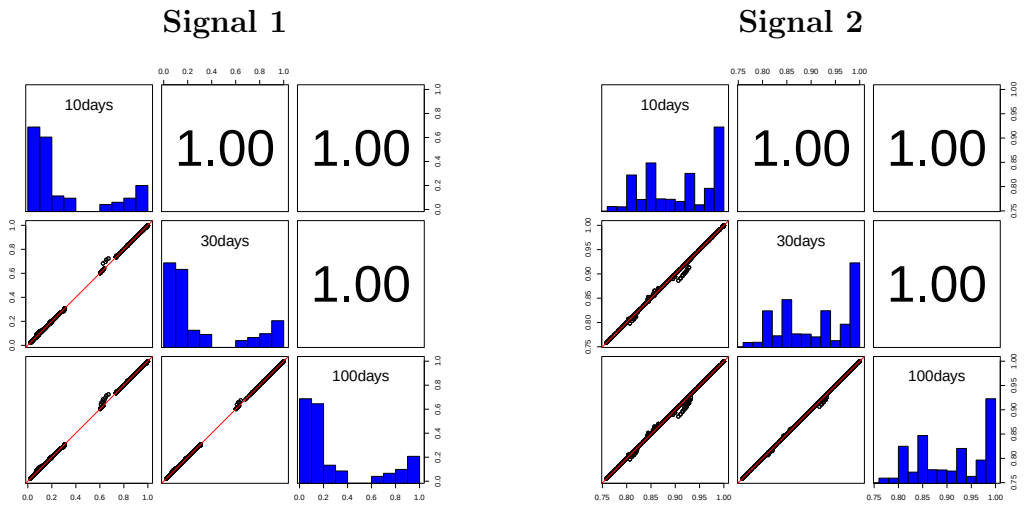

Figure 5.3: **Correlations between specificity scores calculated using different simulation times.** 10 days, 30 days and 100 days were used as the total time for simulations. 57 ligand concentrations ranging from -7 to 7 on log scale and 64 different interactions were considered. Specificity scores calculated using different total simulation time are similar, and 10 days were used for following calculations.

time is not dramatically affected when the simulation time is increased. We compared the specificity scores calculated using 10 days, 30 days and 100 days as the total simulation time and the result is shown in Figure 5.3. For the 64 different combinations of the 6 basic interactions, specificity scores calculated at 57 different ligand concentrations in the absence of the other ligand were plotted. For both model 1 and model 2, although small changes are observed for some interactions and ligand concentrations, the overall agreement is satisfactory.

The system contains 46 variables and 80 rate constants. Models were built in C and the systems of differential equations were solved using the cvode solver in SUNDIALS (SUite of Nonlinear and DIfferential/ALgebraic equation Solvers).

5.3 Results & Discussion

Double-peaked dynamical response in the internalization model.

We first examined the dynamics of the signal in the basic model with internalization of the receptor added. Due to the internalization of the receptor, all ligands will finally be washed out when time is long enough and signal will return to the basal level. A peaked dynamical response would be expected resulting from ligand activation and degradation. Interestingly, the dynamics of the signal in model 1 has two peaks (Figure 5.4(a)). The signal is first increased after ligand addition and decreased over time. However, instead of dropping directly to the basal level, the signal is increased again before the final decay. The trafficking of receptors is shown in Figure 5.4(b) and (c) to help to understand this behavior. In the short time scale (Figure 5.4(b)), the concentration of receptor is dropped quickly due to the binding with ligand (blue). In the mean while, the concentration of LRG is increased (red), which results in the initial increase of the signal. However, due to the internalization of the receptor, the concentration of the receptor on the cell membrane is decreased over time while the concentration of the receptor inside the cell is increased (green). Due to the removal of the ligand from the system, the rate of internalization is reduced overtime and receptors inside the cell are slowly moving back to the cell membrane (Figure 5.4(c)). As a result, the concentration of LRG is increased again, which causes the second increase in the signal. Finally, the signal returns to the basal level when all ligands are removed from the system.

The double-peaked dynamical response can be controlled by multiple factors and the concentration of ligand is one of them. The levels of the two peaks and time to reach them are shown in Figure 5.5 (a) and (b). The height of the first peak can be controlled by the concentration of the ligand (blue). It shows a peaked behavior as previously seen in the basic model. The second peak appears only when the concentration of the

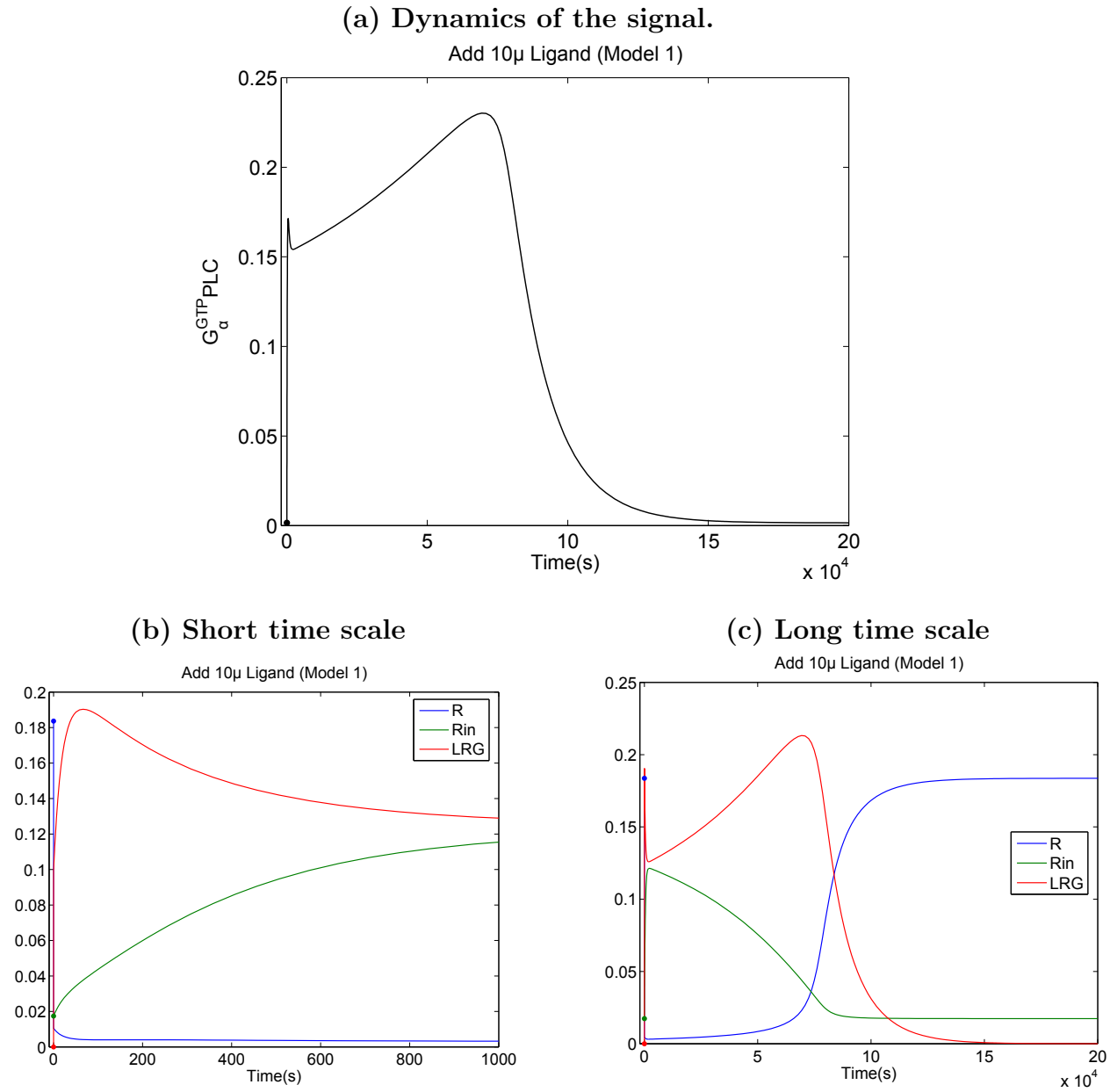

Figure 5.4: **Double-peaked dynamical response.** (a) When internalization of the receptor is considered in the system, the dynamics of the signal in model 1 shows two peaks during the time course. Short time scale (b) and long time scale (c) of the receptor trafficking are plotted. The first peak is related to the internalization of the receptor while the second is affected by the recycling of the receptor.

ligand exceeds a threshold, and its magnitude is not affected by the total concentration of ligand initially added to the system. The first peak is reached at about the same time for different concentrations of ligands, while it takes longer for the second peak to appear

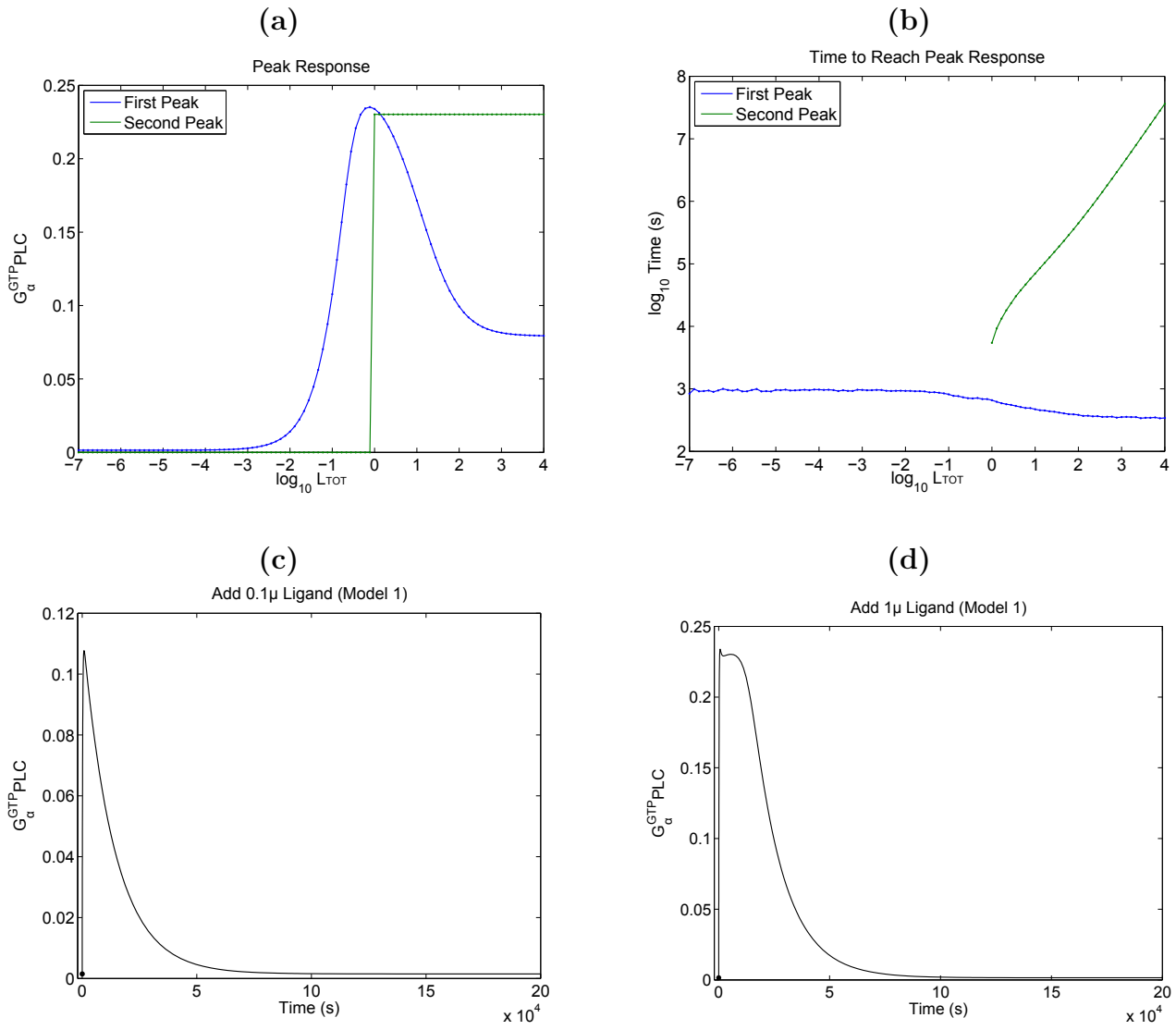

Figure 5.5: **Time and level of the two peaks.** For both figures, the first peak is shown in blue and the second peak is shown in green, if it exists. (a) The level of the first peak is high at intermediate ligand concentration, while low at both high and low ligand concentrations. The second peak only appears when the concentration of ligand is large and the level is about the same. (b) For different ligand concentrations, the first peak is reached at about the same time. while for the second peak, the time it takes to appear increases approximately linearly with the concentration of ligand. (c) Dynamics of the signal as adding 0.1 μ ligand to the system. (d) Dynamics of the signal as adding 1 μ ligand to the system.

when the concentration of ligand is increased. The changes in the levels of the peaks and the time it takes to reach the peaks as changing the concentrations of ligand are

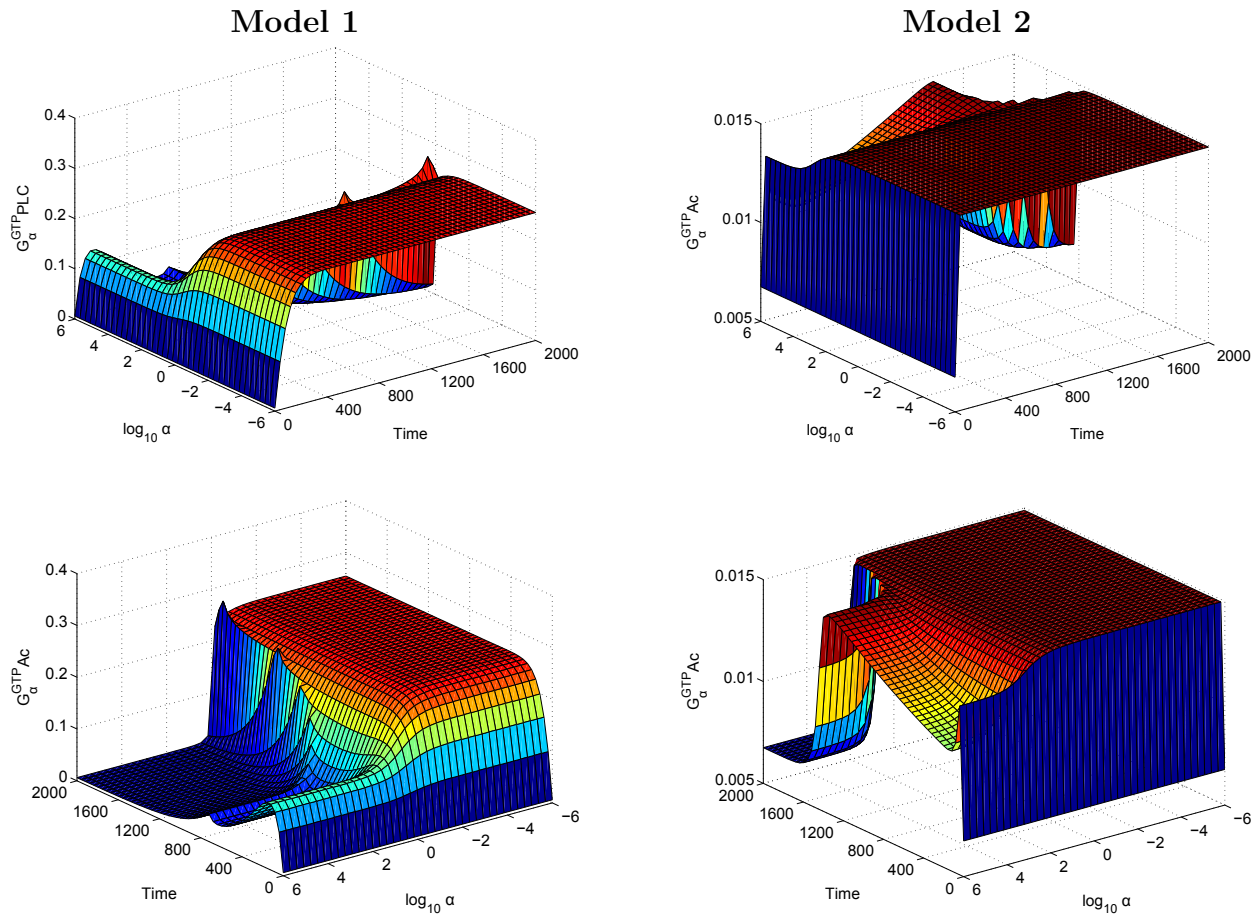

Figure 5.6: **Control of the double-peaked dynamical response.** The rate constant for the ligand-induced internalization (k17) is varied across the x-axis. For both models, double-peaked dynamical response can be observed when the rate of internalization is large. Parameters used here: k15=1/s, k17=1/s for both models, [R1]=1.5 nmol/m^2, [R2]=0.83 nmol/m^2. Other parameters are left unchanged.

illustrated in Figure 5.5 (c) and (d) together with Figure 5.4 (a).

Other factors including the total concentration of the receptor, the rate for internalization and the rate for recycling can also affect the double-peaked dynamical response. Using the original parameters, the double-peaked dynamical response is only observed in model 1. However, by adjusting the parameters associated with the receptor, double-peaked dynamical response can also be obtained in model 2. In Figure 5.6, the impact of the rate of internalization on the dynamical response is demonstrated. Model 1 is shown

on the left and model 2 is shown on the right. The bottom two figures are identical with the top two but rotated for clarity. Since signals at the same time points are needed for the plot and a large number of points reduce the clarity, the peak signal level may not reflect with true maximum of the signal. However, the qualitative behavior should be preserved. Individual simulations at extreme values were also carried out using adaptive time step method to make sure the qualitative behavior is correctly captured. For model 1, double-peaked dynamical response is only observed when the rate of internalization is large. Small rate of internalization inhibit the first peak, while in between the time it takes to reach the second peak is affected by the rate of internalization. Similar behavior is also observed in model 2. When the rate of internalization is low, signal level is directly increased to the maximum and decreased overtime when ligands are removed. However, double-peaked dynamical responses are observed at high rates of internalization. Since the maximum response in model 1 is observed at moderate ligand concentration, during the process of ligand removal, a second peak is more easily to be observed. However, the trafficking of receptors between cell membrane and cytoplasm plays a critical role in controlling the double-peaked dynamical response. A fast internalization result in the initial decrease in the signal. The second increase is caused by the increase in the concentration of the receptor on the cell membrane due to recycling. As long as this mechanism is achieved by properly adjusting the concentration of the receptor and the rates for the internalization and recycling, the double-peaked dynamical response can be obtained.

5.3.1 The effect of internalization on signaling.

In the next step, we examined how signaling specificity can be affected by internalization. Here, we mainly focused on the rate of ligand induced internalization and the effects of nonspecific interactions, left the rates of intrinsic internalization and recycling unchanged. Specificity scores were calculated as described in the method section. For the 6 basic

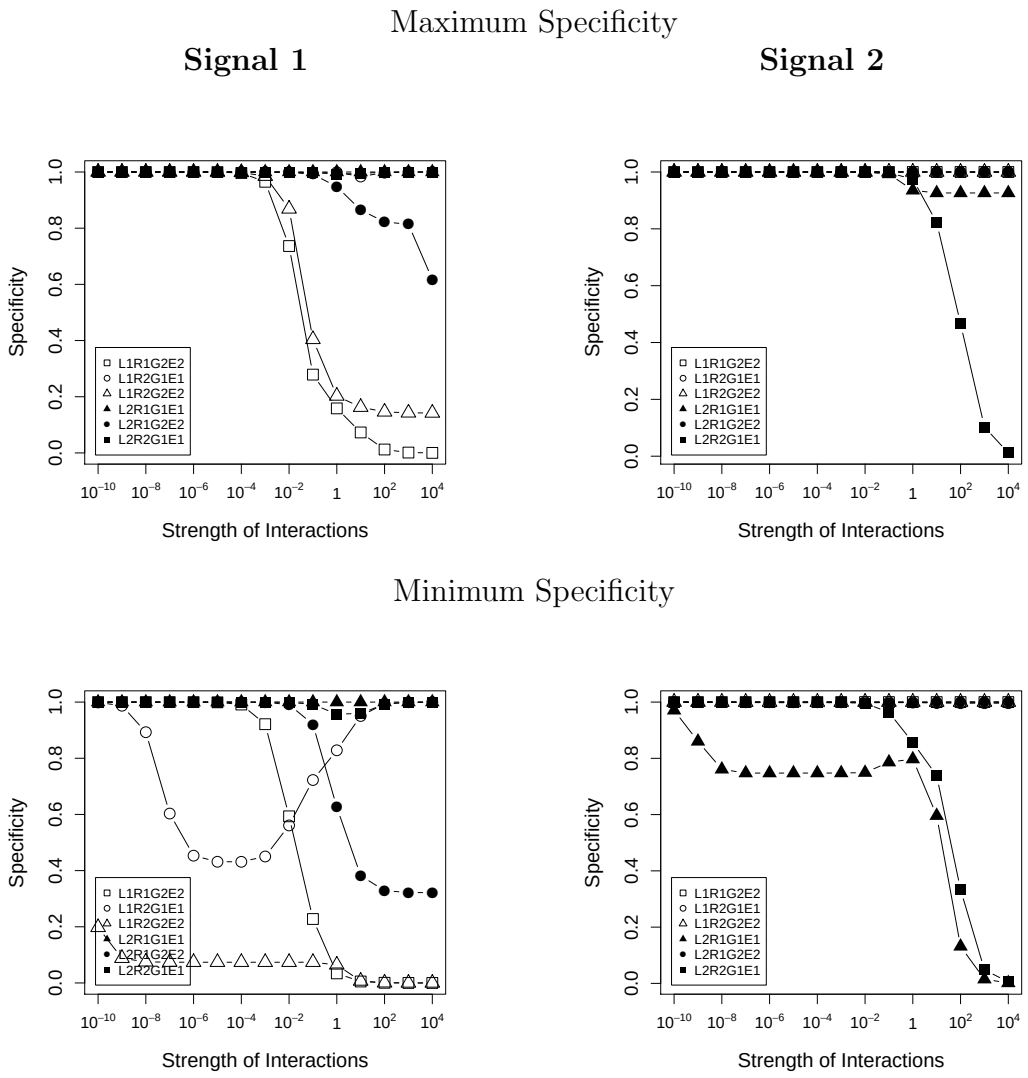

Figure 5.7: **Specificity for the dynaimcs of the signal.** The strengths of the 6 basic interactions are varied along the x-axis, with the specificity scores calculated using the area under the curve of the dynamics shown on the y-axis. The specificity scores calculated here using the area under the curve and calculated using the steady state signal level in Chapter 3 are very similar and controlled in the same way by the strength of interactions.

interactions, maximum and minimum specificities of the two pathways was first examined (Figure 5.7). The specificity calculated using the area under the curve is quite similar to the scores calculated using the steady state signal levels in Chapter 3. When the ligand in one pathway directly interacts with the receptor in the other pathway, specificity of

the pathway can be dramatically reduced (L2R1G1E1▲ for Pathway 1 and L1R2G2E2△ for Pathway 2). Nonspecific interactions between the receptor in one pathway and the G-protein in the other pathway can also significantly lower the specificity when the strength of interaction is strong (L1R1G2E2 □ for Pathway 1 and L2R2G1E1 ■ for Pathway 2). An inverse bell-shaped specificity curve as increasing the strength of interactions are also observed for interaction L1R2G1E1 (○). Although the specificity scores calculated using the area under the curve and using the steady state level in Chapter 3 are not exactly the same, they are very close to each other and controlled in the same way by the strength of nonspecific interactions.

The effect of the rates of interactions on signaling specificity in then examined. We have considered variations in the rates of ligand-induced internalization in the original pathways and also variations in the rates of internalizations induced by the ligand from the other pathway due to nonspecific interactions. From Figure 5.8 to Figure 5.11, the rate for the internalization of L1R1 is varied across rows and the rate for the internalization of L2R2 is varied across columns. In each panel, specificity of Pathway 1 is shown in black and specificity of Pathway 2 is shown in red. Variations in the rate for the internalization of L2R1 are labeled with empty symbols while variations in the rate for the internalization of L1R2 are labeled with solid ones.

The effect of internalization on the maximum and minimum signaling specificities of the two pathways for interaction L1R2G1E1 are shown in Figure 5.8 and Figure 5.9, respectively. The maximum specificity of Pathway 1 is high originally, and it can be decreased when the rate of the internalization of L1R2 is fast (▲ in the 2^{nd} and 3^{rd} rows). Since the effect of L1 on Signal 2 is inhibitory due to the competition for R2, fast internalization of R2 aggravates the reduction of Signal 2 and thus lower the specificity of Pathway 1. The effect of internalization on the minimum specificity is more observable. Since the specificity of Pathway 1 is calculated in the absence of L2, the scaling factor

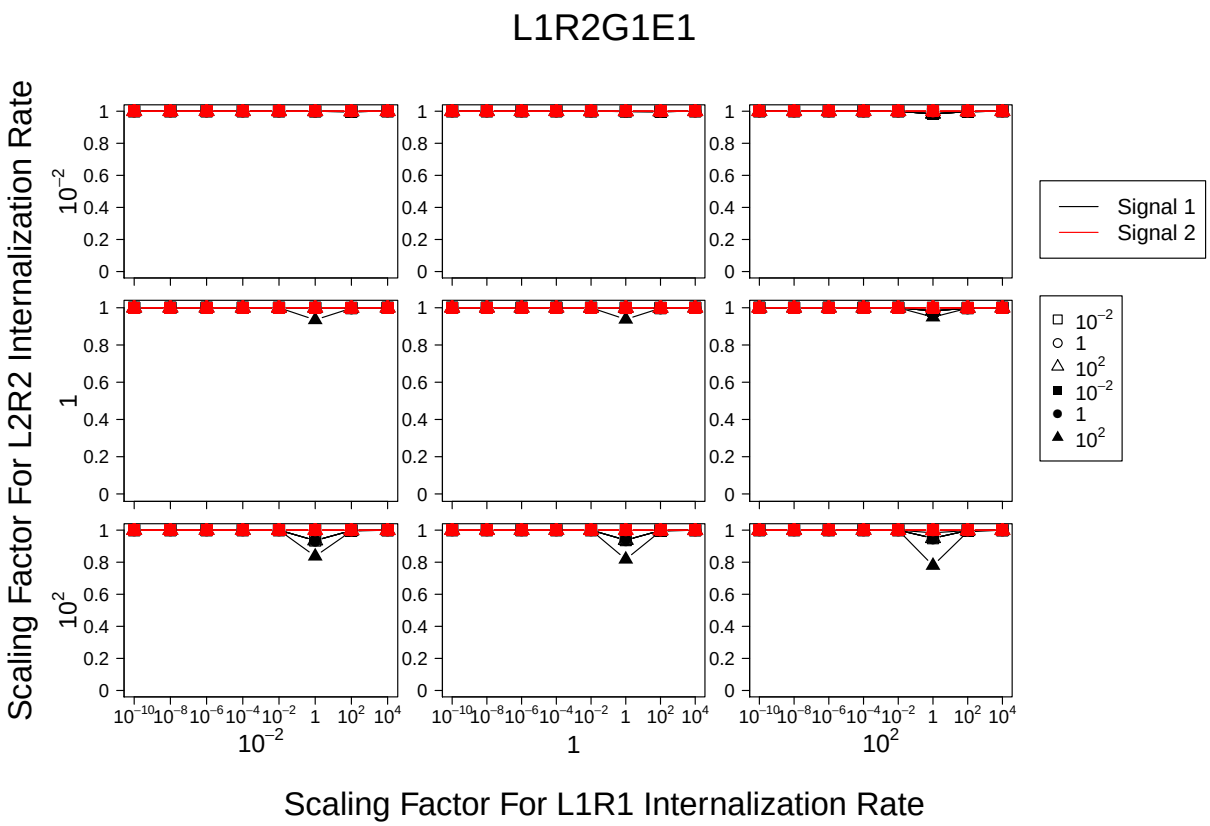

Figure 5.8: **The effects of internalization on the minimum specificities of the two pathways for interaction L1R2G1E1.** The rate for the internalization of L1R1 is varied across rows and the rate for the internalization of L2R2 is varied across columns. In each panel, the scaling factor for the internalization of L2R1 is labeled using empty symbols and that for the internalization of L1R2 is labeled using solid symbols. Specificity of Pathway 1 is shown in black and specificity of Pathway 2 is shown in red.

for the rate of the internalization of L2 does not have any effects and curves labeled with empty symbols and solid circle are all overlapping. As increasing the rate for the internalization of L2R2 from the top row to the bottom row, the overall signaling specificity is decreased. In each panel, if the internalization of L1R2 is even faster (▲), the decrease in the signaling specificity of Pathway 1 is more dramatic. However, if the internalization of L1R2 is slow (■), the specificity of Pathway 1 can be increased.

The effects of internalization on the specificity of Pathway 1 for interaction L1R2G2E2

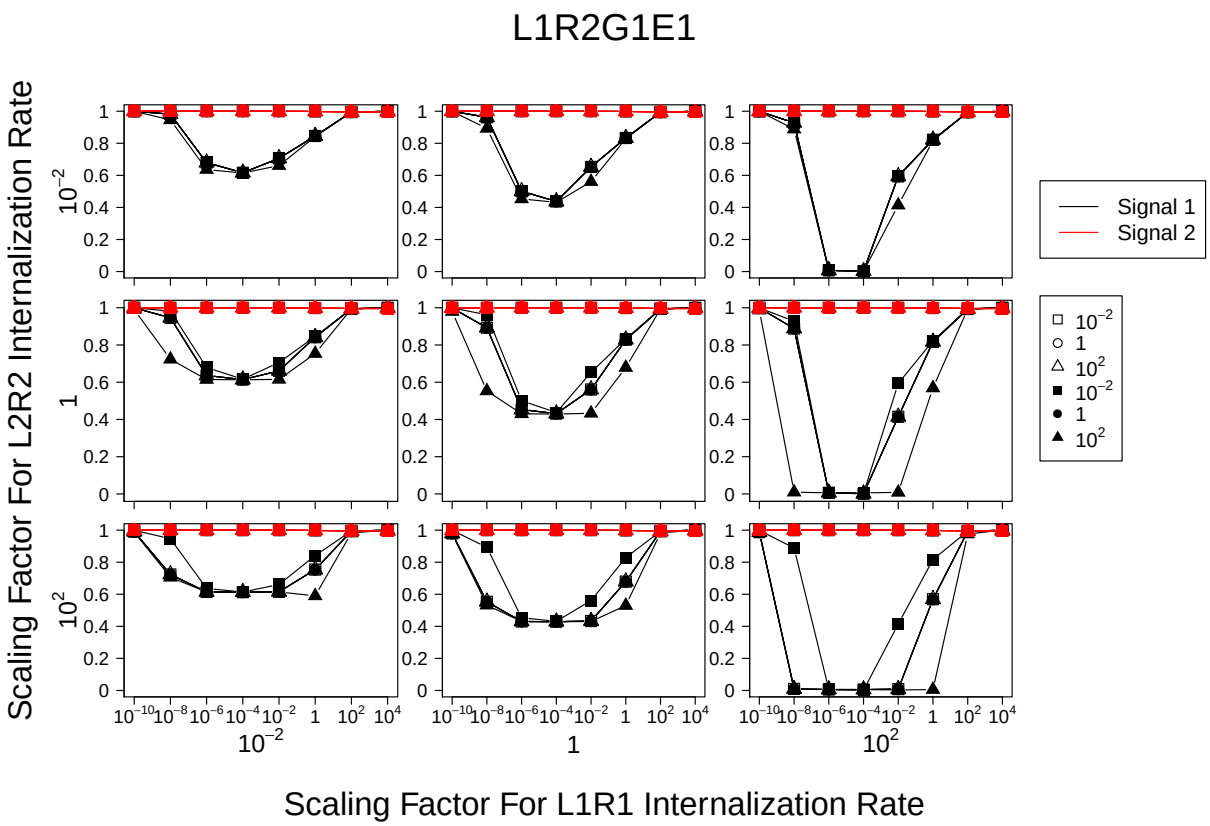

Figure 5.9: **The effects of internalization on the maximum specificities of the two pathways for interaction L1R2G2E2.** The rate for the internalization of L1R1 is varied across rows and the rate for the internalization of L2R2 is varied across columns. In each panel, the scaling factor for the internalization of L2R1 is labeled using empty symbols and that for the internalization of L1R2 is labeled using solid symbols. Specificity of Pathway 1 is shown in black and specificity of Pathway 2 is shown in red.

are opposite. The maximum and minimum signaling specificities of the two pathways for interaction L1R2G2E2 are shown in Figure 5.10 and Figure 5.11, respectively. When the rate for the internalization of L1R2 is fast, the maximum signaling specificity of Pathway 1 can be increased (Figure 5.10, 2^{nd} row and 3^{rd} row ▲). On the opposite, if the rate for the internalization of L1R2 is decreased, the maximum specificity of Pathway can also be decreased (■). For interaction L1R2G2E2, the effect of L1 on Signal 2 is stimulatory. When the internalization of R2 is accelerated by the binding of L1 (▲), the

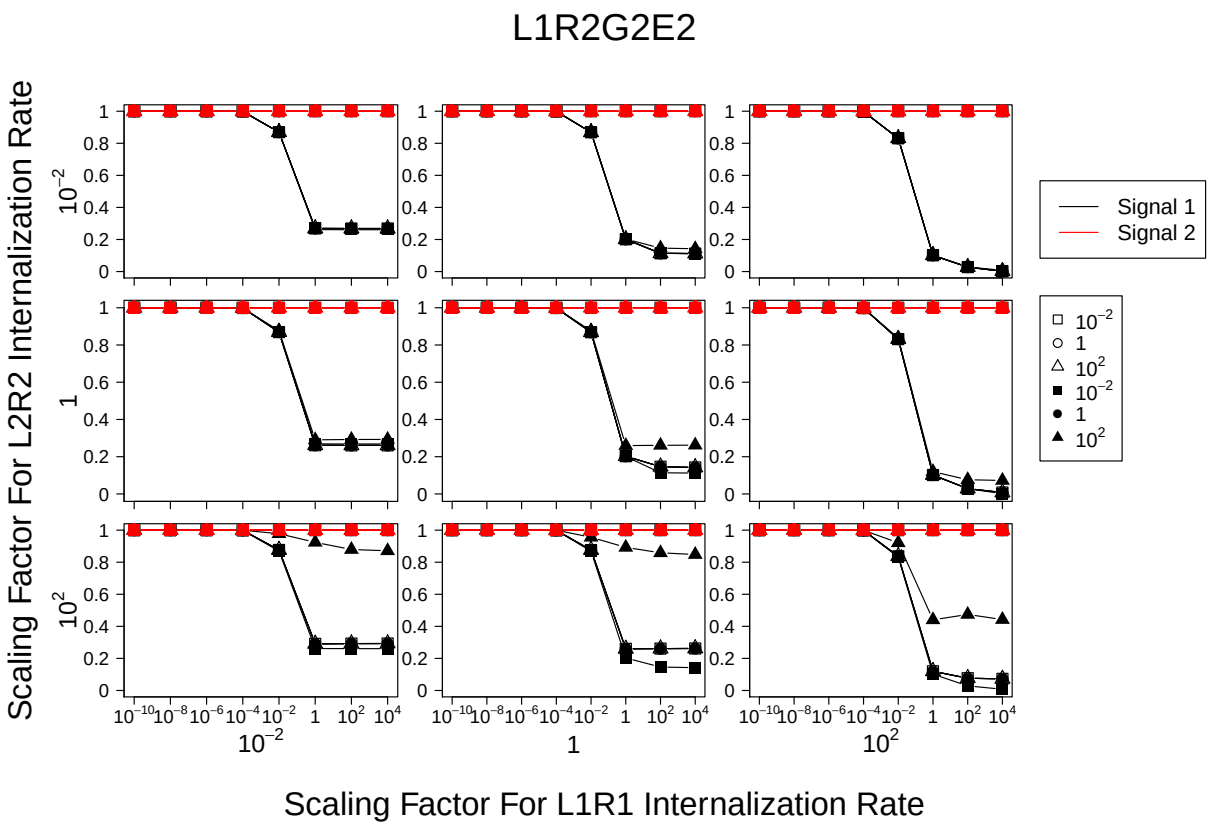

Figure 5.10: **The effects of internalization on the maximum specificities of the two pathways for interaction L1R2G2E2.** The rate for the internalization of L1R1 is varied across rows and the rate for the internalization of L2R2 is varied across columns. In each panel, the scaling factor for the internalization of L2R1 is labeled using empty symbols and that for the internalization of L1R2 is labeled using solid symbols. Specificity of Pathway 1 is shown in black and specificity of Pathway 2 is shown in red.

overall Signal 2 induced by L1 is reduced and the specificity of Pathway 1 is increased. Similarly, when the internalization of R2 is inhibited by the binding of L1, the specificity of Pathway 1 is decreased (■). The minimum specificity of Pathway 1 is affected in the same manner (Figure 5.11). Since the minimum specificity of Pathway 1 is obtained at high concentrations of L1, it can only be increased when the concentration of R2 on the cell membrane is reduced dramatically so that Signal 2 is not activated by L1 (Figure 5.11, 3^{rd} row, 1^{st} and 2^{nd} columns). The internalization of L1R1 can also affect the

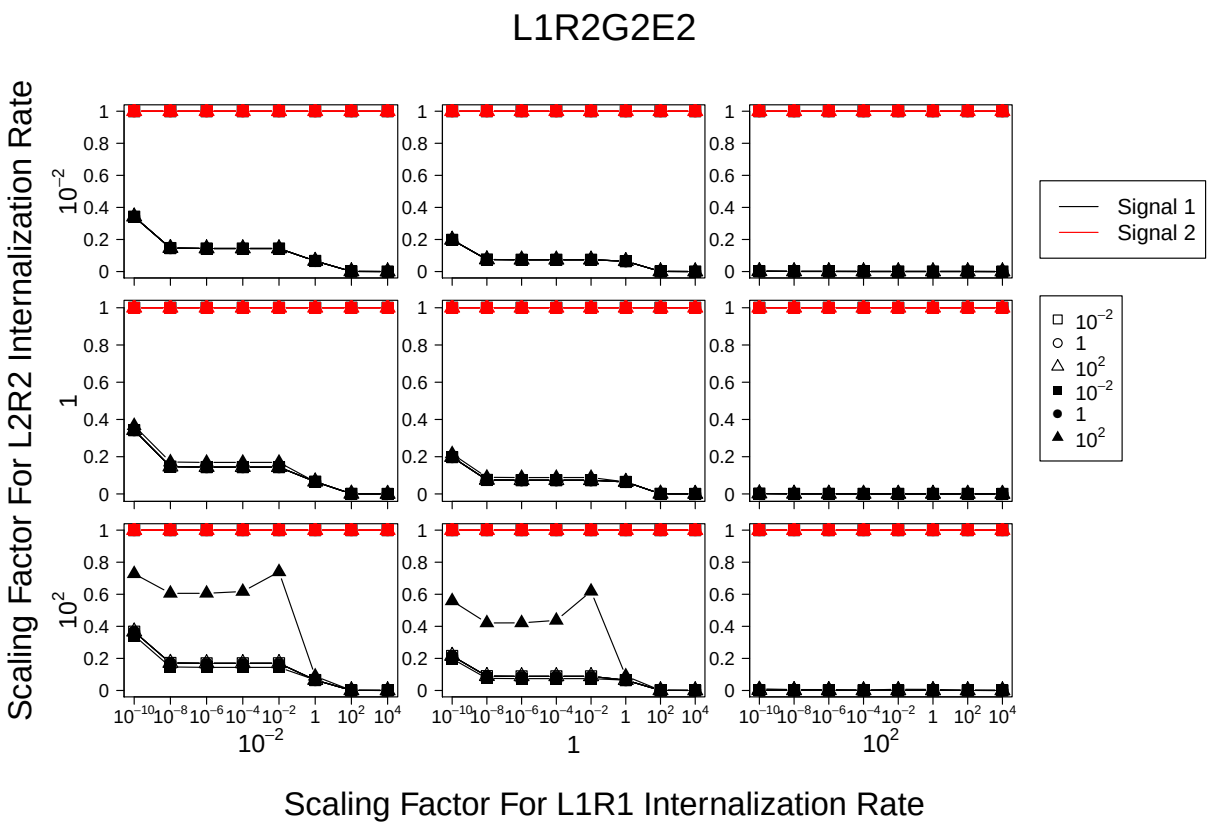

Figure 5.11: **The effects of internalization on the minimum specificities of the two pathways for interaction L1R2G2E2.** The rate for the internalization of L1R1 is varied across rows and the rate for the internalization of L2R2 is varied across columns. In each panel, the scaling factor for the internalization of L2R1 is labeled using empty symbols and that for the internalization of L1R2 is labeled using solid symbols. Specificity of Pathway 1 is shown in black and specificity of Pathway 2 is shown in red.

minimum specificity of Pathway 1. When the internalization of L1R1 is fast, Signal 1 is inhibited and in consequence, the specificity of Pathway 1 is reduced (Figure 5.11, 3^{rd} column).

5.4 Conclusions

In summary, the effects of the internalization of G-protein-coupled receptors on signaling were investigated using mathematical models in this chapter. A double-peaked dynamical response is observed, which is caused by the trafficking of receptors. Signaling

specificity can also be modified by the internalization of receptors, due to its inhibitory effect on signaling.

When nonspecific interactions exist between the binding of ligand from one pathway and the receptor from the other pathway, signaling specificity can be changed due to different rates of the internalizations of the two receptors induced by the ligand. When nonspecific interactions only exist between the binding of receptor from one pathway and the G-protein from the other pathway, specificity will not be significantly changed by the internalization of the receptor since it reduces both signals in the same way.

Although the down-regulation of signaling involves both the desensitization and the internalization of the receptor, we primarily focused on the internalization part and used a single reaction to describe the whole process. A full model considering phosphorylation of the receptor by GRKs and the interactions with β-arrestins has also been built. The rate of of phosphorylation can affect the signaling behavior, but double-peaked dynamical response can still be observed in the full model. Variations in the rates of internalizations considered here may come from specificity of enzymatic activity of GRKs or the binding of β-arrestins.

In our internalization model, besides temporarily altering the distribution of receptors between inside the cell and on the cell membrane, the major effect of internalization is to remove the ligands away from the system. Since the differential equation model is continuous and the rate of internalization is proportional to the concentration of ligand-receptor complex, the concentration of ligand will not return to exactly 0. However, the concentration change of ligand will decay to 0 when time approaches infinity. When the decrease in the concentration of the ligand passes a threshold, the signal level will reduce monotonically as decreasing the concentration of ligand. More than two peaks may be seen for the dynamics of the signal when the concentration of ligand is large under certain conditions, but the system is not oscillatory.

Chapter 6
Conclusions

Heterotrimeric G-protein-coupled receptors play a critical role in converting extracellular stimuli into cellular responses. In this thesis, ordinary differential equation models are used to investigate this process. We have focused on two main aspects: to explain the diverse signaling patterns and to examine the effects of specificity in the individual reactions on the overall signaling specificity.

We have shown that variations of the model parameters can result in qualitatively different signaling patterns. In particular, a switch between a sigmoidal and peaked dose response curve is found to be controlled by the interaction between the ligand-receptor complex and G-protein. In addition, the width of the peak can also be modulated by the parameters in the model such as the rates for the interaction between the receptor and G-protein. More interestingly, both the forward and the backward rates are varied simultaneously for these reactions, which results in an unchanged equilibrium constant. This indicates that the affinity between two molecules may not be enough to explain their roles in a larger signaling network.

Due to the large number of components in the GPCR signaling pathways and their abilities to interact with multiple partners, two signaling pathways may interact with each other. We have examined the effects of such interactions on the signaling specificity of each pathway. The signaling specificity can be affected by the strength of interactions, the presence of other ligands, as well as the expression level of the molecules in the two pathways. When the ligand from one pathway directly interacts with the receptor from the other pathway, signaling specificity can be low even when the strength of interactions is low. A biphasic dose response curve is observed when ligand can interact with two GPCRs to activate the G-protein in its own pathway. This pattern appears in the

presence of high concentration of the ligand for the other pathway and it is the result of the combined activation by two receptors.

Different types of G-protein-coupled receptors coexpressed in cell can form heterodimers. Interactions of the ligand or G-protein to one side of the dimer may alter the ability of the other side of the dimer to interact with its own ligand or G-protein. When the interaction between the ligand and its receptor is inhibited by dimerization, a double-peaked steady state dose response curve is observed. This behavior is a result of a combined activation of the monomer and the dimer in the system. Signaling specificity can be perturbed by the strength of nonspecific interactions, the dimer stability as well as the effects of allosteric regulations. The strength of interactions is more influential than others, especially when the ligand does not directly interact with the receptor in the other pathway.

A double-peaked dynamical response can result from the trafficking of the receptors. The first peak is the result of the internalization of the receptor responding to the initial stimulation. The signal can be increased due to the recycling the receptor to the cell membrane and the second peak appears due to the removal of the ligand. Signaling specificity can also be modified by the internalization of the receptors, due to its inhibitory effect on signaling. When nonspecific interactions exist between the ligand from one pathway and the receptor from the other pathway, different rates of the internalizations of the two receptors induced by the ligand can result in altered signaling specificity.

The diversity and specificity in GPCR signaling pathways observed here raise concerns about the transferability of observations obtained from one system to a related system. Qualitatively different outputs can result from the differences in the details of different pathways, even when their mechanisms are the same. A better understanding in the diversity and specificity in GPCR signaling can provide insights into designing drugs with desired properties. For example, when a drug can initiate multiple signaling

pathways, different combinations of behaviors can be obtained by manipulating the rates of individual reactions. If only one signal is needed and others are considered as side effects, measuring the specificity in different signaling pathways can give insight into how to minimize side effects.

The sensitivity analysis carried out here focused on only one or two parameters at a time, which is helpful for giving straightforward illustrations of the effects of individual reactions on the whole system. However, variation of one parameter only explores the parameter space along one direction and may not be sufficient for understanding the whole parameter space. Understanding the whole parameter space will give insight into how a set of reactions or part of the system can affect the whole system. Some initial studies on sampling the parameters from the whole parameter space and analyzing their effects were carried out. However, the stability of the result from solving the systems of differential equations was an issue when using MATLAB. The cvode solver in the SUNDIALS package may provide more reliable results for further study.

Sensitivity analysis is not only important for understanding the effects of parameters in a model, but also important for understanding the structure of the model. Exhaustively exploring the parameter space will demonstrate the ability of a model to produce different types of behaviors. For example, if considering the LRG complex as the signal in the TCM model, peaked response will not be observed since the concentration of LRG is a monotonic function of L.

The basic model for the initial steps of GPCR signaling pathways can be extended in different ways and here we only focused on considering two pathways and the regulations on the receptors. Other directions may include regulations by other molecules such as RGS proteins, $G_{\beta}\gamma$ signaling, downstream signaling and their possible feedback effects and others. For future work, a sampling-based sensitivity analysis framework should be established and applied to the basic model as well as different types of extended models.

Bibliography

[1] Terry Kenakin. Principles: receptor theory in pharmacology. *Trends in pharmacological sciences*, 25(4):186–92, April 2004.

[2] H P Rang. The receptor concept: pharmacology's big idea. *British journal of pharmacology*, 147:S9–S16, January 2006.

[3] Shigeki Takeda, Shiro Kadowaki, Tatsuya Haga, and Hirotomo Takaesu. Identification of G protein-coupled receptor genes from the human genome sequence. *FEBS Lett.*, 520:1–3, June 2002.

[4] Robert Fredriksson, Malin C Lagerström, Lars-Gustav Lundin, and Helgi B Schiöth. The G-protein-coupled receptors in the human genome form five main families. Phylogenetic analysis, paralogon groups, and fingerprints. *Molecular pharmacology*, 63(6):1256–72, June 2003.

[5] Demetrios K Vassilatis, John G Hohmann, Hongkui Zeng, Fusheng Li, Jane E Ranchalis, Marty T Mortrud, Analisa Brown, Stephanie S Rodriguez, John R Weller, Abbie C Wright, John E Bergmann, and George a Gaitanaris. The G protein-coupled receptor repertoires of human and mouse. *Proceedings of the National Academy of Sciences of the United States of America*, 100(8):4903–8, April 2003.

[6] Allen M Spiegel and Lee S Weinstein. Inherited diseases involving g proteins and g protein-coupled receptors. *Annual review of medicine*, 55(2):27–39, January 2004.

[7] Torsten Schöneberg, Angela Schulz, Heike Biebermann, Thomas Hermsdorf, Holger Römpler, and Katrin Sangkuhl. Mutant G-protein-coupled receptors as a cause of human diseases. *Pharmacology & therapeutics*, 104(3):173–206, December 2004.

[8] Edgar Jacoby, Rochdi Bouhelal, Marc Gerspacher, and Klaus Seuwen. The 7 TM G-protein-coupled receptor target family. *ChemMedChem*, 1(8):761–82, August 2006.

[9] John P Overington, Bissan Al-Lazikani, and Andrew L Hopkins. How many drug targets are there? *Nature reviews. Drug discovery*, 5(12):993–6, December 2006.

[10] Malin C Lagerström and Helgi B Schiöth. Structural diversity of G protein-coupled receptors and significance for drug discovery. *Nature reviews. Drug discovery*, 7(4):339–57, April 2008.

[11] William M Oldham and Heidi E Hamm. Heterotrimeric G protein activation by G-protein-coupled receptors. *Nature reviews. Molecular cell biology*, 9(1):60–71, January 2008.

[12] Bas Vroling, Marijn Sanders, Coos Baakman, Annika Borrmann, Stefan Verhoeven, Jan Klomp, Laerte Oliveira, Jacob de Vlieg, and Gert Vriend. GPCRDB: information system for G protein-coupled receptors. *Nucleic acids research*, 39(Database issue):D309–19, January 2011.

[13] Steven M Foord, Tom I Bonner, Richard R Neubig, Edward M Rosser, Jean-phillipe Pin, Anthony P Davenport, Michael Spedding, and Anthony J Harmar. International Union of Pharmacology . XLVI . G Protein-Coupled Receptor List. *Pharmacological reviews*, 57(2):279–288, June 2005.

[14] Joel Bockaert and Jean Philippe Pin. Molecular tinkering of G protein-coupled receptors : an evolutionary success. *EMBO members' review*, 18(7):1723–1729, April 2000.

[15] Susana R Neves, Prahlad T Ram, and Ravi Iyengar. G protein pathways. *Science (New York, N.Y.)*, 296(5573):1636–9, May 2002.

[16] Edda Klipp and Wolfram Liebermeister. Mathematical modeling of intracellular signaling pathways. *BMC neuroscience*, 7(Suppl 1):S10, January 2006.

[17] Narat J Eungdamrong and Ravi Iyengar. Modeling cell signaling networks. *Biology of the cell / under the auspices of the European Cell Biology Organization*, 96(5):355–62, June 2004.

[18] Hans V Westerhoff, Alexey Kolodkin, Riaan Conradie, Stephen J Wilkinson, Frank J Bruggeman, Klaas Krab, Jan H van Schuppen, Hanna Hardin, Barbara M Bakker, Martijn J Moné, Katja N Rybakova, Marco Eijken, Hans J P van Leeuwen, and Jacky L Snoep. Systems biology towards life in silico: mathematics of the control of living cells. *Journal of mathematical biology*, 58(1-2):7–34, January 2009.

[19] Hans a Kestler, Christian Wawra, Barbara Kracher, and Michael Kühl. Network modeling of signal transduction: establishing the global view. *BioEssays : news and reviews in molecular, cellular and developmental biology*, 30(11-12):1110–25, November 2008.

[20] Regina Samaga and Steffen Klamt. Modeling approaches for qualitative and semi-quantitative analysis of cellular signaling networks. *Cell communication and signaling : CCS*, 11(1):43, January 2013.

[21] Jennifer J Linderman. Modeling of G-protein-coupled receptor signaling pathways. *The Journal of biological chemistry*, 284(9):5427–31, February 2009.

[22] Domitille Heitzler, Pascale Crépieux, Anne Poupon, Frédérique Clément, François Fages, and Eric Reiter. Towards a systems biology approach of-G protein-coupled receptor signalling: challenges and expectations. *Comptes rendus biologies*, 332(11):947–57, November 2009.

[23] A De Lean, J M Stadel, and R J Lefkowitz. A ternary complex model explains the agonist-specific binding properties of the adenylate cyclase-coupled beta-adrenergic receptor. *The Journal of biological chemistry*, 255(15):7108–17, August 1980.

[24] Philippe Samamasb, Susanna Cotecchialf, Tommaso Costal, and Robert J Lefkowitzs. A Mutation-induced Activated State of the beta 2-Adrenergic Receptor. Extending the ternary complex model. *The journal of biological chemistry*, March 1993.

[25] J M Weiss, P H Morgan, M W Lutz, and T P Kenakin. The cubic ternary complex receptor-occupancy model I. model description. *Journal of theoretical biology*, 178(2):151–167, January 1996.

[26] J M Weiss, P H Morgan, M W Lutz, and T P Kenakin. The cubic ternary complex receptor-occupancy model II. Understanding Apparent Affinity. *Journal of theoretical biology*, 178(2):169–182, January 1996.

[27] J M Weiss, P H Morgan, M W Lutz, and T P Kenakin. The cubic ternary complex receptor-occupancy model III. resurrecting efficacy. *Journal of theoretical biology*, 181(4):381–97, August 1996.

[28] L. D. Shea, R. R. Neubig, and J. J. Linderman. Timing is everything: The role of kinetics in g protein activation. *life sciences*, 68(6):647–658, 2000.

[29] Tamara L. Kinzer-Ursem and Jennifer J. Linderman. Both ligand- and cell-specific parameters control ligand agonism in a kinetic model of G protein-coupled receptor signaling. *PLoS computational biology*, 3(1):e6, 2007.

[30] P J Woodroffe, L J Bridge, J R King, C Y Chen, and S J Hill. Modelling of the activation of G-protein coupled receptors: drug free constitutive receptor activity. *Journal of mathematical biology*, 60(3):313–46, March 2010.

[31] P J Woodroffe, L J Bridge, J R King, and S J Hill. Modelling the activation of G-protein coupled receptors by a single drug. *Mathematical biosciences*, 219(1):32–55, May 2009.

[32] Stuart Maudsley, Bronwen Martin, and Louis M Luttrell. The Origins of Diversity and Specificity in G Protein-Coupled Receptor Signaling. *The journal of pharmacology and experimental therapeutics*, 314(2):485–494, April 2005.

[33] S. Offermanns. G-proteins as transducers in transmembrane signalling. *Progress in Biophysics and molecular biology*, 83(2):101–130, October 2003.

[34] T. M. Cabrera-Vera, J. Vanhauwe, T. O. Thomas, M. Medkova, A. Preininger, M. R. Mazzoni, and H. E. Hamm. Insights into G protein structure, function, and regulation. *Endocrine reviews*, 24(6):765–781, December 2003.

[35] R. Fredriksson and H. B. Schiöth. The repertoire of g-protein-coupled receptors in fully sequenced genomes. *Molecular pharmacology*, 67(5):1414–1425, February 2005.

[36] E. H. Hurowitz, J. M. Melnyk, Y. J. Chen, H. Kouros-Mehr, M. I. Simon, and H. Shizuya. Genomic characterization of the human heterotrimeric g protein α, β, γ subunit genes. *DNA Research*, 7(2):111–123, April 2000.

[37] Swiss Institute of Bioinformatics (SIB) and European Bioinformatics Institute (EBI). Swiss-Prot. http://www.ebi.ac.uk/swissprot/.

[38] Monika Frank, Leonore Thümer, Martin J Lohse, and Moritz Bünemann. G Protein activation without subunit dissociation depends on a $G_{\alpha i}$-specific region. *The Journal of biological chemistry*, 280(26):24584–90, July 2005.

[39] G. J. Digby, P. R. Sethi, and N. A. Lambert. Differential dissociation of g protein heterotrimers. *The journal of physiology*, 586(14):3325–3335, May 2008.

[40] L. Busconi, P. M. Boutin, and B. M. Denker. N-terminal binding domain of g_α subunits: involvement of amino acids 11-14 of $g_{\alpha o}$ in membrane attachment. *The biochemical journal*, 323:239–244, April 1997.

[41] N. Barkai and S. Leibler. Robustness in simple biochemical networks. *Nature*, 387(6636):913–917, June 1997.

[42] A R Asthagiri and D A Lauffenburger. A computational study of feedback effects on signal dynamics in a mitogen-activated protein kinase (MAPK) pathway model. *Biotechnology progress*, 17(2):227–39, 2001.

[43] R P Araujo, E F Petricoin, and L a Liotta. A mathematical model of combination therapy using the EGFR signaling network. *Bio Systems*, 80(1):57–69, April 2005.

[44] Seongho Ryu, Shih-Chieh Lin, Nadia Ugel, Marco Antoniotti, and Bud Mishra. Mathematical modeling of the formation of apoptosome in intrinsic pathway of apoptosis. *Systems and synthetic biology*, 2(1-2):49–66, June 2008.

[45] U S Bhalla and R Iyengar. Emergent properties of networks of biological signaling pathways. *Science (New York, N.Y.)*, 283(5400):381–7, January 1999.

[46] L J Bridge, J R King, S J Hill, and M R Owen. Mathematical modelling of signalling in a two-ligand G-protein coupled receptor system: agonist-antagonist competition. *Mathematical biosciences*, 223(2):115–32, February 2010.

[47] Vladimir L Katanaev and Matey Chornomorets. Kinetic diversity in G-protein-coupled receptor signalling. *The Biochemical journal*, 401(2):485–95, January 2007.

[48] J P Kukkonen, J Näsman, and K E Akerman. Modelling of promiscuous receptor-Gi/Gs-protein coupling and effector response. *Trends in pharmacological sciences*, 22(12):616–22, December 2001.

[49] Patrick Flaherty, Mala L Radhakrishnan, Tuan Dinh, Robert a Rebres, Tamara I Roach, Michael I Jordan, and Adam P Arkin. A dual receptor crosstalk model of G-protein-coupled signal transduction. *PLoS computational biology*, 4(9):e1000185, January 2008.

[50] Charin Modchang, Wannapong Triampo, and Yongwimon Lenbury. Mathematical modeling and application of genetic algorithm to parameter estimation in signal transduction: trafficking and promiscuous coupling of G-protein coupled receptors. *Computers in biology and medicine*, 38(5):574–82, May 2008.

[51] C Y Chen, Y Cordeaux, S J Hill, and J R King. Modelling of signalling via G-protein coupled receptors: pathway-dependent agonist potency and efficacy. *Bulletin of mathematical biology*, 65(5):933–58, September 2003.

[52] C Y Chen and J R King. Modelling the effect of caveolae on G-protein activation. *Bulletin of mathematical biology*, 68(4):863–88, May 2006.

[53] Mohammad Fallahi-Sichani and Jennifer J Linderman. Lipid raft-mediated regulation of G-protein coupled receptor signaling by ligands which influence receptor dimerization: a computational study. *PloS one*, 4(8):e6604, January 2009.

[54] H. Rabitz, M. Kramer, and D. Dacol. Sensitivity analysis in chemical kinetics. *Annual Review of Physical Chemistry*, 34:419–461, October 1983.

[55] D. Hu and J. M. Yuan. Time-dependent sensitivity analysis of biological networks: coupled MAPK and PI3K signal transduction pathways. *The journal of physical chemistry. A.*, 110(16):5361–5370, April 2006.

[56] Y. Chu, A. Jayaraman, and J. Hahn. Parameter sensitivity analysis of IL-6 signaling pathways. *IET Systems Biology*, 1(6):342–352, November 2007.

[57] Upinder S Bhalla. Signaling in small subcellular volumes. I. Stochastic and diffusion effects on individual pathways. *Biophysical journal*, 87(2):733–44, August 2004.

[58] Sudhir Sivakumaran, Sridhar Hariharaputran, Jyoti Mishra, and Upinder S. Bhalla. The Database of Quantitative Cellular Signaling: management and analysis of chemical kinetic models of signaling networks. *Bioinformatics*, 19:408–415, 2003.

[59] Naama Barkai and Ben-Zion Shilo. Variability and robustness in biomolecular systems. *Molecular cell*, 28(5):755–60, December 2007.

[60] Bryan C Daniels, Yan-jiun Chen, James P Sethna, Ryan N Gutenkunst, and Christopher R Myers. Sloppiness, robustness and evolvability in systems biology. *Current opinion in biotechnology*, 19(2), August 2008.

[61] G Berstein, J L Blank, a V Smrcka, T Higashijima, P C Sternweis, J H Exton, and E M Ross. Reconstitution of agonist-stimulated phosphatidylinositol 4,5-bisphosphate hydrolysis using purified m1 muscarinic receptor, Gq/11, and phospholipase C-beta 1. *The Journal of biological chemistry*, 267(12):8081–8, April 1992.

[62] Lisa a Catapano and Husseini K Manji. G protein-coupled receptors in major psychiatric disorders. *Biochimica et biophysica acta*, 1768(4):976–93, April 2007.

[63] Rosamaria Lappano and Marcello Maggiolini. G protein-coupled receptors: novel targets for drug discovery in cancer. *Nature reviews. Drug discovery*, 10(1):47–60, January 2011.

[64] Yasushi Okuno, Akiko Tamon, Hiroaki Yabuuchi, Satoshi Niijima, Yohsuke Minowa, Koichiro Tonomura, Ryo Kunimoto, and Chunlai Feng. GLIDA: GPCR–ligand database for chemical genomics drug discovery–database and tools update. *Nucleic acids research*, 36(Database issue):D907–12, January 2008.

[65] D W Bonhaus, L K Chang, J Kwan, and G R Martin. Dual activation and inhibition of adenylyl cyclase by cannabinoid receptor agonists: evidence for agonist-specific trafficking of intracellular responses. *The Journal of pharmacology and experimental therapeutics*, 287(3):884–8, December 1998.

[66] Jörg Schaber, Bente Kofahl, Axel Kowald, and Edda Klipp. A modelling approach to quantify dynamic crosstalk between the pheromone and the starvation pathway in baker's yeast. *The FEBS journal*, 273(15):3520–33, August 2006.

[67] Lee Bardwell, Xiufen Zou, Qing Nie, and Natalia L Komarova. Mathematical models of specificity in cell signaling. *Biophysical journal*, 92(10):3425–41, May 2007.

[68] Bo Hu, Wouter-Jan Rappel, and Herbert Levine. Mechanisms and constraints on yeast MAPK signaling specificity. *Biophysical journal*, 96(12):4755–63, June 2009.

[69] Xiufen Zou, Tao Peng, and Zishu Pan. Modeling specificity in the yeast MAPK signaling networks. *Journal of theoretical biology*, 250(1):139–55, January 2008.

[70] Natalia L Komarova, Xiufen Zou, Qing Nie, and Lee Bardwell. A theoretical framework for specificity in cell signaling. *Molecular systems biology*, 1:2005.0023, January 2005.

[71] C D Rios, B a Jordan, I Gomes, and L a Devi. G-protein-coupled receptor dimerization: modulation of receptor function. *Pharmacology & therapeutics*, 92(2-3):71–87, 2001.

[72] Graeme Milligan. G protein-coupled receptor dimerization: function and ligand pharmacology. *Molecular pharmacology*, 66(1):1–7, July 2004.

[73] Sonia Terrillon and Michel Bouvier. Roles of G-protein-coupled receptor dimerization. *EMBO reports*, 5(1):30–4, January 2004.

[74] Beata Jastrzebska, Dimitrios Fotiadis, Geeng-Fu Jang, Ronald E Stenkamp, Andreas Engel, and Krzysztof Palczewski. Functional and structural characterization of rhodopsin oligomers. *The Journal of biological chemistry*, 281(17):11917–22, April 2006.

[75] Juan J Carrillo, Juan F Lo, and Graeme Milligan. Multiple Interactions between Transmembrane Helices Generate the Oligomeric alpha 1b -Adrenoceptor. *Molecular pharmacology*, 66(5):1123–1137, 2004.

[76] Steven C Prinster, Chris Hague, and Randy A Hall. Heterodimerization of G Protein-Coupled Receptors : Specificity and Functional Significance. 57(3):289–298, 2005.

[77] M Bouvier. Oligomerization of G-protein-coupled transmitter receptors. *Nature reviews. Neuroscience*, 2(4):274–86, April 2001.

[78] M K Dean, C Higgs, R E Smith, R P Bywater, C R Snell, P D Scott, G J Upton, T J Howe, and C a Reynolds. Dimerization of G-protein-coupled receptors. *Journal of medicinal chemistry*, 44(26):4595–614, December 2001.

[79] Mei Bai. Dimerization of G-protein-coupled receptors: roles in signal transduction. *Cellular Signalling*, 16(2):175–186, February 2004.

[80] Graeme Milligan. G-protein-coupled receptor heterodimers: pharmacology, function and relevance to drug discovery. *Drug discovery today*, 11(11-12):541–9, June 2006.

[81] Graeme Milligan. G protein-coupled receptor hetero-dimerization: contribution to pharmacology and function. *British journal of pharmacology*, 158(1):5–14, September 2009.

[82] Raphael Rozenfeld and Lakshmi a Devi. Receptor heteromerization and drug discovery. *Trends in pharmacological sciences*, 31(3):124–30, March 2010.

[83] Vicent Casadó, Antoni Cortés, Josefa Mallol, Kamil Pérez-Capote, Sergi Ferré, Carmen Lluis, Rafael Franco, and Enric I Canela. GPCR homomers and heteromers: a better choice as targets for drug development than GPCR monomers? *Pharmacology & therapeutics*, 124(2):248–57, November 2009.

[84] Michelle a Uberti, Randy a Hall, and Kenneth P Minneman. Subtype-specific dimerization of alpha 1-adrenoceptors: effects on receptor expression and pharmacological properties. *Molecular pharmacology*, 64(6):1379–90, December 2003.

[85] B a Jordan, N Trapaidze, I Gomes, R Nivarthi, and L a Devi. Oligomerization of opioid receptors with beta 2-adrenergic receptors: a role in trafficking and mitogen-activated protein kinase activation. *Proceedings of the National Academy of Sciences of the United States of America*, 98(1):343–8, January 2001.

[86] Jean-Pierre Vilardaga, Viacheslav O Nikolaev, Kristina Lorenz, Sébastien Ferrandon, Zhenjie Zhuang, and Martin J Lohse. Conformational cross-talk between alpha2A-adrenergic and mu-opioid receptors controls cell signaling. *Nature chemical biology*, 4(2):126–31, February 2008.

[87] S R George, T Fan, Z Xie, R Tse, V Tam, G Varghese, and B F O'Dowd. Oligomerization of mu- and delta-opioid receptors. Generation of novel functional properties. *The Journal of biological chemistry*, 275(34):26128–35, August 2000.

[88] Brigitte Ilien, Nicole Glasser, Jean-Pierre Clamme, Pascal Didier, Etienne Piemont, Raja Chinnappan, Sandrine B Daval, Jean-Luc Galzi, and Yves Mely. Pirenzepine promotes the dimerization of muscarinic M1 receptors through a three-step binding process. *The Journal of biological chemistry*, 284(29):19533–43, July 2009.

[89] Laura Albizu, Christophe Breton, Jean-philippe Pin, Maurice Manning, Bernard Mouillac, Claude Barberis, and Thierry Durroux. Probing the Existence of G Protein-Coupled Receptor Dimers by Positive and Negative Ligand-Dependent Cooperative Binding. 70(5):1783–1791, 2006.

[90] Maud Kamal, Pascal Maurice, and Ralf Jockers. Expanding the Concept of G Protein-Coupled Receptor (GPCR) Dimer Asymmetry towards GPCR-Interacting Proteins. *Pharmaceuticals*, 4(2):273–284, January 2011.

[91] M. Fallahi-Sichani and J. J. Linderman. Lipid raft-mediated regulation of G-protein coupled receptor signaling by ligands which influence receptor dimerization: A computational study. *PLoS One*, 4:e6604, 2009.

[92] Rafael Franco, Vicent Casadó, Josefa Mallol, Sergi Ferré, Kjell Fuxe, Antonio Cortés, Francisco Ciruela, Carmen Lluis, and Enric I Canela. Dimer-based model for heptaspanning membrane receptors. *Trends in biochemical sciences*, 30(7):360–6, July 2005.

[93] , Ferre Sergi, Fuxe Kjell, Cortes Antoni, Ciruela Francisco, Lluis Carmen, and Canela Enric I. The Two-State Dimer Receptor Model : A General Model for Receptor Dimers. *Molecular pharmacology*, 69(6):1905–1912, February 2006.

[94] D Armstrong and P G Strange. Dopamine D2 receptor dimer formation: evidence from ligand binding. *The Journal of biological chemistry*, 276(25):22621–9, June 2001.

[95] Thierry Durroux. Principles: a model for the allosteric interactions between ligand binding sites within a dimeric GPCR. *Trends in pharmacological sciences*, 26(7):376–84, July 2005.

[96] Xavier Rovira, Jean-Philippe Pin, and Jesús Giraldo. The asymmetric/symmetric activation of GPCR dimers as a possible mechanistic rationale for multiple signalling pathways. *Trends in pharmacological sciences*, 31(1):15–21, January 2010.

[97] Peter J Woolf and Jennifer J Linderman. An algebra of dimerization and its implications for G-protein coupled receptor signaling. *Journal of theoretical biology*, 229(2):157–68, July 2004.

[98] Peter J Woolf and Jennifer J Linderman. Untangling ligand induced activation and desensitization of G-protein-coupled receptors. *Biophysical journal*, 84(1):3–13, January 2003.

[99] Christopher J Brinkerhoff, Peter J Woolf, and Jennifer J Linderman. Monte Carlo simulations of receptor dynamics: insights into cell signaling. *Journal of molecular histology*, 35(7):667–77, September 2004.

[100] Rinshi S Kasai, Kenichi G N Suzuki, Eric R Prossnitz, Ikuko Koyama-Honda, Chieko Nakada, Takahiro K Fujiwara, and Akihiro Kusumi. Full characterization of GPCR monomer-dimer dynamic equilibrium by single molecule imaging. *The Journal of cell biology*, 192(3):463–80, February 2011.

[101] Matthew T Drake, Sudha K Shenoy, and Robert J Lefkowitz. Trafficking of G protein-coupled receptors. *Circulation research*, 99(6):570–82, September 2006.

[102] Wen Yang and Shi-Hai Xia. Mechanisms of regulation and function of G-protein-coupled receptor kinases. *World journal of gastroenterology : WJG*, 12(48):7753–7, December 2006.

[103] John T Williams, Susan L Ingram, Graeme Henderson, Charles Chavkin, Mark von Zastrow, Stefan Schulz, Thomas Koch, Christopher J Evans, and Macdonald J

Christie. Regulation of μ-opioid receptors: desensitization, phosphorylation, internalization, and tolerance. *Pharmacological reviews*, 65(1):223–54, January 2013.

[104] a B Tobin. G-protein-coupled receptor phosphorylation: where, when and by whom. *British journal of pharmacology*, 153 Suppl(December 2007):S167–76, March 2008.

[105] Catherine a C Moore, Shawn K Milano, and Jeffrey L Benovic. Regulation of receptor trafficking by GRKs and arrestins. *Annual review of physiology*, 69:451–82, January 2007.

[106] Karim Nagi and Graciela Piñeyro. Regulation of opioid receptor signalling: implications for the development of analgesic tolerance. *Molecular brain*, 4(1):25, January 2011.

[107] Catalina Ribas, Petronila Penela, Cristina Murga, Alicia Salcedo, Carlota García-Hoz, María Jurado-Pueyo, Ivette Aymerich, and Federico Mayor. The G protein-coupled receptor kinase (GRK) interactome: role of GRKs in GPCR regulation and signaling. *Biochimica et biophysica acta*, 1768(4):913–22, April 2007.

[108] Leif Erik Vinge, Kjetil W Andressen, Toril Attramadal, Geir Ø ystein Andersen, Mohammed Shakil Ahmed, Karsten Peppel, Walter J Koch, Neil J Freedman, Finn Olav Levy, Tor Skomedal, Jan-bjø rn Osnes, and Hå vard Attramadal. Substrate Specificities of G Protein-Coupled Receptor Kinase-2 and -3 at Cardiac Myocyte Receptors Provide Basis for Distinct Roles in Regulation of Myocardial Function. *Molecular pharmacology*, 72(3):582–591, September 2007.

[109] Deepak a Deshpande, Barbara S Theriot, Raymond B Penn, and Julia K L Walker. Beta-arrestins specifically constrain beta2-adrenergic receptor signaling and func-

tion in airway smooth muscle. *FASEB journal : official publication of the Federation of American Societies for Experimental Biology*, 22(7):2134–41, July 2008.

[110] T a Riccobene, G M Omann, and J J Linderman. Modeling activation and desensitization of G-protein coupled receptors provides insight into ligand efficacy. *Journal of theoretical biology*, 200(2):207–22, September 1999.

[111] Sharat J Vayttaden, Jacqueline Friedman, Tuan M Tran, Thomas C Rich, Carmen W Dessauer, and Richard B Clark. Quantitative modeling of GRK-mediated beta2AR regulation. *PLoS computational biology*, 6(1):e1000647, January 2010.

[112] Mano Ram Maurya and Shankar Subramaniam. A kinetic model for calcium dynamics in RAW 264.7 cells: 1. Mechanisms, parameters, and subpopulational variability. *Biophysical journal*, 93(3):709–28, August 2007.

[113] Mano Ram Maurya and Shankar Subramaniam. A kinetic model for calcium dynamics in RAW 264.7 cells: 1. Mechanisms, parameters, and subpopulational variability. *Biophysical journal*, 93(3):709–28, August 2007.

[114] Domitille Heitzler, Guillaume Durand, Nathalie Gallay, Aurélien Rizk, Seungkirl Ahn, Jihee Kim, Jonathan D Violin, Laurence Dupuy, Christophe Gauthier, Vincent Piketty, Pascale Crépieux, Anne Poupon, Frédérique Clément, François Fages, Robert J Lefkowitz, and Eric Reiter. Competing G protein-coupled receptor kinases balance G protein and β-arrestin signaling. *Molecular systems biology*, 8(590):590, January 2012.

[115] Scott M. DeWire, Seungkirl Ahn, Robert J. Lefkowitz, and Sudha K. Shenoy. β-Arrestins and Cell Signaling. *Annual Review of Physiology*, 69(1):483–510, March 2007.

Appendix A

Supplementary materials for Chapter 2

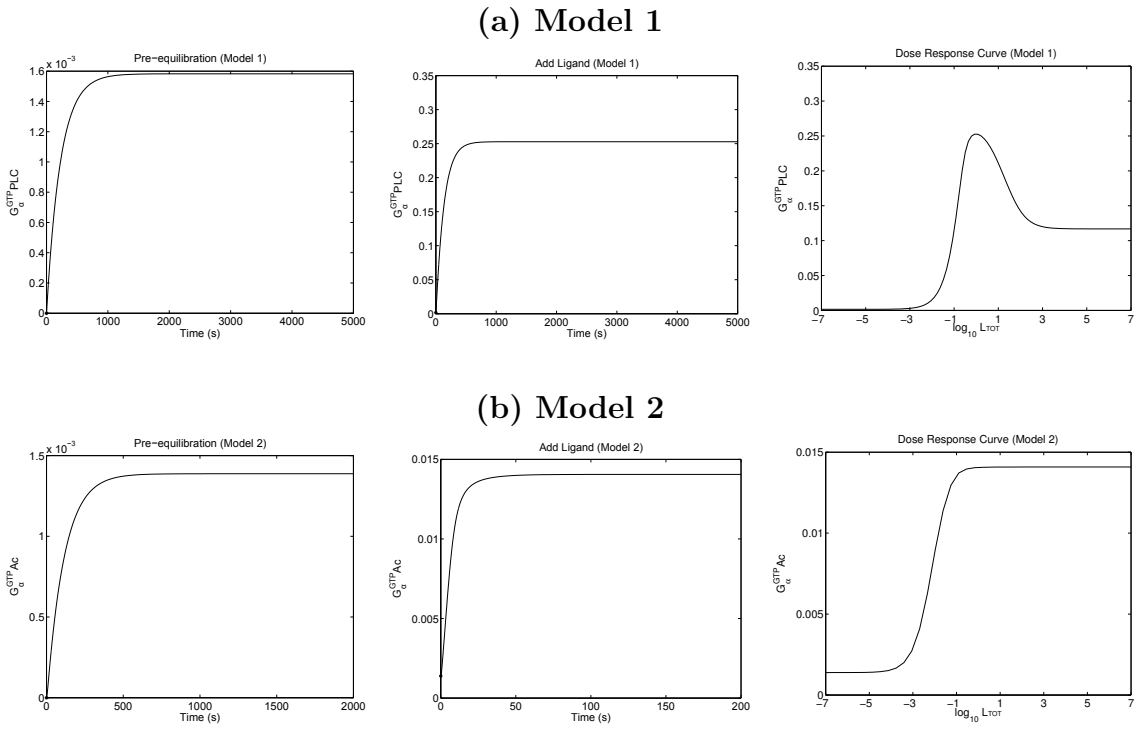

Figure A.1: **Generation of dose-response curves.** Each column shows a step in the generation of a dose-reponse curve: **Left:** Dynamic response during pre-equilibration in the absence of ligand; **Middle:** Dynamic resonse following addition of ligand; **Right:** The dose-response curve, generated from the equilibrium response (the right-most point of the middle panel) for a given ligand concentration. Each row corresponds to data from a given models: Model 1, top; Model 2, bottom.

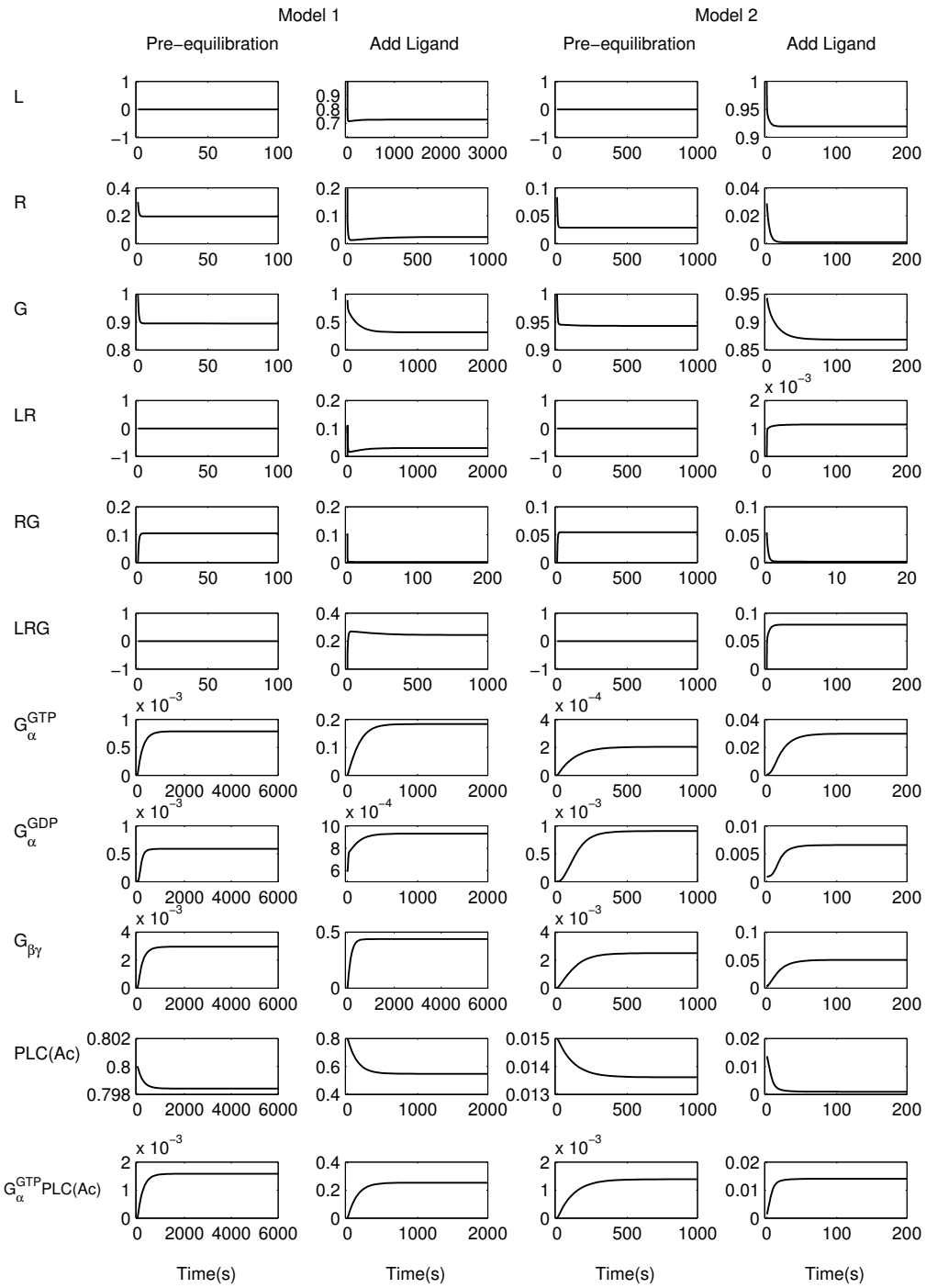

Figure A.2: **Concentration dynamics of models 1 and 2.** The variation in the concentration of each species over times is shown for both Model 1 (left two columns) and Model 2 (right two columns). In each case, the first panel shows the pre-equilibration dynamics, beginning from the presence of only free receptor, G-protein heterotrimer and adenylate cyclase. The second panel then shows the dynamics after addition of ligand.

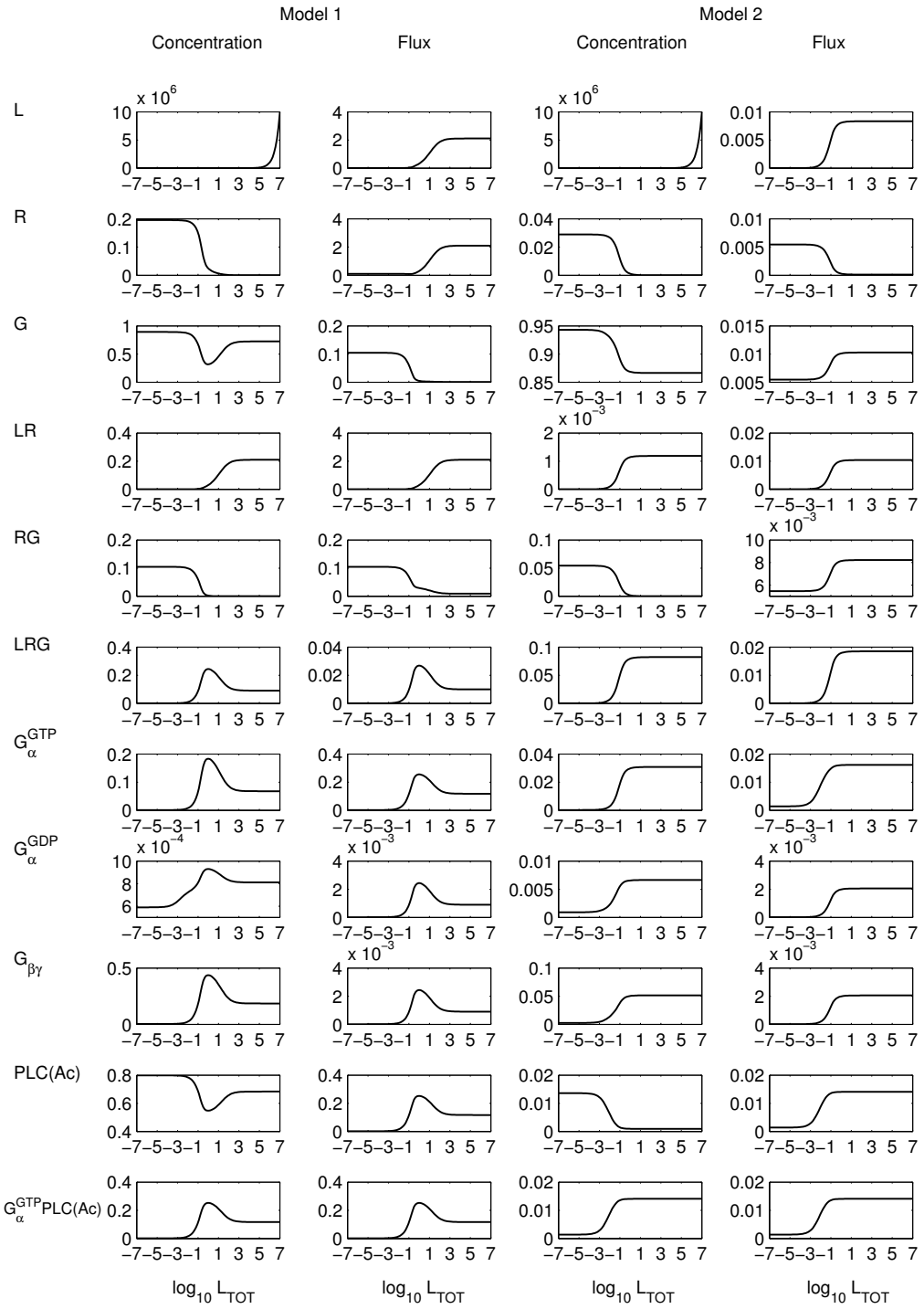

Figure A.3: **Dose-dependent equilibrium concentrations and fluxes of models 1 and 2.** The equilibrium concentration (first panel) and flux (second panel) are shown for each species in both Model 1 (left two columns) and Model 2 (right two columns), as a function in input ligand concentration. Flux is defined as the sum of all rates containing a species as a product; at equilibrium this should be equal to the sum of all rates containing the species as a reactant.

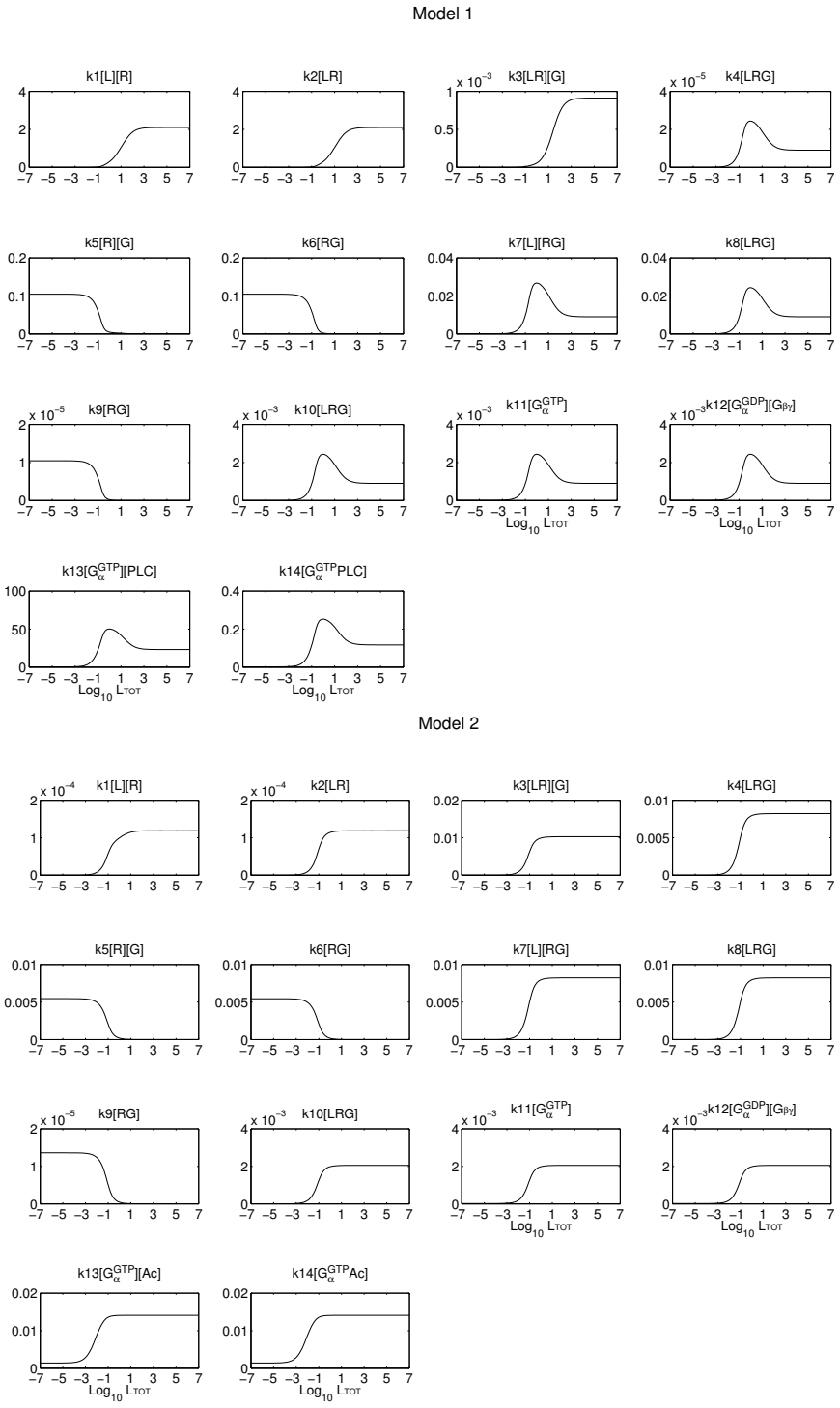

Figure A.4: **Dose-dependent reaction fluxes of models 1 and 2.** The equilibrium flux through each reaction arrow is given as a function of input ligand concentration, for both Model 1 (top panels) and Model 2 (bottom panels).

Table A.1: Convergence of Simulations.[a]

	Model 1			Model 2		
	$\left\|\frac{dx(t=10^5)_i}{dt}\right\|$	$\left\|\frac{dx(t=10^8)_i}{dt}\right\|$	$\max\left(\frac{\Delta x_i}{x_i}\right)$	$\left\|\frac{dx(t=10^5)_i}{dt}\right\|$	$\left\|\frac{dx(t=10^8)_i}{dt}\right\|$	$\max\left(\frac{\Delta x_i}{x_i}\right)$
R	5.80E-11	4.78E-11	9.07E-03	1.02E-10	1.34E-10	1.66E-04
G	5.68E-10	1.02E-11	3.21E-02	3.76E-11	8.63E-11	1.29E-03
E	1.87E-07	3.12E-11	7.70E-02	3.24E-08	7.42E-10	7.65E-03
k1k2	8.86E-11	7.00E-08	3.52E-06	1.53E-11	1.53E-11	2.38E-04
k3k4	6.78E-11	7.36E-10	4.78E-05	5.60E-07	2.46E-06	1.58E-03
k5k6	2.98E-09	4.53E-10	2.03E-03	1.20E-10	3.02E-09	3.49E-04
k7k8	7.76E-10	2.54E-09	3.54E-04	2.89E-10	6.01E-09	9.86E-04
k1k3	1.98E-10	1.36E-11	7.52E-05	4.46E-10	5.75E-10	2.10E-05
k2k4	5.60E-11	2.29E-08	3.14E-03	5.61E-11	1.93E-11	4.06E-04
k1k5	2.32E-12	9.86E-12	7.27E-06	5.79E-11	1.89E-11	2.51E-05
k2k6	5.35E-11	1.96E-09	4.14E-05	1.46E-12	1.03E-12	2.16E-06
k1k7	4.61E-11	2.50E-11	7.88E-05	1.10E-11	8.96E-12	4.62E-04
k2k8	3.86E-07	8.98E-07	1.29E-04	4.85E-10	2.52E-09	1.69E-03
k5k3	5.81E-11	1.69E-10	3.12E-04	1.59E-11	2.13E-11	7.12E-05
k6k4	3.28E-12	1.90E-12	4.70E-03	1.76E-12	1.27E-12	2.96E-04
k5k7	2.14E-11	1.37E-11	4.69E-05	2.45E-11	1.93E-11	1.80E-05
k6k8	8.68E-11	3.56E-07	4.00E-04	2.10E-11	5.85E-10	1.47E-04
k7k3	2.21E-10	1.30E-10	2.31E-05	7.48E-11	5.84E-11	8.84E-05
k8k4	2.63E-11	3.29E-08	5.79E-05	1.37E-12	1.23E-12	1.27E-04
k9	3.51E-12	3.71E-10	6.67E-04	1.37E-11	6.47E-12	1.84E-04
k10	1.06E-11	6.99E-11	1.97E-05	7.33E-10	5.21E-10	8.16E-05
k11	1.51E-07	2.86E-10	4.49E-02	2.87E-08	3.51E-10	6.51E-05
k12	1.17E-06	1.43E-06	6.34E-02	1.39E-08	2.64E-08	1.39E-02
k13k14	1.52E-07	4.58E-12	8.67E+00	6.69E-07	6.27E-12	5.28E+00
k13k14*	–	–	4.10E−04	–	–	1.87E−04

[a] Convergence was assessed by comparing the results from two total simulation times, 1e5 and 1e8 seconds. 1600 simulations were performed for each parameter (or parameter pair) varied; these were analyzed in parallel through consideration of three values: (i, ii) the maximum of the averaged norm of derivatives at the last point of simulation, $\left\|\frac{dx(t)_i}{dt}\right\|$; and (iii) the maximum of relative difference between signal levels using the two simulation times, $\max\left(\frac{\Delta x_i}{x_i}\right)$. The derivatives are all very near 0, and, in most cases extending the simulation results in changes of less than 1%, suggesting the system is very close to a stationary point. For cases where the results differed by more than 1%, the differences were identified (by visual analysis) to be at points with very small absolute values in all but two cases (k13k14 in both models). For these, simulation time was further extended to 1e9 s; the maximal change over this extended period (marked by *) was below 0.1%.

(a) Association of ligand with free receptor

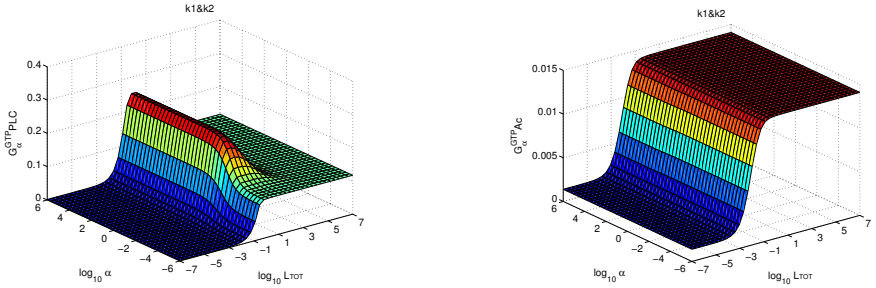

(b) Association of ligand with receptor·G-Protein complex

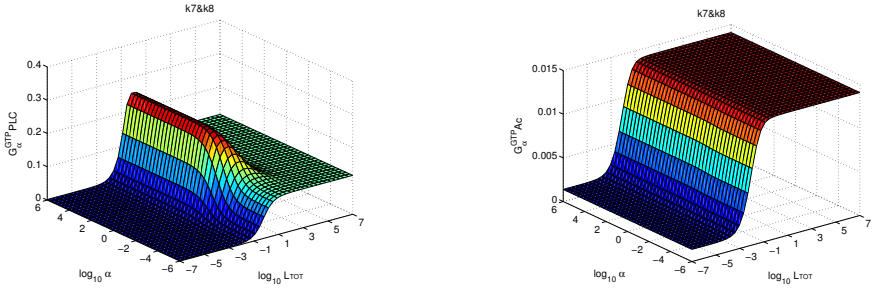

(c) Association of G-protein with ligand-bound receptor

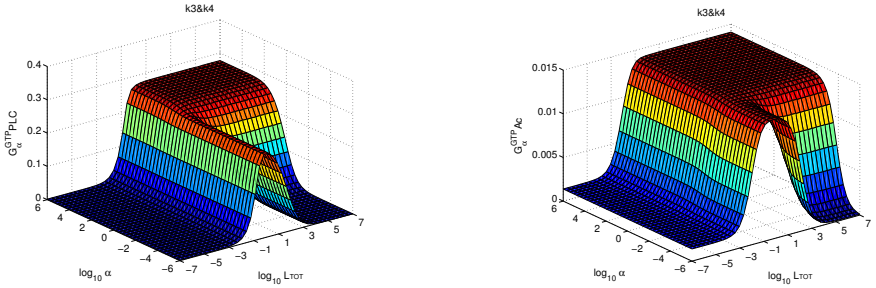

(d) Association of G-protein with unliganded receptor

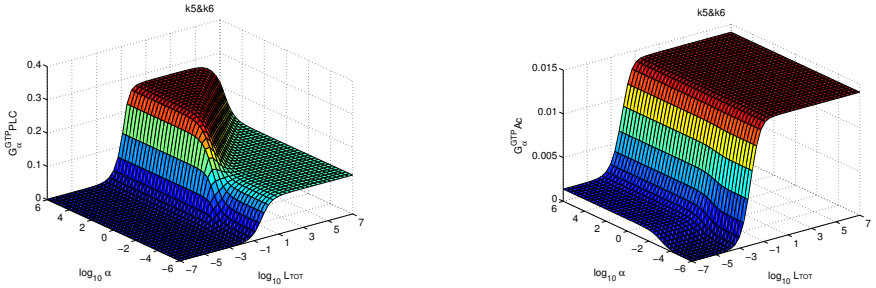

Model 1 **Model 2**

Figure A.5: **Variation of rates of binding equilibria.** The equilibrium concentration of G_α^{GTP}·E is plotted as a function of both added ligand concentration (L_{TOT}) and the parameter scaling factor (α). In these panels, the association and dissociation rate constants of each reaction within the ligand–receptor–G-protein binding square were varied in pairs, multiplying the rate of both forward and reverse reactions by α.

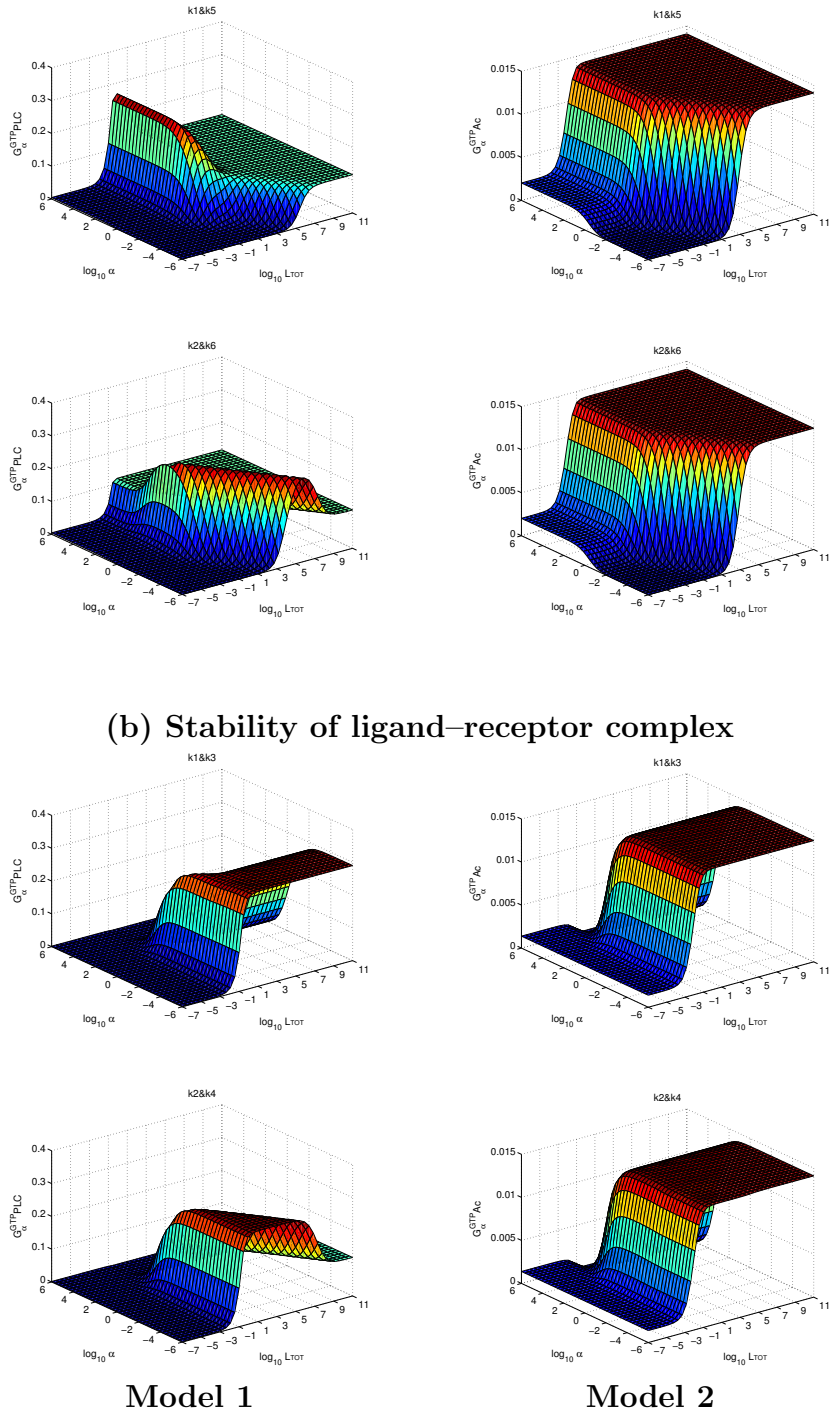

Figure A.6: **Variation of rates at corners of the "binding square" (A).** The equilibrium concentration of G_{α}^{GTP}·E is plotted as a function of both added ligand concentration (L_{TOT}) and the parameter scaling factor (α). In these panels, the rate constants of the association and dissociation reactions sharing a reactant were varied in pairs, multiplying or dividing the rate of each reaction by α, as required for thermodynamic consistency.

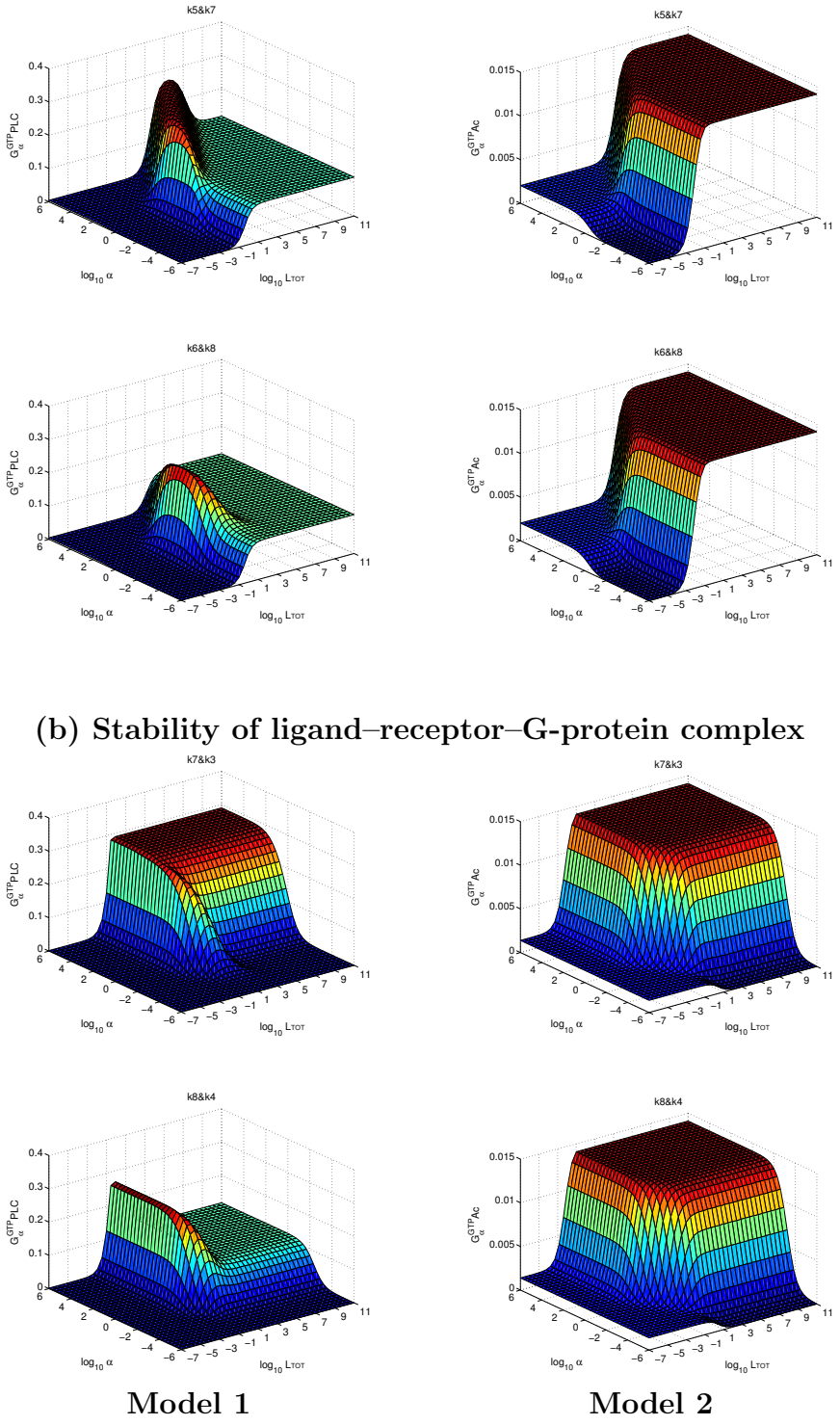

Figure A.7: **Variation of rates at corners of the "binding square" (B).** The equilibrium concentration of G_{α}^{GTP}·E is plotted as a function of both added ligand concentration (L_{TOT}) and the parameter scaling factor (α). In these panels, the rate constants of the association and dissociation reactions sharing a reactant were varied in pairs, multiplying or dividing the rate of each reaction by α, as required for thermodynamic consistency.

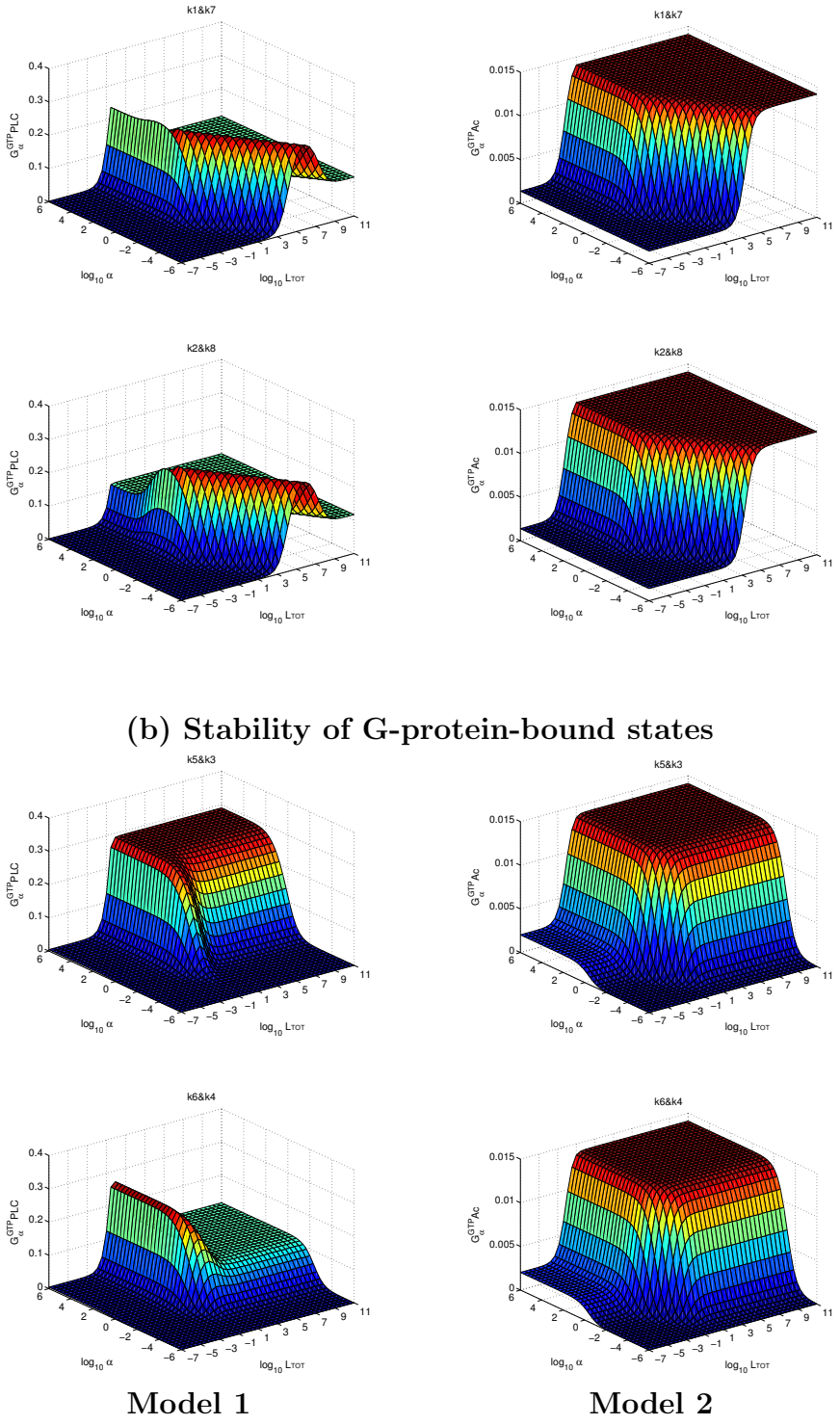

Figure A.8: **Variation of rates on opposite sides of the "binding square".** The equilibrium concentration of G_{α}^{GTP}·E is plotted as a function of both added ligand concentration (L_{TOT}) and the parameter scaling factor (α). In these panels, the rate constants for equivalent reactions on opposing sides of the square of binding-equilibria were varied in pairs, multiplying the rate of both reactions by α.

(a) Activation by unliganded receptor

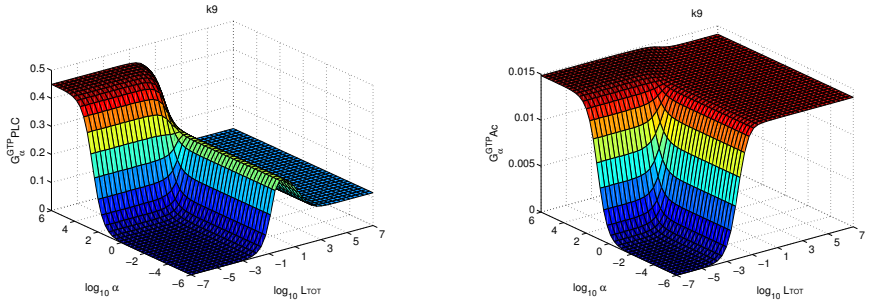

(b) Activation by ligand-bound receptor

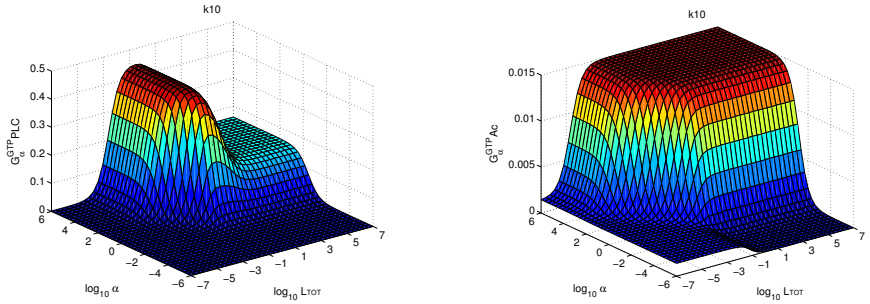

Model 1 **Model 2**

Figure A.9: **Variation of the activation rates.** The equilibrium concentration of G_α^{GTP}·E is plotted as a function of both added ligand concentration (L_{TOT}) and the parameter scaling factor (α). In these panels, the rates of activation (nucleotide exchange) of the G-protein were varied individually, multiplying the reaction rate by α.

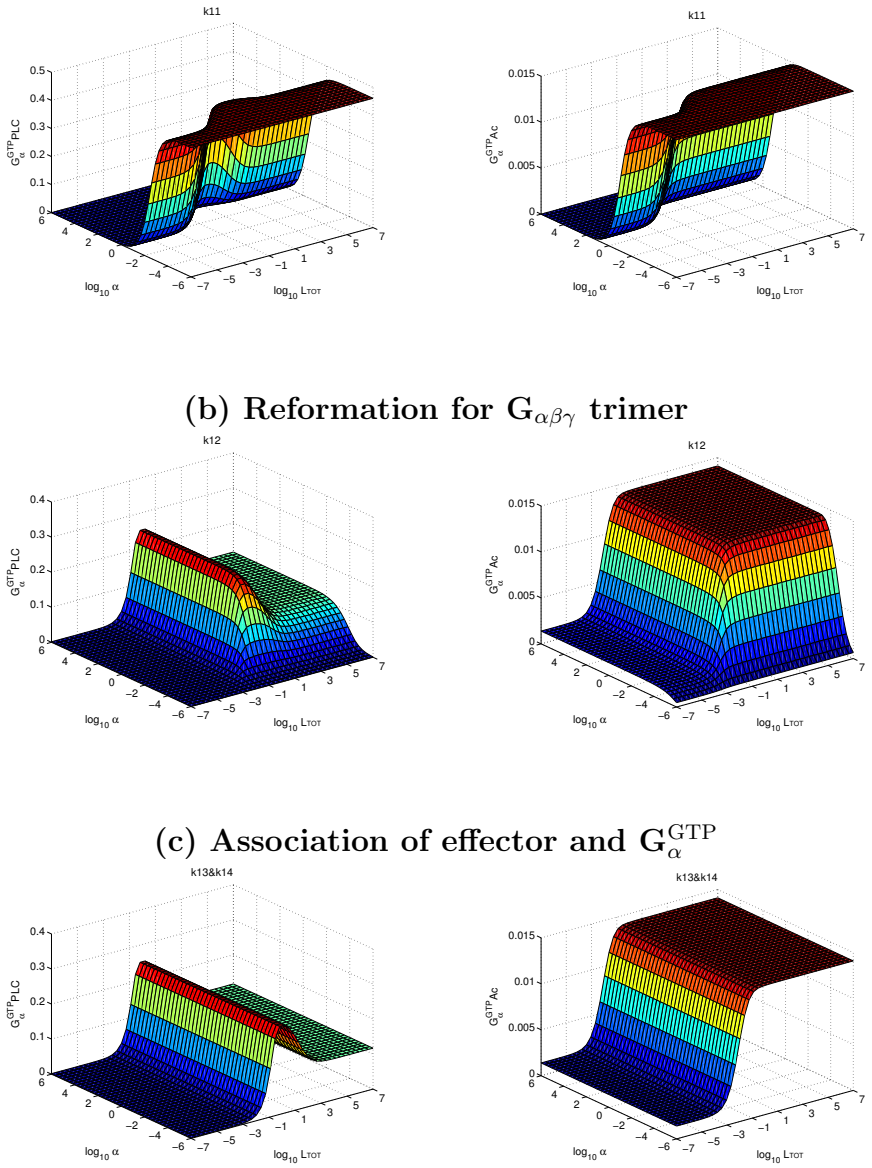

Figure A.10: **Variations of post-activation rate constants.** The equilibrium concentration of $G_\alpha^{GTP}{\cdot}E$ is plotted as a function of both added ligand concentration (L_{TOT}) and the parameter scaling factor (α). In these panels, the rates of post-activation reactions were varied. For GTP hydrolysis and trimer formation, the rates were varied individually, multiplying the reaction rate by α; for effector–G_α^{GTP} binding, both forward and reverse reaction rates were multiplied by α.

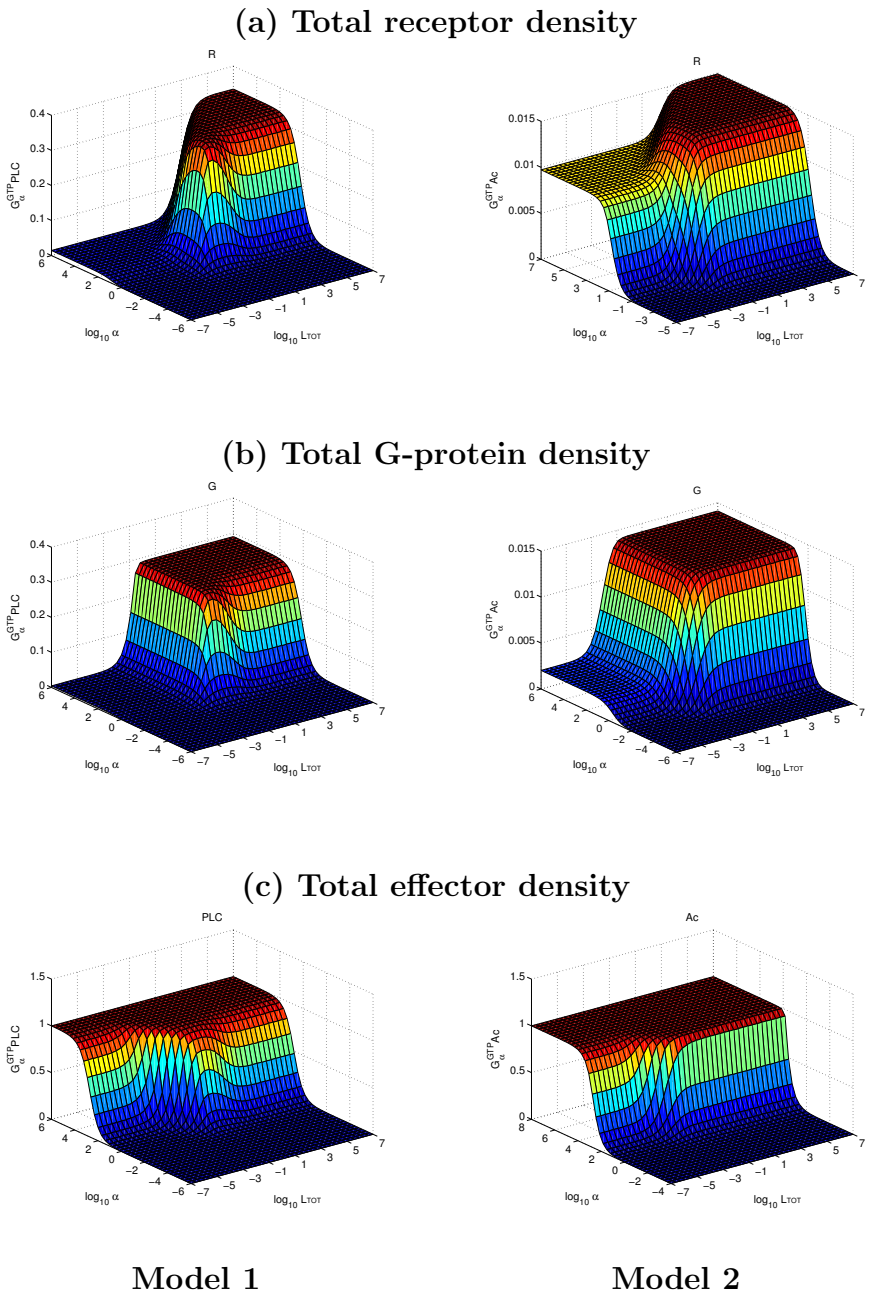

Figure A.11: **Variation of initial concentrations.** The equilibrium concentration of G_{α}^{GTP}·E is plotted as a function of both added ligand concentration (L_{TOT}) and the parameter scaling factor (α). In these panels, the total concentrations of each primary species were varied individually, multiplying the concentration by α.

(a) Evaluated at $t = 10^5$ s.

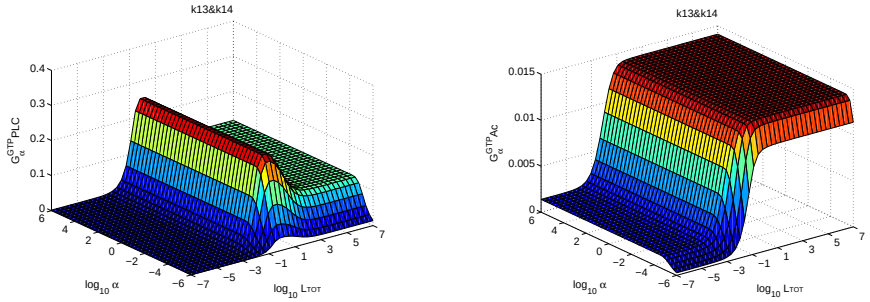

(a) Evaluated at $t = 10^8$ s.

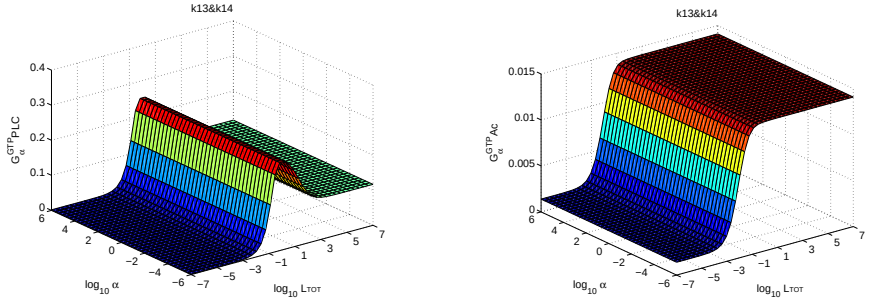

Model 1 **Model 2**

Figure A.12: **Effect of simulation time on the influence of effector–G_α^{GTP} rates.** The equilibrium concentration of G_α^{GTP}·E is plotted as a function of both added ligand concentration (L_{TOT}) and the parameter scaling factor (α); both forward and reverse reaction rates for the association of G_α^{GTP} and effector (k13 and k14) were multiplied by α, preserving the equilibrium binding constant. In **(a)** the total simulation time was 10^5 s, while in **(b)** the simulation was extended to 10^8 s. With very long simulation times, these rates do not affect the result, but low rates cause a very slow approach to equilibrium, effectively reducing the output signal on moderate time scales.